UNIONE EUROPEA
Fondo Sociale Europeo

Ministero dell'Università
e della Ricerca

PON
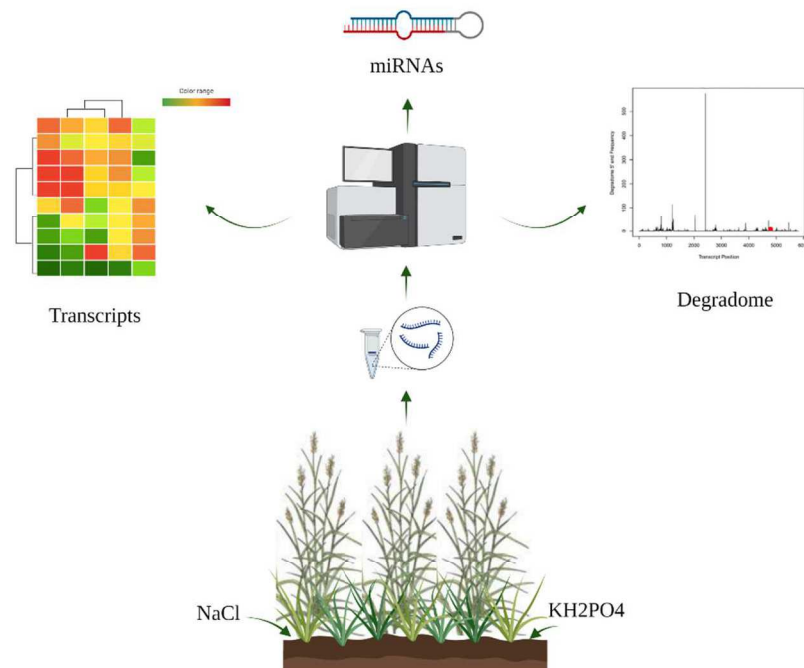RICERCA
E INNOVAZIONE
2014 - 2020

UNIVERSITY OF MOLISE

Department of Biosciences and Territory

DOCTORAL THESIS

An integrated next generation sequencing approach to define and improve the productive efficiency of the energy crop *Arundo donax*

SILVIA ROTUNNO

Supervisor: Professor Gabriella Stefania Scippa

Co-supervisors: Prof. Claudia Cocozza

Dr. Laura Miozzi

UNIONE EUROPEA
Fondo Sociale Europeo

Ministero dell'Università e della Ricerca

PON
RICERCA E INNOVAZIONE
2014 - 2020

UNIVERSITY OF MOLISE

Department of Biosciences and Territory

DOCTORAL THESIS

"ENVIRONMENTAL BIOLOGY"

Cycle XXXIII

An integrated next generation sequencing approach to define and improve the productive efficiency of the energy crop *Arundo donax*

S.S.D. BIO 01

Doctoral coordinator:

Professor Giovanni Fabbrocino

Supervisor: PhD student:

Professor Gabriella Stefania Scippa   **Silvia Rotunno**

An integrated next generation sequencing approach to define and improve the productive efficiency of the energy crop *Arundo donax*

SILVIA ROTUNNO

Supervisor:

Prof. Gabriella Stefania Scippa

University of Molise

Department of Biosciences and Territory

Pesche (IS), Italy

Co-supervisors:

Prof. Claudia Cocozza

University of Florence

Department of Agriculture, Food, Environment and Forestry

Firenze (FI), Italy

Dr. Laura Miozzi

National Research Council

Institute for Sustainable Plant Protection

Torino (TO), Italy

CONTENTS

List of publication

I. Impact of high or low levels of phosphorus and high sodium in soils on productivity and stress tolerance of *Arundo donax* plants

Claudia Cocozza, Federico Brilli, Laura Miozzi, Sara Pignattelli, Silvia Rotunno, Cecilia Brunetti, Cristiana Giordano, Susanna Pollastri, Mauro Centritto, Gian Paolo Accotto, Roberto Tognetti, Francesco Loreto.

(2019). Plant Science, 289:110260.

https://doi.org/10.1016/j.plantsci.2019.110260

II. Identification of abiotic stress responsive microRNAs and their targets in the bioenergy crop *Arundo donax L.* by using high-throughput sequencing

Silvia Rotunno, Claudia Cocozza, Vitantonio Pantaleo, Paola Leonetti, Loris Bertoldi, Giorgio Valle, Gian Paolo Accotto, Francesco Loreto, Gabriella Stefania Scippa, Laura Miozzi.

In preparation

III. Modulation of class III peroxidase pathways and phenylpropanoids in *Arundo donax* under salt and phosphorus stress

Claudia Cocozza, Paola Bartolini, Cecilia Brunetti, Laura Miozzi, Sara Pignattelli, Alessandra Podda, Gabriella Stefania Scippa, Dalila Trupiano, Silvia Rotunno, Federico Brilli, Bianca Elena Maserti.

In preparation

INTRODUCTION

In 2015, United Nations (UN) Member States has adopted the 2030 Agenda for Sustainable Development in order to "protect the planet and improve the lives and prospects of everyone, everywhere" (https://www.un.org/sustainabledevelopment/). The Agenda is organized in 17 Sustainable Development Goals (SDGs), ranging from ending poverty to gaining gender equality to mitigating climate change. Affordable and clean energy is the mission of goal 7: ensuring sustainable energy at accessible price, promoting technological development and innovation are the topics involved. Efforts towards this goal will lead to environmental, social and health advantages.

Based on these premises, the European Union (EU) Parliament and Council has enacted different directives on the promotion of the use of energy from renewable sources over the past years, namely the 2009/28/CE and the EU 2015/1513.The last directive EU 2018/2001 set the targets on energy consumption, sustainability and greenhouse gas emissions by 2030: "Member States shall collectively ensure that the share of energy from renewable sources in the Union's gross final consumption of energy in 2030 is at least 32%" (art. 3, par. 1) and "set an obligation on fuel suppliers to ensure that the share of renewable energy within the final consumption of energy in the transport sector is at least 14 % by 2030" (art. 25, par. 1). Italy has reached the overall national target for 2020 fixed at 17%, contributing to the final goal of 30% by 2030 (Table 1).

	Target for share of energy from renewable sources in gross final consumption of energy, 2020	Target for share of energy from renewable sources in gross final consumption of energy, 2030
Belgium	13%	17.5%
Bulgaria	16%	25%
Czech Republic	13%	20.8%
Denmark	30%	55%
Germany	18%	30%
Estonia	25%	42%
Ireland	16%	15.8% to 27.7%

Greece	18%	35%
Spain	20%	42%
France	23%	33%
Croatia	20%	36.4%
Italy	**17%**	**30%**
Cyprus	13%	22.9%
Latvia	40%	45%
Lithuania	23%	45%
Luxembourg	11%	25%
Hungary	13%	21%
Malta	10%	11.5%
Netherlands	14%	27%
Austria	34%	45% to 50%
Poland	15%	21%
Portugal	31%	47%
Romania	24%	at least 34%
Slovenia	25%	27%
Slovak Republic	14%	18%
Finland	38%	50%
Sweden	49%	65%
United Kingdom*	15%	22% to 29%
EU	**30%**	**32%**

Table 1: data taken from National energy and climate plans (NECPs) (https://ec.europa.eu/energy/topics/energy-strategy/national-energy-climate-plans_en). *even though UK has left EU on February 2020, their NECP was submitted shortly before the end of 2020 (ending of the transition period).

The article 29 focus on sustainability and greenhouse gases (GHGs) emissions saving criteria for biofuels, bioliquids and biomass fuels. GHGs emission is only one of the parameter to consider for Life Cycle Analysis (LCA), a system used for life-cycle energy quantification and environmental impacts (Dunn, 2019) (Fig. 1). Agronomic practices, including fertilization, irrigation and land usage, are also crucial in assessing sustainability.
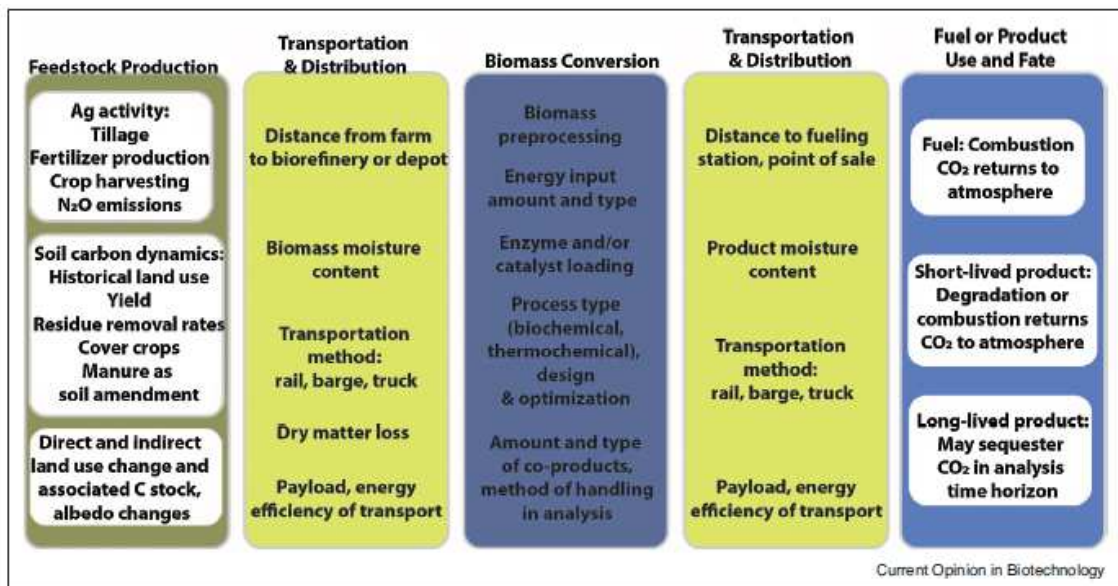
Fig. 1: Stages of biofuel and bioproduct LCA and influencing factors (from Dunn 2019).

In 2019, the *Food and Land Use Coalition* (FOLU) wrote a global report (https://www.foodandlandusecoalition.org/global-report/) that claimed the need to "focus on bioenergy crops that lower the pressure on land and that do not compete with food production or restoration of natural ecosystems or degraded lands". Protect, restore and promote sustainable use of terrestrial ecosystems, sustainably manage forests, combat desertification, halt and reverse land degradation and halt biodiversity loss are the main topics of SDG 15.

Taken together, the SDGs 7 and 15 can be brought back to SDG 13 on climate action. Land exploitation for food or bioenergy production is responsible for rising of GHGs emissions. Actions to mitigate the negative effects of climate changes require shifting economies towards carbon neutrality. The urgency for action was underlined at the COP26 (Conference of the Parties), that took place in Glasgow in November 2020, even though the final agreement seemed bland (https://unfccc.int/process-and-meetings/conferences/glasgow-climate-change-conference-october-november-2021/outcomes-of-the-glasgow-climate-change-conference).

1.1 *Arundo donax L.*

1.1.1 *A. donax* origin and genetics

Arundo donax L., also known as common reed or giant cane (Fig. 2), is a perennial grass plant, belonging to *Arundo* genus of the *Poaceae* family. This genus includes six species, as reported in the Taxonomy database from NCBI: *A. donax* L., *A. plinii* Turra, *A. collina* Ten., *A. donaciformis* Loisel, *A. formosana* Hack and *A. micrantha* Lam.

Fig. 2: Arundo donax field in Sesto Fiorentino (Italy)

A. donax is largely found in subtropical and temperate regions. It has been introduced in the Mediterranean basin from the South-Western Asia (Iran, Afghanistan, Pakistan) around 1500 AD (Hardion et al, 2014). Cytogenetic analysis on Mediterranean populations revealed a 2n=18x ploidy genome constituted by around 108-110 chromosomes. Estimated DNA content (2C) is 4.9 pg, corresponding to a haploid genome of 2,401Mbp (1 pg = 980Mbp) and 54-55 chromosomes (Bucci et al, 2013; Hardion et al, 2015). Starting from *A. plinii*, a fertile specie with 72 chromosomes, and *Phragmites australis*, another fertile specie belonging to the Poaceae family, with 96 chromosomes, two hypothesis have been proposed to explain the uneven ploidy of *A. donax,* (Fig. 3):

- hypothesis 1: *A. plinii* underwent a chromosome doubling producing a fertile tetraploid that crossed with a diploid *A. plinii* created a sterile triploid (108 chromosomes). The addition of two chromosomes resulted in the aneuploid *A. donax*.

- hypothesis 2: *A. plinii* tetraploid crossed with *P. australis* to produce a sterile hybrid (120 chromosomes). The loss of 10 chromosomes resulted in the aneuploid *A. donax*.
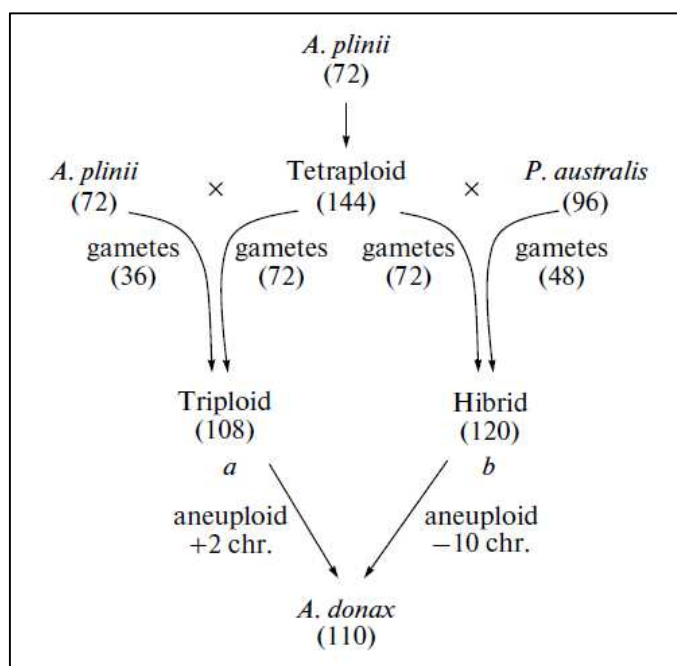
Fig. 3: Phylogenetic origin of *A. donax*. Number of chromosomes are reported in brackets (from Bucci et al, 2013)

Similar ploidity (18x) is reported in North America, with 105 chromosomes (Touchell et al, 2016), while in Australia, *A. donax* is reported as heptaploid (7x), with 84 chromosomes (Haddadchi et al, 2013).

Because of the ploidy and high number of chromosomes, no genome is available to date. Only *de novo A. donax* transcriptome assemblies, from different tissues and/or under stress conditions, are available: leaf, culm, root and bud samples (Sablok et al, 2014), root and shoot samples under osmotic/water stress (Fu et al, 2016), and leaf samples from three ecotypes under different water regimens (Evangelistella et al, 2017).

As result of aneuploidy, arundo is a sterile species, and spreads through rhyzomes or stem fragments. It is found almost everywhere; from subtropical to warm regions. Its fast growth rate, easily overcomes the native vegetation, disrupting the original ecosystem; this is the reason why this plant is listed among the 100 World's Worst Invasive Alien Species (Global Invasive Species Database 2021. http://www.iucngisd.org/gisd/).

Since arundo reproduces asexually, the variability is assured by epigenetic modifications. DNA methylation seems to be the most relevant epigenetic mechanism leading to phenotype diversification, giving arundo the ability to colonize and adapt to different habitats. Methylation patterns could influence gene expression through gene silencing or transposable elements (TEs) activation (Guarino et al, 2019). Considering that 37.55% of

arundo genome is represented by TEs, their activation could have a great impact on variability (Lwin et al, 2017).

Thanks to new techniques (i.e. CRISPR/Cas9) and new studies, the actual limits of genetics improvement of *A. donax* traits involved in biomass production, lignin content and stress resistance would be overcome and increase its importance among bioenergetics crops (Danelli et al, 2020).

1.1.2 *A. donax* as energy crop

Interest around *A. donax* as energy crop has increased along the years. This is due to *A. donax* peculiarities, such as fast growth rate, low input needs, ability of growing in marginal lands and minimal/null competition with feed/food production (Pilu et al, 2013; D'Imporzano et al, 2018; Ren et al, 2019). Its ability to cope with stresses, mostly abiotic, is widely reported (Cocozza et al,, 2020; Docimo et al,, 2019; Haworth et al,, 2019; Shaheen et al,, 2018) and it can also be employed for phytoremediation (Cano-Ruiz et al, 2020; Cristaldi et al, 2020).

Excluding the first year of implantation, *A. donax* does not require irrigation, pesticides and/or fertilizers treatments. Despite being a C3 plant, it shows very high photosynthetic rate (37 μmol m^{-2} s^{-1}) and productivity like C4 species (Sánchez et al,, 2015). During its life cycle (12-15 years), it can produce an average of 40 t/ha of biomass, with lower cost of production compared to other bioenergetics crops (Corno et al, 2014) (Table 2).

	€ ha^{-1} year^{-1}
Arundo	700-1,000
Corn, sorghum, rye and triticale	1,187-2,136
Crop rotation (i.e. triticale plus corn or sorghum)	2,903-3,343

Table 2: estimated cost production of bioenergetics crops in Italy (data from Corno et al, 2014)

Second generation biofuels are defined as fuels produced by non-food biomass, such as switchgrass, mischantus, arundo. First generation biofuels, instead, derive from food biomass, such as sugar cane, sugar beet, corn or wheat. Comparing bioethanol yields, arundo produces 11,000 L ha^{-1}, 50% more than sugar cane and sugar beet, and 20% more than mischantus. In terms of biomethane production, arundo yield (12,618 ± 3,588 Nm^3

CH_4 ha^{-1}, as average) is higher than other energy crops, even if its anaerobic biogasification potential is lower (Corno et al, 2014).

The main limiting factor in the biofuel production from arundo and other lignocellulosic biomasses is recalcitrance, i.e. the difficulty of freeing sugars needed for fermentation process from cell wall structure (Zeng et al, 2014). Lignin is the principal plant cell wall component: it confers rigidity to the wall itself, allowing plants to grow in height; it is involved in mineral transport; it is a barrier against pathogens and it is involved in stress resistance (Liu et al, 2018).

Arundo is one of the highest grass species; however, its lignin content is similar to the others, with an average value of 21%, compared to 19% in switchgrass, 20% of sugarcane and 23% of mischantus (Pilu et al, 2013).

Lignin in cell wall is composed of three subunits, sinapyl alcohol (S, its radical is called syringil); coniferyl alcohol (G, its radical is called guaiacylt) and p-coumaryl alcohol (H, its radical is called hydroxyphenyl), polymerized by peroxidases (POD) and laccases (LAC) in secondary cell walls. These subunits are known as monolignols and their synthesis take part in the phenylpropanoids pathway. Phenylalanine ammonia-lyase (PAL) and cinnamic acid 4-hydroxylase (C4H) catalyze the synthesis of p-coumaric acid from phenylalanine. The p-coumaric acid is hydroxylated by 4-coumarate 3-hydroxylase (C3H) into caffeic acid. The caffeic acid/5-hydroxyconiferaldehyde 3/5-O-methyltransferase (COMT), then, is responsible of the 3-O-methylation of caffeic acid into ferulic acid. These hydroxycinnamates are converted to the corresponding CoA esters by 4-hydroxycinnamate: CoA ligase (4CL). Another way to synthetize caffeoyl CoA via the hydroxycinnamoylCoA: shikimate hydroxycinnamoyl transferase (HCT) and coumaroyl shikimate 3′-hydroxylase (C3H). The resulting caffeoyl CoA is 3-O-methylated by caffeoyl CoA 3-O-methyltransferase (CCoAOMT). CoA esters are converted to corresponding aldehydes and alcohols by cinnamoyl CoA reductase (CCR) and cinnamyl alcohol dehydrogenase (CAD), respectively. COMT and ferulic acid/coniferaldehyde 5-hydroxylase (F5H) are involved in the flux from G to S monolignol (Fig. 4; Liu et al, 2018; Zeng et al, 2020). The caffeoyl shikimate esterase (CSE), that converts caffeoyl CoA to caffeic acid, is found in some species, while in others, including *Brachypodium distachyon*, *Zea mays*, and *Sorghum bicolor*, is absent (Ha et al, 2016). Also tyrosine ammonia-lyase is not always present: in some monocots,

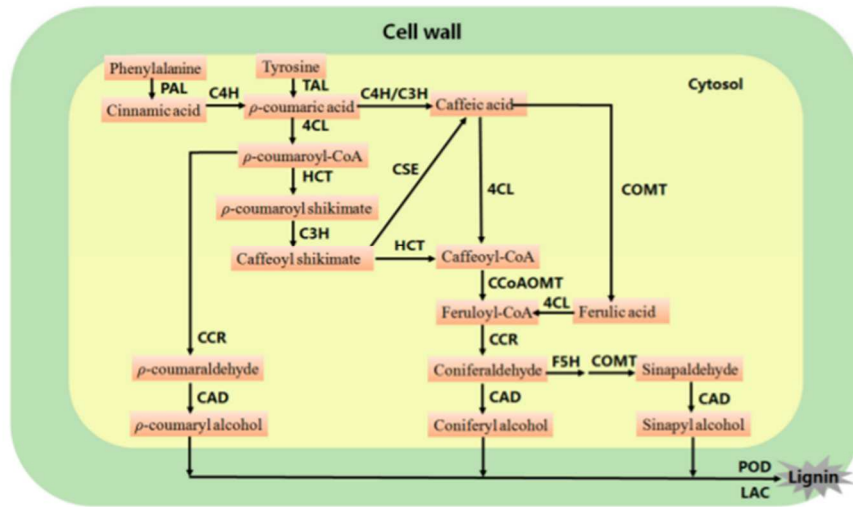PAL has also the ability to use tyrosine as substrate for p-coumaric acid synthesis (Jun et al, 2018).

Fig. 4: Lignin biosynthesis pathway. Enzyme symbols are explained in the text above (from Liu et al, 2018)

Pretreatment processes to increase sugars degradability can be applied, but they affect energetic costs and contribute to pollution. Modifications in lignin content and composition could be a solution: accessibility to cellulose, hemicellulose and other sugars could be improved, increasing the bioenergetics yield; however, they can cause unwanted effects on other metabolic processes, such as stress tolerance/resistance, undermining agronomics productivity (Baxter and Stewart, 2013).

Salt stress has an impact on lignin deposition during secondary cell walls formation; however, key enzymes could be diversely affected by salinity (Le Gall et al, 2015). For example, in soybean roots and vessels a higher lignin deposition, following salt treatment, was determined (Neves et al, 2010; Sánchez-Aguayo et al, 2004). In rice plants, after treatment with 200 mM of NaCl, a lower expression of PAL and COMT was observed (Li et al, 2010); while CCoAOMT expression is increased in rice and Arabidopsis roots under salt stress (Salekdeh et al, 2002; Lee et al, 2004). Transcription factors (TFs) should also be taking into account. TFs involved in lignin synthesis regulation belongs to MYB, MADS-box and WRKY families (Liu et al, 2018). In *Arabidopsis*, overexpression of MYB58 and MYB63 seem to be promote lignification (Zhou et al, 2009); and the transcription factor AGL5, a MADS-box member, regulates a class III peroxidase PRX17 (Cosio et al, 2017). In *Medicago sativa L.*, down-regulation of a WRKY transcription

factor exhibited increased lignin level and enhanced biomass yield (Gallego-Gilardo et al, 2016). Also in *Miscanthus × giganteus*, overexpression of WRKY12 seems to repress lignin biosynthesis, through repression of CAD (Zeng et al, 2020). Indeed, *A. donax* should be considered 'moderately sensitive' to salt. In their work, Nackley and Kim (2014) demonstrated that arundo was able to maintain 50% of its growth when salinity is under 12 dS/m. This finding was also confirmed by the work of De Stefano and co-authors (2018) and promising evidences on salinity tolerance combined with high temperatures were reported by Di Mola and co-authors (2018). The S/G (syringyl/guaiacyl monomers) ratio measures the monomers yield during lignin depolymerization and it used as a predicting factor for recalcitrance: S/G ratio of *A. donax* is around 1.13-1.32, suggesting a lower efficiency in glucose release and bioethanol production with respect to other annual crops, as miscanthus, sorghum or wheat (Seca et al, 2000; Pilu et al, 2012). In *Arabidopsis*, plants where LAC17 gene was silenced, showed a higher S/G ratio, demonstrating that LAC17 is directly involved in G monomers deposition (Berthet et al, 2011). In rice, overexpression of a F5H gene OsCAld5H1 increased the content of S units (Takeda et al, 2017).

1.2 Eutrophication and salinization

More than 16% of the total land area (about 52 million hectares) in the European Union is affected by degradation process. Eight major threats were identified: soil sealing, erosion, loss of organic matter, decline in biodiversity, contamination, compaction, hydro-geological risks and salinization. In 2005 the Soil Atlas of Europe was released as a collection of more than 40 National soil surveys and soil science institutions cooperating across Europe within the European Soil Bureau Network (ESBN) (https://esdac.jrc.ec.europa.eu/content/soil-atlas-europe).

Nitrogen (N) and phosphorus (P) are essential elements for plant growth, but their natural replenishment in soils is slow, so application through use of fertilizers is necessary (Liu and Chen, 2014). However, massive use of fertilizers leads to an excessive N and P supply that is not absorbed by plants and is dispersed into soils, causing eutrophication of water bodies and soils contaminations (Cordell et al, 2009). According to data stored in the Fertilizer archive by FAO (http://www.fao.org/faostat/en/#data/RA), an increment by 2.3 fold in P fertilization and by 7.4 in N fertilization from 1961 to 2022 was observed. Moreover, P fertilizers brings the risk of being trace elements sources, mainly arsenic,

cadmium, copper, chromium, mercury, nickel, lead, and zinc (https://www.fao.org/documents/card/en/c/cb4827en). Great efforts are made in reducing N fertilization, via EU directives (91/676/EEC) and national legislations, but still poor attention is paid to P fertilization. Within the framework of EU's Common Agricultural Policy (CAP), some guidelines about more sustainable soils management are given, targeting the use of fertilizers and organic farming, but not explicitly targeting P management (Garske et al, 2020). P excess in soils is known to interfere with several aspects of plant metabolism such as starch biosynthesis (Fredeen et al, 1989), isoprenoids emission (Fernández-Martínez et al,, 2018), nitrate assimilation (Rufty et al,, 1990), and nutrients absorption (Gatiboni, L. 2018). Furthermore, excess of P supply causes leaf chlorosis and necrosis, inhibition of photosynthesis and Rubisco activity, lipid peroxidation and ROS accumulation (Takagi et al, 2020).

Fertilization associated to hydro-geological risk, water deficiency and sea level raising is responsible of increasing salts in soils. Salinization affects over 1 million hectares of soils in the EU, mainly in the Mediterranean basin (FAO 2008). The types of salt affected soils (SASs) in Europe are principally of two types: saline soils (Solonchak), defined by high amount of soluble salt accumulation; and alkaline soils (Solonetz), defined by high alkalinity and high exchangeable sodium percentage (ESP). Characteristics of SASs by The Global Map of Salt-Affected Soils (GSASmap) are reported in the table below (https://www.fao.org/documents/card/en/c/cb7247en).

EC (dS/m)	Salinity intensity	Effect on crop growth	ESP (%)	Sodicity hazard
<0.75	None	None	<15	None
0.75-2	Slight	None	15-30	Slight
2-4	Moderate	Yields of sensitive crops may be restricted	30-50	Moderate
4-8	Strong	Yields of many crops are limited	50-70	High
8-15	Very strong	Only tolerant crops yield satisfactorily	>70	Extreme
>15	Extreme	Only a few very tolerant crops yield satisfactorily		

Table 3: type of SASs. EC is Electrical Conductivity of soil saturated paste extract, in ds/m, and measures soil salinity; ESP is the Exchangeable Sodium Percentage, in %, and measures soil sodicity (from FAO document).

Salts, particularly sodium salts, cause impairment in the normal plant metabolism, affecting nutrient uptake, photosynthetic capacity and plant growth. Salinity significantly reduces P uptake in plants because phosphate ions precipitate with calcium (Ca^{2+}) ions (Grattan and Grieve, 1998) and induces both ion toxicity and nutrient deficiency through the induction of osmotic and oxidative stress (Almeida Machado and Serralheiro, 2017; Munns and Tester, 2008).

1.3 Plants responses to abiotic stresses

Environmental adverse conditions such as drought, flooding, salinity, heath, cold, heavy metal contamination and nutrient deficiency, are known as abiotic stresses, in opposition to biotic stresses, which indicate pathogens as bacteria, viruses, fungi, or nematodes. Abiotic stresses affect plants growth causing yield loss, and plants, which are sessile organisms, had to develop mechanisms to cope with them (Zhu et al, 2016).

Since this thesis focused on the response of *Arundo donax* to salt stress and excess of P supply, only these abiotic stresses will be further described.

The *Salt Overly Sensitive* (SOS) pathway was the first abiotic stress signaling pathway established and it is considered the major pathway involved in salt stress response (Zhu et al, 2000). SOS consists of three proteins: SOS1, SOS2 and SOS3. SOS1 is a Na+/H+ antiporter; SOS2 is a serine /threonine kinase; and SOS3 is an EF-hand calcium-binding protein. Salts stress elicits Ca+ signaling, resulting in Ca+ binding to SOS3 that in turn binds to and activates SOS2. SOS2 is then able to phosphorylate SOS1, which in turn regulates Na^+ efflux at cellular level and is responsible for long distance transport of Na^+ from root to shoots (Gupta and Huang, 2014). Moreover, the SOS3-SOS2 complex regulates a vacuolar Na^+/H^+ exchange (NHX), that transport Na^+ from the cytoplasm to the vacuole (Yang et al, 2018). A link between SOS pathway and circadian clock under salt/osmotic stress has been recently discovered (Kim et al, 2013; Park et al, 2013). The protein GIGANTEA (GI) binds SOS2, inhibiting its kinase activity, under normal conditions; however, under salt stress, the binding between SOS3 and SOS2, frees GI, that is degraded by the proteasome (Park et al, 2016). SOS2 is a member of the sucrose non-fermenting 1-related protein kinase (SnRKs) family. SnRK2s are involved in osmotic

stress and ABA signaling, whereas SnRK3s are involved in salt and nutrient stresses (Hrabak et al, 2003). The role of ABA in drought and salt-stress responses is already known (Zhu et al, 2002). Other mechanisms involved in salt stress and osmotic stress responses are the activation of the mitogen-activated protein kinase (MAPK) cascades (Mishra et al, 2006) and the increased level ROS scavengers, such as superoxide dismutase, catalase and peroxidases.

Concerning toxicity, symptoms caused by excess of P were reported in leaf of many plants, such as rice, wheat, barley, and Arabidopsis (Aung et al,, 2006; Wang et al,, 2009; Liu et al,, 2010). Excess of P is correlated to Zn and Fe deficiency in rice: accumulation in cells increases phytic acid synthesis, causing Zn e Fe precipitation. During P toxicity, Zn-SOD activity is diminished, while Fe-SOD activity showed no modification, implying that Zn deficiency is more severe than Fe deficiency (Takagi et al, 2020). Evidences of ethylene involvement in P excess are supported by upregulation of genes AtACS11 and AtACS7, isoform of 1-aminocyclopropane -1-carboxylate synthase (ACS), and several ethylene-related genes in *A. thaliana* (Shukla et al, 2017).

1.4 microRNAs involvement in stress responses

Several studies have shown that microRNAs (miRNAs) are strongly involved in the response to abiotic and biotic stress (Li et al, 2017) and that, plants can activate their physiological responses to stress by expressing some miRNAs, and act on stress-related target genes (Sun et al, 2019). miRNAs are a class of small RNA (sRNA) molecules of 20-24 bp involved in the post-transcriptional regulation of a variety of fundamental biological aspects in eukaryotic organisms, including plants (Bartel 2004). miRNAs are transcribed by RNA polymerase II from MIR genes. These sequences, called primary miRNAs (pri-miRNAs), contain a self-complementary region that is processed by Dicer complex; the first cleavage removes the non-complementary part, originating the miRNAs precursor (pre-miRNA), while the second cleavage originates a small double-stranded RNA molecule, known as miRNA/miRNA* duplex, with 2 nt 3' overhangs. AGO1/HSP90 complex binds the duplex and free the miRNA guide strand, originating a mature RISC complex, that is transported into the cytoplasm, where it can perform its function: cleaving the target transcript or inhibiting the translation of the target (Kurihara & Watanabe, 2004; Manavella et al, 2019, Pegler et al, 2019). MIR genes are mostly

intergenic and organized in miRNA families, some of them common to land plants and others originated after eudicots/monocots divergency (Cuperus et al, 2011). Conserved MIR genes originated from genome duplication and rearrangements, so they can be found in multiple loci. As a consequence, conserved miRNAs are highly expressed. Novel MIR genes, instead, are often found in single copy, as they are recently emerged, and novel miRNAs show low expression levels (Voinnet, 2009).

The most representative salt stress-responsive miRNAs include miR156, miR319, miR528, miR396 (Kumar et al, 2018; Sun et al, 2019).

miR156 overexpression is linked to many biological processes, including abiotic stress tolerance. Indeed, in a 2 years open-field research project in USA, miR156 transgenic switchgrass plants showed delayed flowering and increased biomass production (Johnson et al, 2017). Furthermore, its role in salinity tolerance has been reported in many species, such as wheat and alfalfa (Zeeshan et al, 2021; Arshad et al, 2017).

miR319 is involved in plant development, abiotic resistance, and cell wall biosynthesis by targeting TEOSINTE BRANCHED1, CYCLOIDEA, and PCF (TCP) family of transcription factors. In switchgrass, overexpression of miR319 suppresses the activity of the gene PvPCF5, part of TCP pathway, reducing lignin content, by increasing lignin monomer S/G ratio. (Liu et al, 2020). The same miR319-PvPCF5 module could be involved in salinity tolerance via enhancement of ethylene biosynthesis (Liu et al, 2019).

The role of miR528, a monocot specific miRNA, in regulating salinity tolerance is well established. It plays its function through down-regulation of a gene encoding for L-ascorbate oxidase (AAO) in *O. sativa* and *A. stolonifera* (Yuan et al, 2015; Wang et al, 2021). Under salt stress, low level of AAO maintains a high ascorbate redox state and limits H_2O_2 accumulation, contributing to ROS scavenging and resistance to oxidative stress.

The conserved miR396 is involved in plant growth and response to abiotic stresses through regulating Growth Regulating Factor (GRF) transcription factor genes. Transgenic overexpression of osa-miR396 into creeping bentgrass (*A. stolonifera*) resulted in altered plant development, less root biomass and increased capacity to tolerate salt stress (Yuan et al, 2019). The role of miR396 in salt stress is also reported in *M. truncatula* (Cao et al, 2018).

Two miRNAs, the miR397 and miR408, are related to lignin through regulation of laccase genes. In *P. trichocarpa* and *A. thaliana*, miR397 overexpression down-regulates the activity of laccase 17, an enzyme involved in the last step of lignin synthesis (Lu et al, 2013; Wang et al, 2014). Laccases are a specific group of copper protein, whose codified genes are generally targeted by miR408. miR408 is Cu-mir (i.e., dependent on copper metabolism) and is conserved among more than 30 plant species and its overexpression is related to increasing photosynthesis rate in Arabidopsis, rice and tobacco, enhancing biomass yield (Song et al, 2018; Pan et al, 2018). Another Cu-mir is miR398, that targets two Cu/Zn superoxide dismutases (CSD1 and CSD2) in higher plants. Under salinity stress in *A. thaliana*, miR398 levels are negatively correlated to CSD1 mRNA levels, suggesting also a role in salinity stress for miR398 (Jagadeeswaran et al, 2009).

Nutrient-responsive miRNAs are expressed mainly under nutrients deficiency. Under P deficiency, miR399 and miR827 are overexpressed. miR399 targets three genes: the Pi:H$^+$ transporter (PHT1), the DEAD box helicase and the phosphate2 (PHO2), which encodes a putative ubiquitin-conjugating enzyme (UBC) (Hsieh et al, 2009; Fujii et al,, 2005). miR827 targets gene encoding proteins containing SPX domain, which is involved in Pi-sensing, Pi transport in yeast and Pi xylem loading in plants (Hackenberg et al,, 2013). miR395, involved in sulphur metabolism via targeting ATP sulphurylases (APSs) coding genes, is down-regulated under P deficiency (Kumar et al, 2017). As a matter of fact, nutrients deficiencies are often related each another.

Examples listed above are the proof that a fine regulation of different miRNAs-targets could lead to improved preferred traits of crops. Therefore, understanding the relationship among miRNAs and their targets could be the key for biotechnological improvement of crops production (Zhang and Wang, 2015). Focusing on bioenergy crops, improvements would consist in increasing quantity and quality of produced biomass, without losing the ability to face stresses.

1.5 Next Generation Sequencing technologies

The term Next Generation Sequencing (NGS) indicates technologies involving high-throughput approaches to DNA/RNA sequencing, where millions of sequences are processed in parallel in order to obtain a consensus sequence.

The advent of NGS technologies has revolutionized the biological sciences. Thanks to their ability to produce higher amount of data in a shorter time and at lower cost in respect to the classical approaches such as Sanger sequencing and microarray (Table 4),

NGS vs Sanger sequening	NGS vs microarray
High sensitivity: higher sequencing depth enables higher sensitivity (down to 1%)	Discovery mode: detection of novel transcripts, gene fusions, single nucleotide variants, indels (small insertions and deletions), and other previously unknown changes without the use of probes
Higher discovery power: identification of novel variants by increasing the number of targets sequenced in a single run	Broad dynamic coverage: NGS outcomes are discrete, digital sequencing read counts, and can quantify expression across a larger dynamic range. The results are not limited by background at the low end and signal saturation at the high end
Higher mutation resolution	Higher specificity and sensitivity: NGS allows detection of a higher percentage of differentially expressed genes and also genes with low copy numbers
Higher sample throughput	Simple detection of rare and low-abundance transcripts: the broad range of sequence coverage also allows detection of rare transcripts, single transcripts per cell, or weakly expressed genes
Higher detection limits: sequencing samples that have low input amounts starting from 10 ng of input DNA and enormous data produced with the same amount of input DNA compared to Sanger method	

Sequencing of emergency situations as outbreaks	

Table 2: Advantages of NGS over Sanger sequencing and microarrays. (Table from Meera et al, 2019).

NGS technologies have been proven to be extremely useful and scientists from clinical to environmental research to agriculture have started to use them routinely to answer many biological questions.

The NGS platforms currently available are:

- ABI SOLiD (Sequencing by Oligo Ligation Detection) system was purchased by Applied Biosystem in 2006 and released at the end of 2007. It is a two-base sequencing based on ligation sequencing (https://www.thermofisher.com/it/en/home/brands/applied-biosystems.html);
- Illumina purchased in 2007 Solexa, which released the Genome Analyzer in 2006. It uses sequencing by synthesis (SBS) technology (https://emea.illumina.com/);
- Ion Torrent, commercialized by Thermo Fischer in 2006, uses semiconductor sequencing technology (https://www.thermofisher.com/it/en/home/brands/ion-torrent.html).

Among them, Illumina sequencing technology is the most popular and is responsible for generating more than 90% of the world's sequencing data (Data calculations on file. Illumina, Inc. 2015) (Liu et al, 2012; Meera et al, 2019).

Thanks to NGS, the genome of many model species has been assembled. However, the use of NGS technologies for genome assembly of non-model species, particularly in plants, has still shortcomings, such as the genome duplication, the heterozygosity, the ploidy level, and repetitive sequence composition (Unamba et al, 2015; Hirsh and Buell, 2013).

In order to overcome these obstacles, more specialized NGS methodologies can be applied, each one addressing a specific issue. For example, *de novo* (genome or transcriptome) sequencing, metagenomics sequencing, RNA sequencing, smallRNA sequencing or degradome sequencing, only to mention some of them.

RNA-sequencing (RNA-seq) is the methodology used for sequencing all RNA molecules transcribed, so, it is useful in gene discovery and gene expression. Different tissues and

different stages of development need different sets of proteins, so different mRNAs are transcribed. Moreover, responses to both biotic and abiotic stresses, different growth conditions and phenotypes lead to differential mRNAs transcription. Reads form RNA-seq can also be used for *de novo* transcriptome assembly, in case genome reference is missing (Unamba et al, 2015), and for variants calling, when a genome reference is available (Piskol et al, 2013).

smallRNA-sequencing (smallRNA-seq) is useful in miRNAs discovery, not only conserved miRNAs, but also novel miRNAs. Novel miRNAs are phylogenetically younger than conserved miRNAs, and usually expressed at lower levels. NGS technologies, thanks to their high sensitivity, could help in miRNAs discovery, also in non model crops, lacking a reference genome (Lakhotia et al, 2014). Furthermore, as RNA-seq, it gives a spatial and temporal picture of miRNAs in the samples, giving hints to understand their function (Axtell and Bartel, 2005).

Degradome-sequencing (deg-seq), also referred to as parallel analysis of RNA ends (PARE), is a modified version of 5'-Rapid Amplification of cDNA Ends (RACE) using high-throughput sequencing methods. Thanks to this methodology, all 5'cap deprived RNA molecules can be identified and sequenced (German et al, 2008; Addo-Quaye et al, 2008). Those RNA molecules can be remnants of miRNAs cleavage, but also remnants from generical endonucleases activities. This is the reason why a combined analysis with RNA-seq data and small-RNA data is required in order to identify deg-reads derived from miRNA's activity.

The world of NGS technologies is still developing. New platforms, such as single molecule real-time (SMRT) sequencing by PacBio or nanopore sequencing, are now arising, giving new opportunities, especially in the diagnostic and clinical field (Thompson and Milos, 2011).

References

Addo-Quaye, C., Eshoo, T. W., Bartel, D. P., & Axtell, M. J. (2008). Endogenous siRNA and miRNA targets identified by sequencing of the Arabidopsis degradome. Curr Biol, 18(10), 758-762. doi:10.1016/j.cub.2008.04.042

Arshad, M., Gruber, M. Y., Wall, K., & Hannoufa, A. (2017). An Insight into microRNA156 Role in Salinity Stress Responses of Alfalfa. Front Plant Sci, 8, 356. doi:10.3389/fpls.2017.00356

Aung, K., Lin, S. I., Wu, C. C., Huang, Y. T., Su, C. L., & Chiou, T. J. (2006). pho2, a phosphate overaccumulator, is caused by a nonsense mutation in a microRNA399 target gene. Plant Physiol, 141(3), 1000-1011. doi:10.1104/pp.106.078063

Axtell, M. J., & Bartel, D. P. (2005). Antiquity of microRNAs and their targets in land plants. Plant Cell, 17(6), 1658-1673. doi:10.1105/tpc.105.032185

Bartel, D. P. (2004). MicroRNAs: genomics, biogenesis, mechanism, and function. Cell, 116(2), 281-297. doi:10.1016/s0092-8674(04)00045-5

Baxter, H. L., & Stewart, C. N. (2013). Effects of altered lignin biosynthesis on phenylpropanoid metabolism and plant stress. Biofuels, 4(6), 635-650. doi:10.4155/bfs.13.56

Berthet, S., Demont-Caulet, N., Pollet, B., Bidzinski, P., Cézard, L., Le Bris, P., Borrega, N., Hervé, J., Blondet, E., Balzergue, S., Lapierre, C., & Jouanin, L. (2011). Disruption of LACCASE4 and 17 results in tissue-specific alterations to lignification of *Arabidopsis thaliana* stems. Plant Cell, 23(3), 1124-1137. doi:10.1105/tpc.110.082792

Bucci, A., Cassani, E., Landoni, M., Cantaluppi, E., & Pilu, R. (2013). Analysis of chromosome number and speculations on the origin of *Arundo donax* L. (Giant Reed). Cytology and Genetics, 47(4), 237-241. doi:10.3103/S0095452713040038

Cano-Ruiz, J., Ruiz Galea, M., Amorós, M. C., Alonso, J., Mauri, P. V., & Lobo, M. C. (2020). Assessing *Arundo donax* L. in vitro-tolerance for phytoremediation purposes. Chemosphere, 252, 126576. doi:10.1016/j.chemosphere.2020.126576

Cao, C., Long, R., Zhang, T., Kang, J., Wang, Z., Wang, P., Sun, H., Yu, J., & Yang, Q. (2018). Genome-Wide Identification of microRNAs in Response to Salt/Alkali Stress in. Int J Mol Sci, 19(12). doi:10.3390/ijms19124076

Cocozza, C., Brilli, F., Pignattelli, S., Pollastri, S., Brunetti, C., Gonnelli, C., Tognetti, R., Centritto, M., & Loreto, F. (2020). The excess of phosphorus in soil reduces physiological performances over time but enhances prompt recovery of salt-stressed *Arundo donax* plants. Plant Physiol Biochem, 151, 556-565. doi:10.1016/j.plaphy.2020.04.011

Cordell, D., Drangert, J.-O., & White, S. (2009). The story of phosphorus: Global food security and food for thought. Global Environmental Change, 19(2), 292-305. doi:https://doi.org/10.1016/j.gloenvcha.2008.10.009

Corno, L., Pilu, R., & Adani, F. (2014). *Arundo donax* L.: a non-food crop for bioenergy and bio-compound production. Biotechnol Adv, 32(8), 1535-1549. doi:10.1016/j.biotechadv.2014.10.006

Cosio, C., Ranocha, P., Francoz, E., Burlat, V., Zheng, Y., Perry, S. E., Ripoll, J. J., Yanofsky, M., & Dunand, C. (2017). The class III peroxidase PRX17 is a direct target of the MADS-box transcription factor AGAMOUS-LIKE15 (AGL15) and participates in lignified tissue formation. New Phytol, 213(1), 250-263. doi:10.1111/nph.14127

Cristaldi, A., Oliveri Conti, G., Cosentino, S. L., Mauromicale, G., Copat, C., Grasso, A., Zuccarello, P., Fiore, M., Restuccia, C., & Ferrante, M. (2020). Phytoremediation potential of *Arundo donax* (Giant Reed) in contaminated soil by heavy metals. Environ Res, 185, 109427. doi:10.1016/j.envres.2020.109427

Cuperus, J. T., Fahlgren, N., & Carrington, J. C. (2011). Evolution and functional diversification of MIRNA genes. The Plant cell, 23(2), 431–442. doi:10.1105/tpc.110.082784

D'Imporzano, G., Pilu, R., Corno, L., & Adani, F. (2018). *Arundo donax* L. can substitute traditional energy crops for more efficient, environmentally-friendly production of biogas: A Life Cycle Assessment approach. Bioresour Technol, 267, 249-256. doi:10.1016/j.biortech.2018.07.053

Danelli, T., Laura, M., Savona, M., Landoni, M., Adani, F., & Pilu, R. (2020). Genetic Improvement of. Plants (Basel), 9(11). doi:10.3390/plants9111584

De Stefano, R., Cappetta, E., Guida, G., Mistretta, C., Caruso, G., Giorio, P., Albrizio, R., & Tucci, M. (2018). Screening of giant reed (*Arundo donax* L.) ecotypes for biomass production under salt stress. Plant Biosystems - An International Journal Dealing with all Aspects of Plant Biology, 152(5), 911-917. doi:10.1080/11263504.2017.1362059

Di Mola, I., Guida, G., Mistretta, C., Giorio, P., Albrizio, R., Visconti, D., Fagnano M., & Mori, M. (2018). Agronomic and physiological response of giant reed (*Arundo donax* L.) to soil salinity. Italian Journal of Agronomy, 13(1), 31-39. doi:10.4081/ija.2018.995

Docimo, T., De Stefano, R., De Palma, M., Cappetta, E., Villano, C., Aversano, R., & Tucci, M. (2019). Transcriptional, metabolic and DNA methylation changes underpinning the response of *Arundo donax* ecotypes to NaCl excess. Planta, 251(1), 34. doi:10.1007/s00425-019-03325-w

Dunn, J. B. (2019). Biofuel and bioproduct environmental sustainability analysis. Curr Opin Biotechnol, 57, 88-93. doi:10.1016/j.copbio.2019.02.008

Evangelistella, C., Valentini, A., Ludovisi, R., Firrincieli, A., Fabbrini, F., Scalabrin, S., Cattonaro, F., Morgante, M., Mugnozza, G. S., Keurentjes, J. J. B., & Harfouche, A. (2017). *De novo* assembly, functional annotation, and analysis of the giant reed (Biotechnol Biofuels, 10, 138. doi:10.1186/s13068-017-0828-7

Fernández-Martínez, M., Llusià, J., Filella, I., Niinemets, Ü., Arneth, A., Wright, I. J., Loreto F., & Peñuelas, J. (2018). Nutrient-rich plants emit a less intense blend of volatile isoprenoids. New Phytol, 220(3), 773-784. doi:10.1111/nph.14889

Fredeen, A. L., Rao, I. M., & Terry, N. (1989). Influence of Phosphorus Nutrition on Growth and Carbon Partitioning in *Glycine max*. Plant Physiol, 89(1), 225-230. doi:10.1104/pp.89.1.225

Fu, Y., Poli, M., Sablok, G., Wang, B., Liang, Y., La Porta, N., Velikova, V., Loreto, F., Li, M., & Varotto, C. (2016). Dissection of early transcriptional responses to water stress in *Arundo donax* L. by unigene-based RNA-seq. Biotechnol Biofuels, 9, 54. doi:10.1186/s13068-016-0471-8

Fujii, H., Chiou, T. J., Lin, S. I., Aung, K., & Zhu, J. K. (2005). A miRNA involved in phosphate-starvation response in Arabidopsis. Curr Biol, 15(22), 2038-2043. doi:10.1016/j.cub.2005.10.016

Gallego-Giraldo, L., Shadle, G., Shen, H., Barros-Rios, J., Fresquet Corrales, S., Wang, H., & Dixon, R. A. (2016). Combining enhanced biomass density with reduced lignin level for improved forage quality. Plant Biotechnology Journal, 14(3), 895-904. doi:https://doi.org/10.1111/pbi.12439

Garske, B., Stubenrauch, J., & Ekardt, F. (2020). Sustainable phosphorus management in European agricultural and environmental law. Review of European, Comparative & International Environmental Law, 29(1), 107-117. doi:https://doi.org/10.1111/reel.12318

Gatiboni, L. (2018). Soils and Plant Nutrients. In a. L. K. B. K.A. Moore (Ed.), North Carolina Extension Gardener Handbook. NC State Extension, Raleigh, NC.

German, M. A., Pillay, M., Jeong, D. H., Hetawal, A., Luo, S., Janardhanan, P., Kannan, V., Rymarquis, L. A., Nobuta, K., German, R., De Paoli, E., Lu, C., Schroth, G., Meyers, B. C., & Green, P. J. (2008). Global identification of microRNA-target RNA pairs by parallel analysis of RNA ends. Nat Biotechnol, 26(8), 941-946. doi:10.1038/nbt1417

Grattan, S. R., & Grieve, C. M. (1998). Salinity–mineral nutrient relations in horticultural crops. Scientia Horticulturae, 78(1), 127-157. doi:https://doi.org/10.1016/S0304-4238(98)00192-7

Guarino, F., Cicatelli, A., Brundu, G., Improta, G., Triassi, M., & Castiglione, S. (2019). The use of MSAP reveals epigenetic diversity of the invasive clonal populations of *Arundo donax* L. PLoS One, 14(4), e0215096. doi:10.1371/journal,pone.0215096

Gupta, B., & Huang, B. (2014). Mechanism of salinity tolerance in plants: physiological, biochemical, and molecular characterization. Int J Genomics, 2014, 701596. doi:10.1155/2014/701596

Ha, C. M., Escamilla-Trevino, L., Yarce, J. C., Kim, H., Ralph, J., Chen, F., & Dixon, R. A. (2016). An essential role of caffeoyl shikimate esterase in monolignol biosynthesis in *Medicago truncatula*. Plant J, 86(5), 363-375. doi:10.1111/tpj.13177

Hackenberg, M., Shi, B. J., Gustafson, P., & Langridge, P. (2013). Characterization of phosphorus-regulated miR399 and miR827 and their isomirs in barley under phosphorus-sufficient and phosphorus-deficient conditions. BMC Plant Biol, 13, 214. doi:10.1186/1471-2229-13-214

Haddadchi, A., Gross, C.L., & Fatemi, M. (2013).The expansion of sterile *Arundo donax* (Poaceae) in southeastern Australia is accompanied by genotypic variation. Aquat Bot, 104, 153-161. doi:10.1016/j.aquabot.2012.07.006

Hardion, L., Verlaque, R., Rosato, M., Rosselló, J. A., & Vila, B. (2015). Impact of polyploidy on fertility variation of Mediterranean Arundo L. (Poaceae). C R Biol, 338(5), 298-306. doi:10.1016/j.crvi.2015.03.013

Hardion, L., Verlaque, R., Saltonstall, K., Leriche, A., & Vila, B. (2014). Origin of the invasive *Arundo donax* (Poaceae): a trans-Asian expedition in herbaria. Ann Bot, 114(3), 455-462. doi:10.1093/aob/mcu143

Haworth, M., Marino, G., Riggi, E., Avola, G., Brunetti, C., Scordia, D., Testa, G., Thiago Gaudio Gomes, M., Loreto, F., Luciano Cosentino, S., & Centritto, M. (2019). The effect of summer drought on the yield of *Arundo donax* is reduced by the retention of photosynthetic capacity and leaf growth later in the growing season. Ann Bot, 124(4), 567-580. doi:10.1093/aob/mcy223

Hirsch, C. N., & Buell, C. R. (2013). Tapping the promise of genomics in species with complex, nonmodel genomes. Annu Rev Plant Biol, 64, 89-110. doi:10.1146/annurev-arplant-050312-120237

Hrabak, E. M., Chan, C. W., Gribskov, M., Harper, J. F., Choi, J. H., Halford, N., Kudla, J., Luan, S., Nimmo, H. G., Sussman, M. R., Thomas, M., Walker-Simmons, K., Zhu, J. K. & Harmon, A. C. (2003). The Arabidopsis CDPK-SnRK superfamily of protein kinases. Plant Physiol, 132(2), 666-680. doi:10.1104/pp.102.011999

Hsieh, L. C., Lin, S. I., Shih, A. C., Chen, J. W., Lin, W. Y., Tseng, C. Y., Li, W. H., & Chiou, T. J. (2009). Uncovering small RNA-mediated responses to phosphate deficiency in Arabidopsis by deep sequencing. Plant Physiol, 151(4), 2120-2132. doi:10.1104/pp.109.147280

Jagadeeswaran, G., Saini, A., & Sunkar, R. (2009). Biotic and abiotic stress down-regulate miR398 expression in Arabidopsis. Planta, 229(4), 1009-1014. doi:10.1007/s00425-009-0889-3

Jike, W., Sablok, G., Bertorelle, G., Li, M., & Varotto, C. (2018). In silico identification and characterization of a diverse subset of conserved microRNAs in bioenergy crop Arundo donax L. Sci Rep, 8(1), 16667. doi:10.1038/s41598-018-34982-8

Johnson, C. R., Millwood, R. J., Tang, Y., Gou, J., Sykes, R. W., Turner, G. B., Davis, M. F., Sang, Y., Wang, Z. Y., & Stewart, C. N. (2017). Field-grown miR156 transgenic switchgrass reproduction, yield, global gene expression analysis, and bioconfinement. Biotechnol Biofuels, 10, 255. doi:10.1186/s13068-017-0939-1

Jun, S. Y., Sattler, S. A., Cortez, G. S., Vermerris, W., Sattler, S. E., & Kang, C. (2018). Biochemical and Structural Analysis of Substrate Specificity of a Phenylalanine Ammonia-Lyase. Plant Physiol, 176(2), 1452-1468. doi:10.1104/pp.17.01608

Kim, W. Y., Ali, Z., Park, H. J., Park, S. J., Cha, J. Y., Perez-Hormaeche, J., Quintero, F. J., Shin, G., Kim, M. R., Qiang, Z., Ning, L., Park, H. C., Lee, S. Y., Bressan, R. A., Pardo, J. M., Bohnert, H. J., & Yun, D. J. (2013). Release of SOS2 kinase from sequestration with GIGANTEA determines salt tolerance in Arabidopsis. Nat Commun, 4, 1352. doi:10.1038/ncomms2357

Kumar, S., Verma, S., & Trivedi, P. K. (2017). Involvement of Small RNAs in Phosphorus and Sulfur Sensing, Signaling and Stress: Current Update. Front Plant Sci, 8, 285. doi:10.3389/fpls.2017.00285

Kumar, V., Khare, T., Shriram, V., & Wani, S. H. (2018). Plant small RNAs: the essential epigenetic regulators of gene expression for salt-stress responses and tolerance. Plant cell reports, 37(1), 61–75. doi:10.1007/s00299-017-2210-4

Kurihara, Y., & Watanabe, Y. (2004). Arabidopsis micro-RNA biogenesis through Dicer-like 1 protein functions. Proceedings of the National Academy of Sciences of the United States of America, 101(34), 12753–12758. doi:10.1073/pnas.0403115101

Lakhotia, N., Joshi, G., Bhardwaj, A. R., Katiyar-Agarwal, S., Agarwal, M., Jagannath, A., Goel, S., & Kumar, A. (2014). Identification and characterization of miRNAome in root, stem, leaf and tuber developmental stages of potato (*Solanum tuberosum* L.) by high-throughput sequencing. BMC Plant Biol, 14, 6. doi:10.1186/1471-2229-14-6

Le Gall, H., Philippe, F., Domon, J. M., Gillet, F., Pelloux, J., & Rayon, C. (2015). Cell Wall Metabolism in Response to Abiotic Stress. Plants (Basel), 4(1), 112-166. doi:10.3390/plants4010112

Lee, S., Lee, E. J., Yang, E. J., Lee, J. E., Park, A. R., Song, W. H., & Park, O. K. (2004). Proteomic identification of annexins, calcium-dependent membrane binding proteins that

mediate osmotic stress and abscisic acid signal transduction in Arabidopsis. Plant Cell, 16(6), 1378-1391. doi:10.1105/tpc.021683

Li, S., Castillo-González, C., Yu, B., & Zhang, X. (2017). The functions of plant small RNAs in development and in stress responses. Plant J, 90(4), 654-670. doi:10.1111/tpj.13444

Li, X. J., Yang, M. F., Chen, H., Qu, L. Q., Chen, F., & Shen, S. H. (2010). Abscisic acid pretreatment enhances salt tolerance of rice seedlings: proteomic evidence. Biochim Biophys Acta, 1804(4), 929-940. doi:10.1016/j.bbapap.2010.01.004

Liu, F., Wang, Z., Ren, H., Shen, C., Li, Y., Ling, H. Q., Wu, C., Lian, X., & Wu, P. (2010). OsSPX1 suppresses the function of OsPHR2 in the regulation of expression of OsPT2 and phosphate homeostasis in shoots of rice. Plant J, 62(3), 508-517. doi:10.1111/j.1365-313X.2010.04170.x

Liu, L., Li, Y., Li, S., Hu, N., He, Y., Pong, R., Lin, D., Lu, L., & Law, M. (2012). Comparison of Next-Generation Sequencing Systems. Journal of Biomedicine and Biotechnology, 2012, 251364. doi:10.1155/2012/251364

Liu, Q., Luo, L., & Zheng, L. (2018). Lignins: Biosynthesis and Biological Functions in Plants. Int J Mol Sci, 19(2). doi:10.3390/ijms19020335

Liu, Y., & Chen, J. (2014). Phosphorus Cycle☆. In B. Fath (Ed.), Encyclopedia of Ecology (Second Edition) (pp. 181-191). Oxford: Elsevier.

Liu, Y., Li, D., Yan, J., Wang, K., Luo, H., & Zhang, W. (2019). MiR319 mediated salt tolerance by ethylene. Plant Biotechnol J, 17(12), 2370-2383. doi:10.1111/pbi.13154

Liu, Y., Yan, J., Wang, K., Li, D., Han, Y., & Zhang, W. (2020). Heteroexpression of Osa-miR319b improved switchgrass biomass yield and feedstock quality by repression of PvPCF5. Biotechnol Biofuels, 13, 56. doi:10.1186/s13068-020-01693-0

Lu, S., Li, Q., Wei, H., Chang, M. J., Tunlaya-Anukit, S., Kim, H., Liu, J., Song, J., Sun, Y. H., Yuan, L., Yeh, T. F., Peszlen, I., Ralph, J., & Sederoff, R. R. Chiang, V. L. (2013). Ptr-miR397a is a negative regulator of laccase genes affecting lignin content in *Populus trichocarpa*. Proc Natl Acad Sci U S A, 110(26), 10848-10853. doi:10.1073/pnas.1308936110

Lwin, A. K., Bertolini, E., Pè, M. E., & Zuccolo, A. (2017). Genomic skimming for identification of medium/highly abundant transposable elements in *Arundo donax* and *Arundo plinii*. Mol Genet Genomics, 292(1), 157-171. doi:10.1007/s00438-016-1263-3

Machado, R. M., & Serralheiro, R. P. (2017). Soil Salinity: Effect on Vegetable Crop Growth. Management Practices to Prevent and Mitigate Soil Salinization. Horticulturae, 3(2). doi:10.3390/horticulturae3020030

Manavella, P. A., Yang, S. W., & Palatnik, J. (2019). Keep calm and carry on: miRNA biogenesis under stress. Plant J, 99(5), 832-843. doi:10.1111/tpj.14369

Meera Krishna, B., Khan, M. A., & Khan, S. T. (2019). Next-Generation Sequencing (NGS) Platforms: An Exciting Era of Genome Sequence Analysis. In V. Tripathi, P. Kumar, P. Tripathi, A. Kishore, & M. Kamle (Eds.), Microbial Genomics in Sustainable Agroecosystems: Volume 2 (pp. 89-109). Singapore: Springer Singapore.

Mishra, N. S., Tuteja, R., & Tuteja, N. (2006). Signaling through MAP kinase networks in plants. Arch Biochem Biophys, 452(1), 55-68. doi:10.1016/j.abb.2006.05.001

Munns, R., & Tester, M. (2008). Mechanisms of salinity tolerance. Annu Rev Plant Biol, 59, 651-681. doi:10.1146/annurev.arplant.59.032607.092911

Nackley, L., & Kim, S.-H. (2014). A salt on the bioenergy and biological invasions debate: Salinity tolerance of the invasive biomass feedstock *Arundo donax*. GCB Bioenergy, 7. doi:10.1111/gcbb.12184

Neves, G. Y. S., Marchiosi, R., Ferrarese, M. L. L., Siqueira-Soares, R., & Ferrarese-Filho, O. (2010). Root Growth Inhibition and Lignification Induced by Salt Stress in Soybean. Journal of Agronomy and Crop Science, 196, 467-473. doi:10.1111/j.1439-037X.2010.00432.x

Pan, J., Huang, D., Guo, Z., Kuang, Z., Zhang, H., Xie, X., Ma, Z., Gao, S., Lerdau, M. T., Chu, C., & Li, L. (2018). Overexpression of microRNA408 enhances photosynthesis, growth, and seed yield in diverse plants. J Integr Plant Biol, 60(4), 323-340. doi:10.1111/jipb.12634

Park, H. J., Kim, W. Y., & Yun, D. J. (2013). A role for GIGANTEA: keeping the balance between flowering and salinity stress tolerance. Plant Signal Behav, 8(7), e24820. doi:10.4161/psb.24820

Park, H. J., Kim, W. Y., & Yun, D. J. (2016). A New Insight of Salt Stress Signaling in Plant. Mol Cells, 39(6), 447-459. doi:10.14348/molcells.2016.0083

Pegler, J. L., Grof, C. P. L., & Eamens, A. L. (2019). The Plant microRNA Pathway: The Production and Action Stages. Methods Mol Biol, 1932, 15-39. doi:10.1007/978-1-4939-9042-9_2

Pilu, R., Bucci A., Cerino Badone F & Landoni M. (2012). Giant reed (Arundo donax L.): A weed plant or a promising energy crop? Afr. J. Biotechnol, 11(38), 9163-9174. doi: 10.5897/AJB11.4182

Pilu, R., Manca, A., & Landoni, M. (2013). Arundo donax as an energy crop: pros and cons of the utilization of this perennial plant. 2013, 58(1), 6

Piskol, R., Ramaswami, G., & Li, J. B. (2013). Reliable identification of genomic variants from RNA-seq data. Am J Hum Genet, 93(4), 641-65. doi:10.1016/j.ajhg.2013.08.008

Ren, L., Eller, F., Lambertini, C., Guo, W. Y., Brix, H., & Sorrell, B. K. (2019). Assessing nutrient responses and biomass quality for selection of appropriate paludiculture crops. Sci Total Environ, 664, 1150-1161. doi:10.1016/j.scitotenv.2019.01.419

Rufty, T. W., Mackown, C. T., & Israel, D. W. (1990). Phosphorus stress effects on assimilation of nitrate. Plant Physiol, 94(1), 328-333. doi:10.1104/pp.94.1.328

Sablok, G., Fu, Y., Bobbio, V., Laura, M., Rotino, G. L., Bagnaresi, P., Allavena, A., Velikova, V., Viola, R., Loreto, F., Li, M., & Varotto, C. (2014). Fuelling genetic and metabolic exploration of C3 bioenergy crops through the first reference transcriptome of *Arundo donax* L. Plant Biotechnology Journal, 12(5), 554-567. doi:https://doi.org/10.1111/pbi.12159

Salekdeh, G. H., Siopongco, J., Wade, L. J., Ghareyazie, B., & Bennett, J. (2002). Proteomic analysis of rice leaves during drought stress and recovery. Proteomics, 2(9), 1131-1145. doi:10.1002/1615-9861(200209)2:9<1131::AID-PROT1131>3.0.CO;2-1

Seca, A. M., Cavaleiro, J. A., Domingues, F. M., Silvestre, A. J., Evtuguin, D., & Neto, C. P. (2000). Structural characterization of the lignin from the nodes and internodes of *Arundo donax* reed. J Agric Food Chem, 48(3), 817-824. doi:10.1021/jf9910988

Shaheen, S., Ahmad, R., Mahmood, Q., Mubarak, H., Mirza, N., & Hayat, M. T. (2018). Physiology and selected genes expression under cadmium stress in *Arundo donax* L. Int J Phytoremediation, 20(11), 1162-1167. doi:10.1080/15226514.2018.1460312

Shukla, D., Rinehart, C. A., & Sahi, S. V. (2017). Comprehensive study of excess phosphate response reveals ethylene mediated signaling that negatively regulates plant growth and development. Sci Rep, 7(1), 3074. doi:10.1038/s41598-017-03061-9

Song, Z., Zhang, L., Wang, Y., Li, H., Li, S., Zhao, H., & Zhang, H. (2017). Constitutive Expression of miR408 Improves Biomass and Seed Yield in Arabidopsis. Front Plant Sci, 8, 2114. doi:10.3389/fpls.2017.02114

Sun, X., Lin, L., & Sui, N. (2019). Regulation mechanism of microRNA in plant response to abiotic stress and breeding. Mol Biol Rep, 46(1), 1447-1457. doi:10.1007/s11033-018-4511-2

Sánchez, E., Scordia, D., Lino, G., Arias, C., Cosentino, S. L., & Nogués, S. (2015). Salinity and Water Stress Effects on Biomass Production in Different *Arundo donax* L. Clones. Bioenergy Research, 8(4), 1461-1479. doi:http://dx.doi.org/10.1007/s12155-015-9652-8

Sánchez-Aguayo, I., Rodríguez-Galán, J. M., García, R., Torreblanca, J., & Pardo, J. M. (2004). Salt stress enhances xylem development and expression of S-adenosyl-L-methionine synthase in lignifying tissues of tomato plants. Planta, 220(2), 278-285. doi:10.1007/s00425-004-1350-2

Takagi, D., Miyagi, A., Tazoe, Y., Suganami, M., Kawai-Yamada, M., Ueda, A., Suzuki, Y., Noguchi, K., Hirotsu, N., & Makino, A. (2020). Phosphorus toxicity disrupts Rubisco activation and reactive oxygen species defence systems by phytic acid accumulation in leaves. Plant Cell Environ, 43(9), 2033-2053. doi:10.1111/pce.13772

Takeda, Y., Koshiba, T., Tobimatsu, Y., Suzuki, S., Murakami, S., Yamamura, M., Rahman, M. M., Takano, T., Hattori, T., Sakamoto, M., & Umezawa, T. (2017). Regulation of coniferaldehyde 5-hydroxylase expression to modulate cell wall lignin structure in rice. Planta, 246(2), 337-349. doi:10.1007/s00425-017-2692-x

Thompson, J. F., & Milos, P. M. (2011). The properties and applications of single-molecule DNA sequencing. Genome Biology, 12(2), 217. doi:10.1186/gb-2011-12-2-217

Touchell, D. H., Ranney, T. G., Panthee, D. R., Gehl, R. J., & Krings, A. (2016). Genetic Diversity, Cytogenetics, and Biomass Yields among Taxa of Giant Reeds (Arundo Species), J. Amer. Soc. Hort. Sci., 141(3), 256-263. doi:10.21273/JASHS.141.3.256

Unamba, C. I., Nag, A., & Sharma, R. K. (2015). Next Generation Sequencing Technologies: The Doorway to the Unexplored Genomics of Non-Model Plants. Front Plant Sci, 6, 1074. doi:10.3389/fpls.2015.01074

Voinnet, O. (2009). Origin, biogenesis, and activity of plant microRNAs. Cell, 136(4), 669-687. doi:10.1016/j.cell.2009.01.046

Wang, C., Ying, S., Huang, H., Li, K., Wu, P., & Shou, H. (2009). Involvement of OsSPX1 in phosphate homeostasis in rice. Plant J, 57(5), 895-904. doi:10.1111/j.1365-313X.2008.03734.x

Wang, C. Y., Zhang, S., Yu, Y., Luo, Y. C., Liu, Q., Ju, C., Zhang, Y. C., Qu, L. H., Lucas, W. J., Wang, X., & Chen, Y. Q. (2014). MiR397b regulates both lignin content and seed number in Arabidopsis via modulating a laccase involved in lignin biosynthesis. Plant Biotechnol J, 12(8), 1132-1142. doi:10.1111/pbi.12222

Wang, M., Guo, W., Li, J., Pan, X., Pan, L., Zhao, J., Zhang, Y., Cai, S., Huang, X., & Liu, Q. (2021). The miR528- AO Module Confers Enhanced Salt Tolerance in Rice by Modulating the Ascorbic Acid and Abscisic Acid Metabolism and ROS Scavenging. J Agric Food Chem, 69(31), 8634-8648. doi:10.1021/acs.jafc.1c01096

Yang, Y., Guo, Z., Liu, Q., Tang, J., Huang, S., Dhankher, O. P., & Yuan, H. (2018). Growth, physiological adaptation, and NHX gene expression analysis of *Iris halophila* under salt stress. Environ Sci Pollut Res Int, 25(25), 25207-25216. doi:10.1007/s11356-018-2593-y

Yuan, S., Li, Z., Li, D., Yuan, N., Hu, Q., & Luo, H. (2015). Constitutive Expression of Rice MicroRNA528 Alters Plant Development and Enhances Tolerance to Salinity Stress and Nitrogen Starvation in Creeping Bentgrass. Plant Physiol, 169(1), 576-593. doi:10.1104/pp.15.00899

Yuan, S., Zhao, J., Li, Z., Hu, Q., Yuan, N., Zhou, M., Xia, X., Noorai, R., Saski, C., Li, S., & Luo, H. (2019). MicroRNA396-mediated alteration in plant development and salinity stress response in creeping bentgrass. Hortic Res, 6, 48. doi:10.1038/s41438-019-0130-x

Zeeshan, M., Qiu, C. W., Naz, S., Cao, F., & Wu, F. (2021). Genome-Wide Discovery of miRNAs with Differential Expression Patterns in Responses to Salinity in the Two Contrasting Wheat Cultivars. Int J Mol Sci, 22(22). doi:10.3390/ijms222212556

Zeng, X., Sheng, J., Zhu, F., Wei, T., Zhao, L., Hu, X., Zheng, X., Zhou, F., Hu, Z., Diao, Y., & Jin, S. (2020). Genetic, transcriptional, and regulatory landscape of monolignol biosynthesis pathway in *Miscanthus × giganteus*. Biotechnol Biofuels, 13, 179. doi:10.1186/s13068-020-01819-4

Zeng, Y., Zhao, S., Yang, S., & Ding, S. Y. (2014). Lignin plays a negative role in the biochemical process for producing lignocellulosic biofuels. Curr Opin Biotechnol, 27, 38-45. doi:10.1016/j.copbio.2013.09.008

Zhang, B., & Wang, Q. (2015). MicroRNA-based biotechnology for plant improvement. J Cell Physiol, 230(1), 1-15. doi:10.1002/jcp.24685

Zhou, J., Lee, C., Zhong, R., & Ye, Z. H. (2009). MYB58 and MYB63 are transcriptional activators of the lignin biosynthetic pathway during secondary cell wall formation in Arabidopsis. Plant Cell, 21(1), 248-266. doi:10.1105/tpc.108.063321

Zhu, J. K. (2000). Genetic analysis of plant salt tolerance using Arabidopsis. Plant Physiol, 124(3), 941-948. doi:10.1104/pp.124.3.941

Zhu, J. K. (2002). Salt and drought stress signal transduction in plants. Annu Rev Plant Biol, 53, 247-273. doi:10.1146/annurev.arplant.53.091401.143329

Zhu, J. K. (2016). Abiotic Stress Signaling and Responses in Plants. Cell, 167(2), 313-324. doi:10.1016/j.cell.2016.08.029

Cover image created with BioRender.com

1.   PROJECT BACKGROUND AND OBJECTIVES

Due to climate change and intensive agriculture, soils quality is fast degrading and the selection of stress tolerant second generation bioenergetic crops, able to growth on marginal lands avoiding competition with food/feed crops, is becoming no longer postponable.

Thanks to its low agronomics input needs and its high rate of CO_2 assimilation, *Arundo donax* L. is a promising bioenergetic crop and it is to preferred to other ones, such as sugarcane, corn, sorghum or poplar.

However, bioenergy production from arundo, as well as from others bioenergy crops, is limited by the problem of the recalcitrance, defined as the resistance to enzymatic degradation of lignocellulosic biomass into fermentable sugars.

The amount of lignocellulosic biomass is linked to the lignin deposition and is reported in the literature to be related to stress responses. Therefore, investigating what happen in arundo under stress conditions mimicking the situation of marginal lands is useful to clarify the mechanisms used by this plant to face stresses with the final aim of improving the quality and quantity of biomass and, consequently, biofuel production.

This work aims to use an omics approach to investigate the molecular responses of *A. donax* to salt and phosphorus excess and fits into a larger project dedicated to study how arundo faces stresses, both biotic and abiotic, in order to identify mechanisms of resistance and adaptation to promote plant health in agriculture and forestry.

The project called "CROPSTRESS – System performance of non-food crops to drought stress: development of a plant ideotype", was founded by the SIR2014 program of the Italian Ministry of University and Research (RBSI14VV35), and was mainly developed at the Institute for Sustainable Plant Protection (IPSP), part of the National Research Council (CNR) of Italy. Its objective was to gain information on bioenergetics crop *A. donax* grown under abiotic constraints, such as drought and salinity, in order to address innovative mitigation strategies in the agricultural sector. Biochemical, physiological, molecular mechanisms and proteomics would have been explored during the three-year project.

Within the framework of the CROPSTRESS project, *A. donax* plants were grown in controlled conditions and supplied with five different nutrient solutions:

1) Hoagland solution (Control, C);

2) Hoagland solution deprived of phosphorus (no phosphorus supply, -P);

3) Hoagland solution complemented with 8.0 mM KH_2PO_4 (excess of phosphorus, +P);

4) Hoagland solution complemented with 200 mM NaCl (excess of salt, +Na);

5) Hoagland solution complemented with both 200 mM NaCl and 8.0 mM KH_2PO_4 (excess of phosphorus and salt, +NaP).

Plant phenotyping, quantification of metabolites and ultrastructural imaging of leaves were conducted at different time points (after 9, 21 and 43 days of treatments, and after 1 month of wash out). Transcriptomics data were obtained from samples at the end of treatments (i.e., 43 days) (Fig. 5).
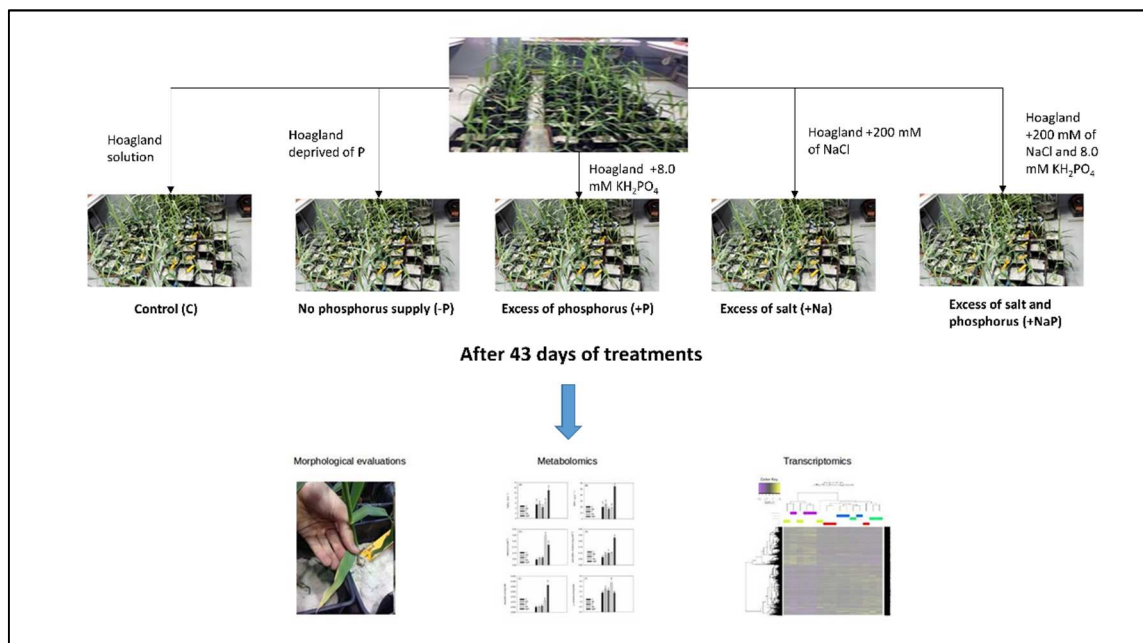

Fig. 5: CROPSTRESS project design.

My PhD project started from leaf samples collected during the CROPSTRESS project at the end of treatments (+P, +Na and +NaP samples, specifically) and aimed to:

- investigate the lignin pathway at transcriptional level, in order to expand our knowledge about lignin biosynthesis in *A. donax* with the final aim of enhancing cellulose accessibility and improving biomass yield;

- study the transcriptional and post-transcriptional plant responses to salt stress and/or eutrophication, mimicking real conditions of marginal lands;

- study the relationship between lignin production and salt stress and/or eutrophication responses.

-P treatment was left from the analysis because the PhD project focused on salt stress and/or eutrophication.

A combination of different next generation sequencing approaches were used:

- *RNA-seq*, to study the transcriptional response to stresses;
- *smallRNA-seq,* to identify microRNAs (miRNAs) and study their expression during stresses;
- *Deg-seq*, to identify target transcripts of miRNAs.

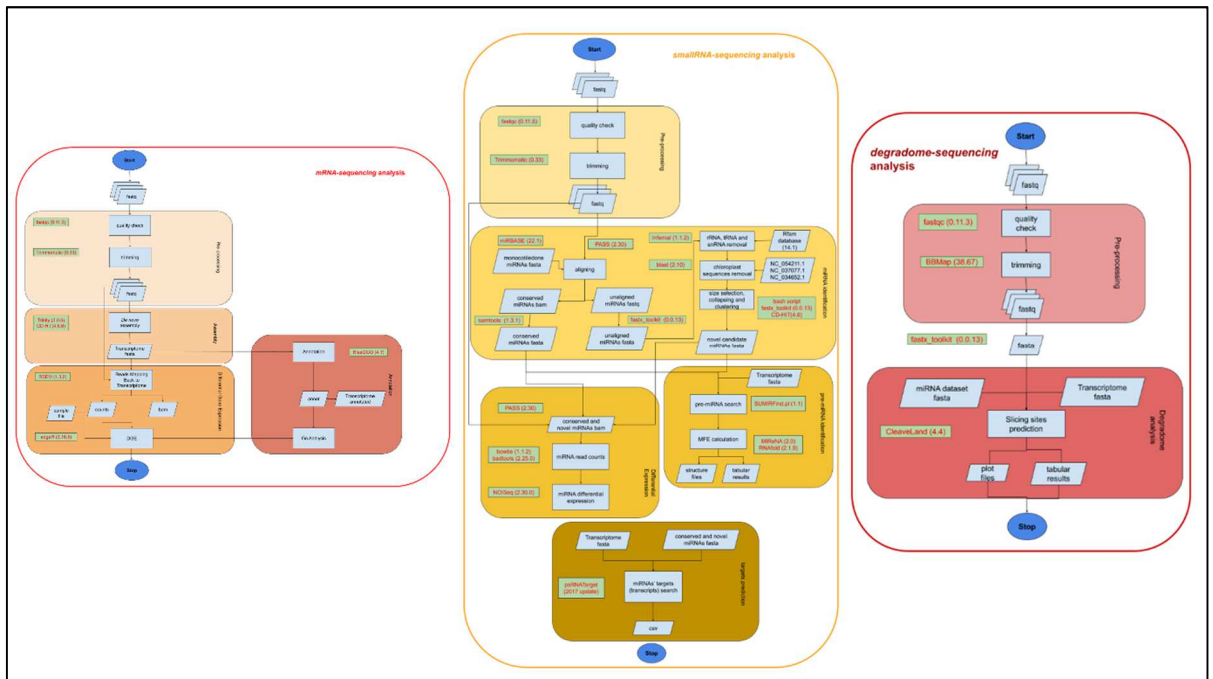Bioinformatics pipelines for sequencing data analysis are summarized in fig. 6.

Fig 6: Pipelines developed for bioinformatics analysis of sequencing data.

Below, the three papers reporting the results obtained during the PhD program:

I. **Impact of high or low levels of phosphorus and high sodium in soils on productivity and stress tolerance of *Arundo donax* plants**
Claudia Cocozza, Federico Brilli, Laura Miozzi, Sara Pignattelli, Silvia Rotunno, Cecilia Brunetti, Cristiana Giordano, Susanna Pollastri, Mauro Centritto, Gian Paolo Accotto, Roberto Tognetti, Francesco Loreto.
(2019). Plant Science, 289:110260.
https://doi.org/10.1016/j.plantsci.2019.110260

II. **Identification of abiotic stress responsive microRNAs and their targets in the bioenergy crop *Arundo donax L.* by using high-throughput sequencing**
Silvia Rotunno, Claudia Cocozza, Vitantonio Pantaleo, Paola Leonetti, Loris Bertoldi, Giorgio Valle, Gian Paolo Accotto, Francesco Loreto, Gabriella Stefania Scippa, Laura Miozzi.
In preparation

III. **Modulation of class III peroxidase pathways and phenylpropanoids in *Arundo donax* under salt and phosphorus stress**
Claudia Cocozza, Paola Bartolini, Cecilia Brunetti, Laura Miozzi, Sara Pignattelli, Alessandra Podda, Gabriella Stefania Scippa, Dalila Trupiano, Silvia Rotunno, Federico Brilli, Bianca Elena Maserti.
In preparation

PAPER I

Impact of high or low levels of phosphorus and high sodium in soils on productivity and stress tolerance of Arundo donax plants

Claudia Cocozza, Federico Brilli, Laura Miozzi, Sara Pignattelli, Silvia Rotunno, Cecilia Brunetti, Cristiana Giordano, Susanna Pollastri, Mauro Centritto, Gian Paolo Accotto, Roberto Tognetti, Francesco Loreto

ABSTRACT

The potential of *Arundo donax* to grow in degraded soils, characterized by excess of salinity (Na+), and phosphorus deficiency (-P) or excess (+P) also coupled with salinity (+NaP), was investigated by combining in vivo plant phenotyping, quantification of metabolites and ultrastructural imaging of leaves with a transcriptome-wide screening. Photosynthesis and growth were impaired by +Na, -P and +NaP. While +Na caused stomatal closure, enhanced biosynthesis of carotenoids, sucrose and isoprene and impaired anatomy of cell walls, +P negatively affected starch production and isoprene emission, and damaged chloroplasts. Finally, +NaP largely inhibited photosynthesis due to stomatal limitations, increased sugar content, induced/repressed a number of genes 10 time higher with respect to +P and +Na, and caused appearance of numerous and large plastoglobules and starch granules in chloroplasts. Our results show that *A. donax* is sensitive to unbalances of soil ion content, despite activation of defensive mechanisms that enhance plant resilience, growth and biomass production of *A. donax* under these conditions

Impact of high or low levels of phosphorus and high sodium in soils on productivity and stress tolerance of *Arundo donax* plants

Claudia Cocozza[a,b,*,1], Federico Brilli[a,1], Laura Miozzi[c], Sara Pignattelli[a], Silvia Rotunno[c,d], Cecilia Brunetti[e], Cristiana Giordano[e], Susanna Pollastri[a], Mauro Centritto[a], Gian Paolo Accotto[c], Roberto Tognetti[f,g], Francesco Loreto[h,i]

[a] *National Research Council of Italy, Institute for the Sustainable Plant Protection (CNR - IPSP), Via Madonna del Piano 10, 50019 Sesto Fiorentino, Italy*
[b] *Department of Agriculture, Food, Environment and Forestry, Via San Bonaventura 13, 50145 Florence, Italy*
[c] *National Research Council of Italy, Institute for the Sustainable Plant Protection (CNR - IPSP), Strada delle Cacce 73, 10135 Torino, Italy*
[d] *Department of Biosciences and Territory, University of Molise, contrada Fonte Lappone, 86090 Pesche, Italy*
[e] *National Research Council of Italy, Institute for BioEconomy (IBE), Via Madonna del Piano 10, 50019 Sesto Fiorentino, Italy*
[f] *Department of Agriculture, Environment and Food Sciences, University of Molise, Via Francesco De Sanctis, 86100 Campobasso, Italy*
[g] *The EFI Project Centre on Mountain Forests (MOUNTFOR), Edmund Mach Foundation, 38010 San Michele all'Adige, Italy*
[h] *National Research Council of Italy, Department of Biology, Agriculture, and Food Sciences, Piazzale Aldo Moro 7, Roma, Italy*
[i] *Department of Biology, University of Naples Federico II, Via Cinthia, 80126 Napoli, Italy*

ARTICLE INFO

ABSTRACT

The potential of *Arundo donax* to grow in degraded soils, characterized by excess of salinity (Na+), and phosphorus deficiency (-P) or excess (+P) also coupled with salinity (+NaP), was investigated by combining in vivo plant phenotyping, quantification of metabolites and ultrastructural imaging of leaves with a transcriptome-wide screening. Photosynthesis and growth were impaired by +Na, -P and +NaP. While +Na caused stomatal closure, enhanced biosynthesis of carotenoids, sucrose and isoprene and impaired anatomy of cell walls, +P negatively affected starch production and isoprene emission, and damaged chloroplasts. Finally, +NaP largely inhibited photosynthesis due to stomatal limitations, increased sugar content, induced/repressed a number of genes 10 time higher with respect to +P and +Na, and caused appearance of numerous and large plastoglobules and starch granules in chloroplasts. Our results show that *A. donax* is sensitive to unbalances of soil ion content, despite activation of defensive mechanisms that enhance plant resilience, growth and biomass production of *A. donax* under these conditions.

1. Introduction

Giant reed, *Arundo donax* L., is a non-food perennial rhizomatous invasive grass species that belongs to the family *Poaceae* [1], able to colonize a wide spectrum of habitats, from very wet loam to relatively dry sandy soils [2]. *A. donax* is a C3 plant displaying an unusually high photosynthetic rate and a fast-growing habit that make its cultivation suitable for biomass and bioenergy production [3,4]. Tolerance of this plant to abiotic stress has been demonstrated across a range of stressful conditions, thus allowing this plant to survive in degraded and marginal lands [5,6]. *A. donax* is able to maintain a high leaf-level photosynthesis and biomass gain under drought [7,83] and withstand salinity [6]. In particular, efficient stomatal regulation in *A. donax* is induced by

increased foliar ABA content in response to drought [8]. Moreover, *A. donax* is able to adjust the size of xylem vessels to regulate vulnerability to embolism under drought conditions [9]. Recently, it has been found that symbiosis with arbuscular mycorrhiza can increase the performance of *A. donax* under saline conditions [10]. *A. donax* leaves constitutively produce a large amount of isoprene [11], which can act as an antioxidant [12] and makes chloroplast membrane resistant to stresses [10,13], thus protecting plants against the occurrence of abiotic stresses [14]. However, there is no clear pattern in isoprene emission in response to abiotic stress in grasses, such as *Arundo* and *Phragmites*, because isoprene emission increased in *A. donax* following drought [7], decreased in *Phragmites australis* (the common reed, and a close relative of *A. donax*) plants exposed to high P concentrations [15], and was

---

* Corresponding author at: University of Florence, Department of Agricultural and Forest Economics, Engineering, Sciences and Technologies, Via San Bonaventura 13, 50145 Florence, Italy.
E-mail address: claudia.cocozza@unifi.it (C. Cocozza).
[1] Authors contributed equally to this work.

unaltered in salt-stressed *A. donax* [10].

Phosphorus (P) is an essential element for many key enzymes and intermediate metabolites of photosynthesis, sugar metabolism [16] and regulates energy storage reactions and maintains the structural integrity of cellular membranes [17], and unbalanced P availability can seriously impair plant physiological processes and structure [18]. On one hand, P deficiency modifies carbohydrate metabolism by reducing the levels of organic acids available for the tricarboxylic acid cycle [19] that further limits P consumption, thus hampering plants growth and the ability to reproduce and adapt to different environments [20]. On the other hand, P surplus impairs plant performances being negatively correlated to biosynthesis of starch [21] and other secondary metabolites (e.g. isoprenoids [22,23],), and lowers nitrate assimilation in the roots [24].

Intensive exploitation of rock phosphates reserves for fertilization purposes may lead to their depletion by the end of this century [25]. Analysis of plant responses to growth under P deficient conditions and identification of species/varieties capable of maintaining productivity with low P requirements is therefore crucial to food and bioenergy security. In contrast, marginal lands, where high amounts of P are associated with salinity, are not suitable for agriculture. It is well-known that salinity impairs plant performance and productivity [26]. In particular, exposure to high sodium (Na^+) contents in soil increases diffusive [27] and biochemical limitations to photosynthetic CO_2 assimilation [28], decreases transpiration rates, modifies the biosynthesis of both soluble sugars [29] and starch [30], and reduces the content of pigments in leaves [31]. Moreover, excess of Na^+ impairs root nutrient uptake by altering the trans-membrane transport of ions leading to a loss of turgor of plant cells and to further membrane damage following the formation of reactive oxygen species (ROS) [32].

In this study, *A. donax* plants were grown under controlled conditions by providing a nutrient solution deprived of P, or enriched with a high concentration of P in combination with high concentrations of sodium chloride (NaCl). Our investigation aimed to: a) characterise the response of *A. donax* plants to P availability, both under P-deficiency and high P concentration; b) test the performance of *A. donax* under a simultaneous excess of P and Na^+. To this end, we used an integrated approach, by combining physiological and biochemical measurements with transcriptomic analysis. Leaf and root transcriptomes of *A. donax* have been recently explored only in plants that did not undergo any stressful treatment [33] and in plants exposed to water stress [34,35]. Understanding the response of *A. donax* at the molecular level to combined P and Na^+ stress is crucial for implementing adaptation strategies to achieve high biomass yield and productivity in marginal areas for agriculture.

2. Materials and methods

2.1. Plant material, growth conditions, supply of P and Na+

A. donax plants were propagated from rhizomes of plants collected from Sesto Fiorentino (43°81′75″ N, 11°18′88″ E) (Italy). Rhizomes were kept in tap water for one day and then planted in $6\,dm^3$ pots containing quartz sand. All potted plants were then grown in a climatic chamber under controlled environmental conditions (temperature ranging between 24 °C and 26 °C; relative air humidity ranging between 40% and 60%; photosynthetic photon flux density (PPFD) of $700\,\mu mol\,m^{-2}\,s^{-1}$ for 14 h per day (from 06:00 AM to 08:00 PM). All plants were regularly watered twice a week with half strength Hoagland solution [36] for two months before the beginning of the experiment.

The experiment was performed by applying five different nutrient conditions: 1) Hoagland solution (C); 2) Hoagland solution deprived of phosphorus (-P); 3) Hoagland solution complemented with 8.0 mM KH_2PO_4 (+P); 4) Hoagland solution complemented with 200 mM NaCl (+Na); and 5) Hoagland solution complemented with both 200 mM NaCl and 8.0 mM KH_2PO_4 (+NaP). All different solutions were supplied twice a week throughout the experiment (43 days).

2.2. Biometrical traits, leaf determination of C, N, P and Na+

Biometrical traits were measured at 9, 21 and 43 days of treatment (DOT), by counting the number of leaves and by measuring the length of culms. The relative leaf water content (RLWC) of leaves was determined by weight measurements on the second fully expanded leaf at the end of the treatment. Fresh weight (FW) was immediately determined following leaf collection. The same leaf was then immersed into water for 24 h before measuring the turgid weight (TW). Finally, the leaf was oven dried at 80 °C for 48 h before measuring the dry weight (DW). RLWC was calculated according to [37] by using the formula:

RLWC = (FW – DW) / (TW – DW).

Total C and total N concentrations (%) in 1 g of leaves were quantified at the end of the treatment with a Carlo Erba NA 1500 CNS Analyzer (Milan, Italy) through a chromatographic column and a thermal conductivity detector [38].

The concentrations of Na^+ and P ($\mu g\,g^{-1}$ DW) were determined in 1 g of leaves at the end of the treatment. Na^+ concentration was measured by flame atomic absorption spectrometry (Analyst 200, Perkin Elmer), and P concentration was measured by inductively coupled plasma atomic emission spectrometry (ICP-AES; iCAP 6500 Duo; ThermoFisher, Dreieich, Germany), employing appropriate quality standard controls [39].

2.3. CO₂/H₂O gas exchange, chlorophyll fluorescence and isoprene measurements

Gas exchange of both CO_2 and H_2O coupled with chlorophyll fluorescence measurements were performed in treated and control plants at the end of the experiment for two consecutive days, between 10:00 and 14:00, by using a portable gas exchange system equipped with a fluorometer (Li-Cor 6400, Li-Cor Biosciences Inc., NE, USA). The third fully expanded leaf (collected from the culm apex of *A. donax* plants) was clamped in the $2\,cm^2$ Li-Cor cuvette and exposed to a saturating PPFD of $1000\,\mu mol\,m^{-2}\,s^{-1}$, CO_2 concentration of 400 ppm, temperature of 30 °C and relative humidity (RH) ranging between 45 and 50%. Photosynthesis (A), stomatal conductance (g_s) and internal CO_2 concentration (Ci) were calculated according to [40] 10 min after reaching steady-state conditions. The linear electron transport rate (ETR) was calculated from chlorophyll fluorescence measurements of PSII efficiency, according to [41].

Maximum photosynthesis under low O_2 conditions was measured by reducing the concentration of O_2 in the air entering the Li-Cor 6400 from 21% to 2%. We used a nitrogen cylinder connected to a mass flow controller (Rivoira, Italy) that precisely enriched the concentration of N_2 in the air entering the Li-Cor 6400 from 89 to 98%, while CO_2 concentration was maintained at 400 ppm. After collecting the gas exchange measurements under 2% O_2, the concentration of O_2 in the air was restored to 21% and A and g_s were again measured.

The O_2 inhibition of A was calculated from values measured at 21% and at 2% of O_2 (v/v) using the following formula [42]:

$$O_2 \text{ inhibition of photosynthesis} = (A_{2\%\ O2} - A_{21\%\ O2}) * 100 / A_{2\%\ O2}.$$

Isoprene emitted by leaves was collected following CO_2 and H_2O and chlorophyll fluorescence measurements by using the same Li-Cor 6400 system. For each sample, 3 L of the air coming out of the cuvette were diverted in a cartridge filled with 30 mg of Tenax and 30 mg of Carboxen (Gerstel, Mülheim an der Ruhr, Germany) with a precision pump (Elite 5; A.P. Buck, Orlando, FL, USA) set at a flow rate of 200 mL min^{-1} [7]. All cartridges were stored at 4 °C before analysis. Isoprene

2

trapped in the cartridges was quantified through thermo-desorption followed by gas chromatography-electro impact mass spectrometry (7890 GC – 5975 MSD 8 Agilent Tech, Santa Clara, CA, USA). The GC–MS column (J&W Innovax, 50 m, 0.20 mm i.d., 0.4 μm d.f.) was held at 40 °C for 1 min, and then the oven temperature was sequentially increased by $10\,°C\,min^{-1}$ until 130 °C, by $5\,°C\,min^{-1}$ until 210 °C, and finally by $20\,°C\,min^{-1}$ until 260 °C, temperature at which the column was held for 3 min. The mass spectrometer was operated with an electron ionization of 70 eV, in scan mode. Isoprene was identified by using the NIST 11.L 08 library spectral database, and quantified with an isoprene gas standard (99.9%, Sigma-Aldrich) prepared in the laboratory as reported in [10].

During gas exchange measurements and isoprene collection, a charcoal filter (Supelco, Bellafonte, USA) was placed ahead of the Li-Cor 6400 to remove all volatile organic compounds (including isoprene) before reaching the gas exchange cuvette. The filter did not affect CO_2 and H_2O concentrations [43]. The background level of isoprene was measured every day before starting the measurements by collecting 3 L of the air exiting the empty cuvette.

2.4. RNA sequencing

At the end of the treatment, the third fully expanded leaf was collected during the day between 10:00 and 12:00 for RNA extraction and stored at -80 °C. RNA extraction was performed using TRIzol® Reagent (Ambion). The concentration and quality of RNA was determined with a NanoDrop spectrophotometer (Thermo Scientific, Wilmington, USA) and Agilent 2100 Bioanalyzer (Agilent, Santa Clara, CA). According to RNA quality and quantity, three out of four samples for each treatment were selected for RNA sequencing and sent to the HuGeF sequencing service (http://www.hugef-torino.org, Human Genetics Foundation, Turin, Italy). A total of 15 paired-end libraries (2 × 75bp) were constructed using the TruSeq RNA library Prep Kit v2 (Illumina, San Diego, CA) with poly-A enrichment and sequenced on Illumina NextSeq 500. Raw data have been deposited in the Sequence Read Archive (https://www.ncbi.nlm.nih.gov/sra) with SRA accession SRP145569. Assessment of read quality metrics was carried out with FastQC software (http://www.bioinformatics.babraham.ac.uk/projects/fastqc/ version 0.11.3). Quality filtering, adapter cutting and trimming were carried out using Trimmomatic (version 0.33) [44], which can handle fastq paired-end synchronization. After Illumina adapters clipping, the first 12 bases were trimmed due to sequencing biases [45], leading and trailing low quality (below 3) or N bases and reads with low average quality (15) in a 4-bases scan were removed. Finally, reads less than 36 bases long after these steps were dropped.

Trinity software (version 2.0.6) was used for transcript reconstruction. Contigs less than 200 bp and with coverage less than 5 were discarded [46]. Transcript redundancy was reduced with CD-HIT software (version 4.6.6), using a word size of 10 and 95% identity [47]. Trinity software was able to assemble a total of 184,849 transcripts (Table S1). After removing redundancy, we obtained a total of 120,553 transcripts. The quality of our reconstructed transcriptome was tested mapping each paired-end library against it. The percentage of reads mapping back to transcriptome (RMBT) were between 78.66% and 89.87%, perfectly concordant with the expected percentage for RNA-seq experiments. In fact, because of the lack of a reference genome, the percentage of multimapping appears greater then single mapping (Table S2). Based on these results, the assembled transcriptome was considered to be reliable as reference for differential expression analysis.

2.5. Identification of differentially expressed genes (DEGs), functional annotation and enrichment analysis

Reads from each of the 15 libraries were mapped against our reference transcriptome and quantified using RSEM (version 1.3.0) [48].

The quantification was obtained as fragments per kb of the exon per million fragments mapped (FPKM). To identify the differentially expressed genes, Trinity scripts based on the R package edgeR (R version 3.3.2; edgeR version 3.16.5) were used. Pairwise comparisons were made to highlight the differential expression in different conditions. Genes with a false discovery rate cut off of 0.05 (5% FDR) were considered as differentially expressed.

To annotate the genes, blastx searches were performed against NCBI non-redundant database with an e-value cut-off of $1e^{-3}$. Blastx results, saved as xml files, were loaded into Blast2GO tool (version 4.1; database Germany, DE3, version b2g_jan17) [49], and mapping, annotation and InterPro scanning were performed. To associate annotations obtained with Blast2GO to DEGs, the R package Annotation Tools (version 1.44.0) was used [50]. Gene ontology enrichment analysis of DEGs was performed on Blast2GO applying Fisher's Exact Test with a FDR of 0.05. Pathways enrichment analysis of DEGs was carried out with KOBAS tool (v3.0) [51] using *Oryza sativa* var. *japonica* as reference. Pathways were visualized with KEGG Mapper, a collection of tools for KEGG mapping [52].

2.6. Quantification of soluble carbohydrates and starch

The third fully expanded leaf was collected during the day between 10:00 and 12:00 at the end of the experiment for all biochemical measurements (i.e. soluble carbohydrates and starch, and hydrogen peroxide, glutathione, photosynthetic pigments, phenylpropanoid and ABA). Soluble carbohydrates were identified and quantified by HPLC-RI analysis following the protocol of [53]. In detail, 0.3 g of fresh leaf tissue was ground with liquid nitrogen and extracted 3 times with 5 mL of 75% ethanol. The solvent was dried under a vacuum and the resulting pellet was rinsed with 2 mL of ultrapure water. The aqueous extract was purified by solid-liquid extraction through −CH and -SAX pre-packed Bond-Elute cartridges (Varian, Harbor City, CA), and the eluate reduced until dry under a vacuum. Samples were rinsed with ultrapure water and injected in a series 250 LC binary pump equipped with an LC 30-RI detector (Perkin-Elmer). Soluble carbohydrates were separated on a 8 × 300 mm SC1011 column (Showa Denko, Tokyo, Japan) maintained at 88 ± 1 °C. Eluent was ultra-pure water at a flow rate of $0.8\,mL\,min^{-1}$ during a 22-min run. Individual carbohydrates were identified by comparison of retention times with those of authentic standards (Sigma-Aldrich, Milano, Italy). Starch was quantified as reported in [54] on the pellet resulting from the ethanol extraction for the analysis of soluble carbohydrates. Digestion of starch was through an enzyme mixture consisting of 1000 U α-amylase and 5 U of amyloglucosidase. Glucose was quantified through peroxidase-glucose oxidase/o-dianisidine reagent (Sigma-Aldrich, Milano, Italy), reading the absorbance at 525 nm after the addition of sulfuric acid.

2.7. Determination of hydrogen peroxide and glutathione

Hydrogen peroxide (H_2O_2) was measured spectrophotometrically after reaction with potassium iodide (KI), following the modified method of [55]. A sample (0.25 g of fresh leaves) was homogenised with liquid nitrogen and then transferred into a 13 mL tube with 2 mL of 0.1% trichloroacetic acid (TCA); the extract was then centrifuged at 10,000 rpm for 10 min at 4 °C. The reaction consisted 0.5 ml 0.1% TCA leaf extract supernatant, 0.2 mL of 100 mM K-phosphate buffer pH 7.8 and 2 mL 1 M KI. The blank probe consisted of 0.1% TCA in the absence of the leaf extract. The reaction was developed for one hour in darkness and absorbance was measured at 390 nm. The amount of H_2O_2 was calculated using a standard curve prepared with known concentrations of hydrogen peroxide. The results were expressed as $\mu g\,g^{-1}$ leaf FW.

A modification of the method [56] was used for glutathione (GSH) determination. A sample (0.5 g of fresh leaves) was homogenised within liquid nitrogen and then transferred in a 13 mL tube with 1.5 mL of 5% trichloroacetic acid (TCA), the extract was then centrifuged at

3

12,000 rpm for 20 min; after that 0.5 mL of supernatant was mixed in the 13 mL tube with 1.5 mL of 0.2 M tris buffer, pH 8.2, and 0.1 mL of 0.01 M D'TNB [5, 5^l-dithiobis-(2-nitrobenzoic acid)] or Ellman's reagent, and then centrifuged at 3000 rpm for 15 min. The absorbance was read at 412 nm; a standard curve was made with glutathione. The results were expressed as µg g^{-1} leaf FW.

2.8. Analysis of photosynthetic pigments (β-carotene, zeaxanthin) and phenylpropanoid (caffeic acid)

Zeaxantin and β carotene were identified by comparison of their retention times and UV spectra with those of authentic standards. The compounds were quantified at 445 nm and calibrated using the calibration curve of zeaxanthin and β-carotene (from LGC standards, Sigma Aldrich, Italy).

Caffeic acid, a phenylpropanoid, was extracted and purified following the protocol of [53] with some modifications. In detail, 0.3 mg of fresh leaf material was ground with liquid nitrogen and extracted 3 times with 4 mL of 75% aqueous ethanol adjusted to pH 2.5 with formic acid. The supernatant was partitioned 3 times with 4 mL of n-hexane and then dried under a vacuum at 30 °C. The pellet was rinsed with 2 mL of CH$_3$OH/H$_2$O (8:2). Aliquots of 10 µL were injected into the Perkin Elmer liquid chromatography unit reported above. Phenylpropanoid was separated using a 250 x 4.6 mm Zorbax SB-C18 column (5 µm) operating at 30 °C. The eluent was H$_2$O (added with 0.5% formic acid, A) and CH$_3$CN (added with 0.1% formic acid, B). Caffeic acid was separated using a linear gradient solvent system, at a flow rate of 1 mL min^{-1}, during a 58-min run: 0–20 min from 5 to 15% B; 20–30 min at 15% B; 30–40 min from 15 to 25% of B; 40–48 min at 25% of B; 48–58 min from 25 to 100% of B. Caffeic acid was identified using retention times and UV-spectral characteristics of authentic standards (all from Extrasynthese, Lyon-Nord, Genay, France).

2.9. Determination of abscisic acid (ABA)

Abscisic acid (ABA) was extracted and quantified using the protocol of [57]. Briefly, 0.3 mg of fresh leaf material was ground with liquid nitrogen, extraction was performed 3 times with 1.5 mL of CH$_3$OH–H$_2$O (50/50 adjusted to pH 2.5 with HCOOH) for 30 min at 4 °C, and the supernatant was partitioned 3 times with 3 mL of n-hexane. The methanolic fraction was loaded onto Sep-Pak C18 cartridges (Waters, Milford, MA, USA) and then eluted with 1.2 mL of ethyl acetate. The eluate, dried under nitrogen, was rinsed with 500 µL of CH$_3$OH/H$_2$0 (8/2) acidified with formic acid. Aliquots of 3 µL were injected into a liquid chromatography–electrospray ionization (ESI) tandem mass spectrometry (MS-MS) device, consisting of a Shimadzu LCMS-8030 quadruple mass spectrometer detector equipped with an ESI source (all from Shimadzu, Kyoto, Japan), operating in negative ion mode. ABA, was separated using an Agilent Poroshell C18 column (3.0 × 100 mm, 2.7 µm), eluted with a linear gradient solvent, at a flow rate of 0.3 mL min^{-1}, from 95% H$_2$O (with 0.1% of HCOOH, solvent A) to 100% of CH$_3$CN–methanol (50/50, with 0.1% of HCOOH, solvent B) over a 30-

min run. Quantification was conducted in the multiple reaction mode (MRM).

2.10. Hydrogen peroxide (H₂O₂) localization and leaf ultrastructure by Transmission Electron Microscopy (TEM)

Hydrogen peroxide localization in the leaves was estimated cytochemically via determination of cerium perhydroxyde upon reaction of cerium chloride (CeCl$_3$) with endogenous H$_2$O$_2$, following the protocols of [58,59]. At the end of the treatment, portions of approximately 0.15 mm^2 were sampled in the center of the leaf blade and then infiltrated (under vacuum) with 5 mM CeCl$_3$ in 50 mM 3-(N-morpholino)-propane sulfonic acid (pH 7.2). The CeCl$_3$-treated and control leaf samples (without CeCl$_3$-staining) were then fixed in 2.5% of glutaraldehyde, in 0.2 M of phosphate buffer (pH 7.2) for 1 h, and washed then twice with the same buffer, prior to post-fixing with 2% of osmium tetroxide in phosphate buffer (pH 7.2). Leaves were dehydrated in a graded ethanol series (30, 40, 50, 70, 90 and 100%), and gradually embedded in Spurr Resin (Sigma Aldrich). Ultrathin sections were obtained on an LKB IV ultramicrotome, mounted on Formvar coated copper grids, stained with UranylessEm Stain (Electron Microscopy Science) and lead citrate, and examined using a Philips CM12 transmission electron microscope (Philips, Eindhoven, The Netherlands) operating at 80 kV.

2.11. Statistical analysis

Descriptive statistics (means, standard errors) were carried out for all measured parameters. In order to account for variability between samples, a pooled standard deviation was computed from three replicates for each treatment. Normality of the population distribution was tested using the Shapiro-Wilk test. The homogeneity of variances was performed with the Levene's test. Analysis of variance (ANOVA) was applied to test the effect of Na$^+$ and P supply in *A. donax* plants. An LSD post-hoc test was applied to assess significantly different means among treatments (P < 0.05 level). Post-hoc Tukey test was carried out to define differences among groups. All statistical analyses were carried out with OriginPro 8 program (OriginLab, Northampton, MA, USA).

3. Results

3.1. Plant biometrics, gas exchange, chlorophyll fluorescence measurements and isoprene emission

At the end of the experiment, P concentration doubled in + P leaves, but did not decrease significantly in –P leaves, in comparison to the control treatment (Table 1). In the leaves of + Na plants, sodium (Na$^+$) was two order of magnitude higher than in the control. When Na$^+$ and P were both provided in excess (+NaP), an increase of Na$^+$ and a slight reduction in the accumulation of P, in comparison to the leaves of + Na and + P plants, respectively, was observed.

Table 1

Plant biometrical traits (culm length and leaf number), relative water content (RLWC), carbon, nitrogen (N), sodium (Na) and phosphorus (P) content of leaves of *Arundo donax* plants in control conditions (C), without phosphorus supply (-P), with excess supply of phosphorus (+P) or sodium chloride (+Na), and with excess supply of both phosphorus and sodium chloride (+NaP). Data are means of 4 plants per treatment ± SE; different letters indicate statistical difference at P < 0.05 in the same column.

	culm length (cm)	leaf number (n)	RLWC (%)	carbon (%)	N (%)	Na (µg g^{-1} DW)	P (µg g^{-1} DW)
C	90.8 ± 2.0 [a]	16.0 ± 0.2 [ab]	89.6 ± 2.1 [a]	42.4 ± 0.3 [a]	3.4 ± 0.2 [a]	120.9 ± 23.1 [c]	2358.7 ± 168.4 [c]
-P	81.54 ± 2.9 [b]	15.2 ± 0.5 [b]	90.1 ± 0.6 [a]	42.4 ± 0.3 [a]	2.9 ± 0.2 [b]	103.5 ± 31.8 [c]	1766.7 ± 154.4 [c]
+P	91.3 ± 4.3 [a]	16.8 ± 0.5 [a]	91.5 ± 0.6 [a]	41.3 ± 0.6 [a]	3.7 ± 0.1 [a]	151.2 ± 16.3 [c]	5765.4 ± 403.2 [a]
+Na	62.6 ± 3.6 [c]	11.5 ± 0.3 [c]	83.0 ± 2.7 [b]	40.3 ± 0.5 [b]	3.8 ± 0.1 [a]	15098.3 ± 1128.1 [b]	2100.7 ± 109.0 [c]
+NaP	66.4 ± 2.5 [c]	10.7 ± 0.3 [c]	82.3 ± 1.1 [b]	39.5 ± 0.1 [b]	3.4 ± 0.1 [a]	17781.4 ± 1567.9 [a]	4501.3 ± 297.2 [b]

Table 2

Photosynthesis (A), O_2 inhibition of photosynthesis (%), stomatal conductance (g_s), internal CO_2 concentrations (Ci) electron transport rate (ETR), isoprene emission of *Arundo donax* plants in control (C) conditions, without phosphorus supply (-P), with excess supply of phosphorus (+P) or sodium chloride (+Na), and with excess supply of both phosphorus and sodium chloride (+NaP). Data are means of 4 plants per treatment ± SE; different letters indicate statistical difference at $P < 0.05$ in the same column.

	A (μmol m^{-2} s^{-1})	Inhibition of photosynthesis (%)	g_s (mol m^{-2} s^{-1})	Ci (ppm)	ETR	Isoprene (nmol m^{-2} s^{-1})
C	23.4 ± 1.1 [a]	29.9 ± 3.7 [b]	0.32 ± 0.03 [a]	239 ± 11 [a]	159 ± 5 [a]	17.9 ± 2.8 [a]
-P	18.2 ± 0.4 [b]	18.3 ± 2.8 [b]	0.24 ± 0.03 [a]	245 ± 16 [a]	140 ± 7 [a]	20.7 ± 4.4 [a]
+P	21.4 ± 1.2 [a]	26.2 ± 2.7 [b]	0.30 ± 0.05 [a]	250 ± 11 [a]	149 ± 6 [a]	12.0 ± 2.9 [b]
+Na	12.5 ± 2.0 [c]	48.3 ± 9.5 [a]	0.08 ± 0.03 [b]	167 ± 14 [b]	103 ± 19 [b]	25.9 ± 5.4 [a]
+NaP	4.0 ± 0.5 [d]	49.9 ± 12.2 [a]	0.03 ± 0.00 [c]	158 ± 21 [b]	71 ± 5 [b]	20.7 ± 3.3 [a]

Culm length, number of leaves, leaf RLWC, and leaf carbon content were reduced in plants growing under + Na with respect to the control; culm height, leaf number and nitrogen concentration were reduced by -P treatment (Table 1). However, in + NaP plants, culm length, number of leaves, RLWC and carbon content decreased to the same extent as in the + Na plants when compared to the control treatment (Table 1). When examining impacts of the treatments before end-point (Fig. S1), we observed that growth was statistically reduced 9 days after beginning the −P treatment, whereas the negative effect of both + Na and + NaP was dramatically observed only after 21 d. On the other hand, + P plants showed a statistically higher culm length already 9 days after beginning the treatment and a higher leaf number than control plants at the end of the treatment (Fig. S1).

Photosynthesis of *A. donax* decreased in −P, whereas it was similar to controls in + P plants (Table 2). Photosynthesis was also reduced in + Na plants with respect to control plants, and the effect was even stronger in + NaP plants. In both + Na and + NaP plants, the reduction of photosynthesis was associated with reduced gs, Ci, and ETR, when compared to control plants (Table 2).

Isoprene emission from *A. donax* leaves was not affected by -P treatment, but was reduced in + P plants, in comparison to control (Table 2). Isoprene emission was slightly, but not significantly, increased by the + Na and + NaP treatments (Table 2).

3.2. Analysis of differentially expressed genes (DEGs)

The −P treatment showed the lowest impact in term of number of DEGs, and mainly led to gene down-regulation. More DEGs were affected by the + P treatment, where a similar number of up- and down-regulated genes were found (Fig. 1, Table 3). A further increase in the number of DEGs was observed in + Na plants. Finally, the highest number of DEGs (10 time more than other treatments) was observed in + NaP plants (Fig. 1, Table 3). The complete list of DEGs is reported in Table S3.

As a first step to functionally inspect the changing DEGs and identify the associated major biological processes, the transcriptome of *A. donax* leaves was annotated according to Gene Ontology (GO) using the Blast2GO software. A total of 65,802 sequences, representing more than half of the transcripts were annotated to at least one GO term for a total of 313,942 GO terms (Fig. S2). The first top ten hit species found through the blastx search belonged to the *Poaceae* family (Fig. S3), confirming the reliability of the obtained GO annotations. As a second step in our functional characterization, a GO category enrichment analysis was performed with a p-value threshold of 0.05. The GO annotation has a tree configuration with three main branches: Biological Processes (BP), Cellular Component (CC) and Molecular Functions (MF). We focused on the BP branch, as this is usually considered the most informative in the GO category enrichment analysis. In −P treatment, no GO terms were significantly over-represented, while in + P treatment 7 GO terms were over-represented (Table S4), showing a general perturbation of primary metabolic processes (i.e. GO categories *carbohydrate metabolic process* and *generation of precursor metabolites and*
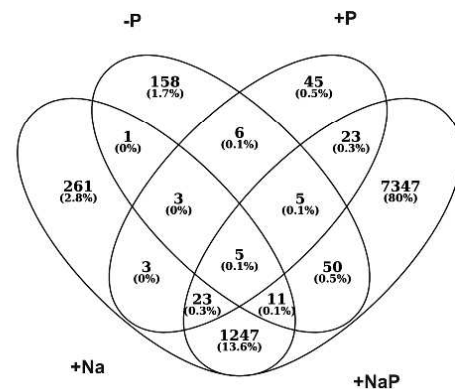

Fig. 1. Venn diagram of differentially expressed genes (FDR < 0.05) in *Arundo donax* plants without phosphorus supply (-P), with excess supply of phosphorus (+P) or sodium chloride (+Na), and with an excess supply of both phosphorus and sodium chloride (+NaP) with respect to control condition.

Table 3

Number of differentially expressed genes (DEGs) at 5% FDR; (-P) low phosphorus, (+P) excess of phosphorus, (+Na) excess of sodium chloride, (+NaP) excess of both phosphorus and sodium chloride, (C) control condition.

	-P vs C	+P vs C	+Na vs C	+NaP vs C
Up-regulated genes	75	258	243	2103
Down-regulated genes	234	198	453	3076
Total number of DEGs	**309**	**456**	**696**	**5179**

energy) as well as of transport and localization processes (i.e. GO categories *transport*, *localization* and *establishment of localization*). For the + Na treatment, 23 GO terms belonging to the BP branch were over-represented and indicated a general impact of the treatment on primary metabolism (i.e. GO categories *carbohydrate metabolic process*, *generation of precursor metabolites and energy*), transport and localization processes (i.e. GO categories *transport*, *localization*), secretory pathway (i.e. GO categories *vesicle targeting*, *rough ER to cis-Golgi*, *COPII vesicle coating*, *vesicle localization*, *vesicle coating*, *vesicle targeting*, *membrane budding*), and *cell death*. Finally, 74 GO terms in the BP branch were over-represented in the list of DEGs related to the + NaP treatment, confirming the stronger impact of this treatment. It is worth noticing that, in this particular case (+NaP), beside the GO categories related to primary metabolism (i.e. GO categories *carbohydrate metabolic process*, *generation of precursor metabolites and energy*, *peptide metabolic process*), *localization* and *transport*, other more focused terms such as those related to response to stress/stimuli (*response to biotic/abiotic stimulus*, *response to stress*, *cellular homeostasis*), growth and development (*cell*

5

Table 4

Carbohydrate and starch content of leaves of *Arundo donax* plants in control conditions (C), without phosphorus supply (-P), with excess supply of phosphorus (+P) or sodium chloride (+Na), and with an excess supply of both phosphorus and sodium chloride (+NaP). Data are means of 4 plants per treatment ± SE; different letters indicate statistical difference at P < 0.05 in the same column.

	sucrose (mg g^{-1} DW)	glucose (mg g^{-1} DW)	fructose (mg g^{-1} DW)	non-structural carbohydrates (mg g^{-1} DW)	starch (mg g^{-1} DW)
C	4.4 ± 0.4 [c]	14.9 ± 0.5 [b]	67.8 ± 2.9 [b]	87.0 ± 3.6 [b]	5.2 ± 0.2 [b]
-P	3.3 ± 0.2 [c]	11.6 ± 0.5 [b]	45.1 ± 0.9 [c]	60.0 ± 14.5 [c]	4.8 ± 0.4 [bc]
+P	4.2 ± 0.3 [c]	14.2 ± 0.9 [b]	73.0 ± 4.6 [b]	91.4 ± 4.2 [b]	1.8 ± 0.5 [c]
+Na	11.4 ± 0.3 [b]	15.0 ± 0.8 [b]	71.4 ± 1.7 [b]	97.8 ± 2.7 [b]	4.3 ± 0.3 [b]
+NaP	14.1 ± 0.6 [a]	37.3 ± 2.7 [a]	166.0 ± 10.6 [a]	217.4 ± 13.1 [a]	7.1 ± 0.2 [a]

differentiation, development process, cellular developmental process, anatomical structure development/morphogenesis, reproduction), *photosynthesis*, secondary metabolism (*amide biosynthetic process, cellular aromatic compound metabolic process, cellular nitrogen compound biosynthetic process, heterocycle metabolic process, macromolecule biosynthetic process, organic substance biosynthetic process, organonitrogen compound biosynthetic process*), cell communication (*signaling, cell communication*) and *cell death* were over-represented. A complete overview of all the over-represented functional categories is shown in Table S4.

3.3. Quantification of soluble carbohydrates and starch, photosynthetic pigments, abscisic acid (ABA), hydrogen peroxide (H₂O₂), glutathione (GSH) and caffeic acid derivative

Carbohydrate biosynthesis was impaired by both –P and + P. A reduction of starch content was found in + P leaves, while in –P leaves the content of sucrose, fructose and non-structural carbohydrates was reduced compared to control plants (Table 4). Consistently, DEG analysis showed a down-regulation of genes coding for ADP-glucose pyrophosphorylase, soluble acid invertases and a sucrose-phosphate synthase, involved in starch and sucrose metabolism pathway, in –P and + P plants (Fig. S4A, B). In contrast, in + Na leaves, the content of sucrose doubled as compared to control, and + NaP treatment further increased the sucrose content and enhanced two-fold the content of glucose, fructose, non-structural carbohydrates and starch, when compared to control plants (Table 4). DEG analysis also revealed an up-regulation of genes coding for enzymes involved in fructose and glucose synthesis in + NaP plants (Fig. S4D).

Hydrogen peroxide (H₂O₂) and glutathione (GSH) strongly accumulated in + NaP plants with respect to all other treatments (Fig. 2A, B). Consistent with these observations, genes involved in the glutathione metabolism were up-regulated to a greater extent in + NaP leaves than in + P leaves (Fig. S4I, Fig. S4H). In + Na and + NaP leaves, leaf ABA content increased two-fold with respect to control plants (Fig. 2C). In these plants, molecular analysis showed a down-regulation of the gene coding for the ABA 8-hydroxylase 3, a key enzyme in ABA catabolism (Table S3). Moreover, three ABA stress-ripening coding genes, involved in response to abiotic stress, were induced in + NaP plants (Table S3).

The content of caffeic acid derivatives was significantly enhanced in + NaP leaves, while the other treatments caused only a moderate increase of these secondary metabolites, with respect to control plants (Fig. 2D). The pathway for biosynthesis of flavonoids was significantly perturbed in + NaP plants. Genes coding for flavonol synthase, trans-cinnamate 4-monooxygenase, flavonoid 3′-monooxygenase and chalcone synthase were up-regulated in + NaP plants with respect to control plants (Fig. S4G). Zeaxanthin and β-carotene were enhanced in + Na leaves with respect to the controls, and zeaxanthin further increased in + NaP plants (Fig. 2E, F). There was no difference in the expression of genes involved in zeaxanthin and β-carotene synthesis in + Na and control leaves. However, a down-regulation of lycopene β-cyclase and phytoene synthase (the genes responsible for β-carotene synthesis) was measured in + NaP plants with respect to controls

(Table S3).

3.4. Transmission electron microscopy images of leaves ultrastructure

The ultrastructure of *A. donax* control leaves showed a peripheral location of organelles, and a large vacuole in the center of the cells (Fig. 3A). Cytoplasmic organelles (nucleus, mitochondria, vacuole, endoplasmic reticula, Golgi apparatus) showed typical structure and distribution, and chloroplasts portrayed distinct granal and stromal thylakoid arrangement and a well-defined stroma matrix where few and little starch granules were present (Fig. 3B).

In + P plants, chloroplasts displayed few small or no starch grains (Fig. 3C), confirming that starch did not accumulate in these leaves, as shown in Table 3. These cells also showed a greater number of larger plastoglobules than control plants (Fig. 3C). In addition, the envelope membrane of few + P chloroplasts appeared damaged, with the thylakoid membranes no longer recognizable (Fig. 3C). Some + P cells also had wavy plasma membranes, large peroxisomes (Fig. 3D), and electron dense cerium perhydroxide precipitates in the cell walls after treatment with CeCl₃, thus indicating the onset of ROS accumulation (Fig. 3C D). Chloroplasts of –P leaves were characterized by an extensive system of grana and stroma lamellae, that also contained a moderate number of plastoglobules (Fig. 3E). The nucleus of –P cells showed poorly condensed chromatin. Moreover, deposition of CeCl₃ was found in cell walls (Fig. 3F) and in bundle sheath cells.

In leaves of + Na plants, the shape of the cells changed from elliptical to wrinkle elongated, and cell walls appeared curled (indicated by white arrows in Fig. 4A). Strong accumulation of H₂O₂ in the cell wall (indicated by the black arrow in Fig. 4B) and large cytoplasmic lipid bodies (Fig. 4B) were detectable in some + Na cells. Moreover, some mesophyll cells were destroyed, and cytoplasmic organelles were no longer recognizable except for swollen or disintegrated chloroplasts (Fig. 4C). Chloroplasts of + Na cells that were still visible showed a wavy outline (indicated by the white arrow in Fig. 4B), significant loss of a clear stromal matrix, with swelling and curling thylakoids, and an increased number of plastoglobules (Fig. 4A, B). In addition, many peroxisomes with scarce electron dense deposits of CeCl₃ were observed (data not shown). Mesophyll cells of + NaP plants contained chloroplasts with numerous and large plastoglobules and very large starch granules (Fig. 4D), matching the reported increase of starch (Table 3) and carotenoid (i.e., zeaxanthin) content of these leaves (Fig. 2E). Large lipid bodies were also present in the cytoplasm of these cells, and CeCl₃ deposits were observed in chloroplasts, peroxisomes and mitochondria (Figs. 4E, F).

4. Discussion

4.1. Impact of high and low level of P on growth

Growth of *A. donax* plants was affected by manipulation of P in soil, highlighting negative effects induced by P starvation in both leaf production and culm elongation (Fig. S1). A two-fold increase of P in the leaves of *A. donax* approached toxic levels, as confirmed by early
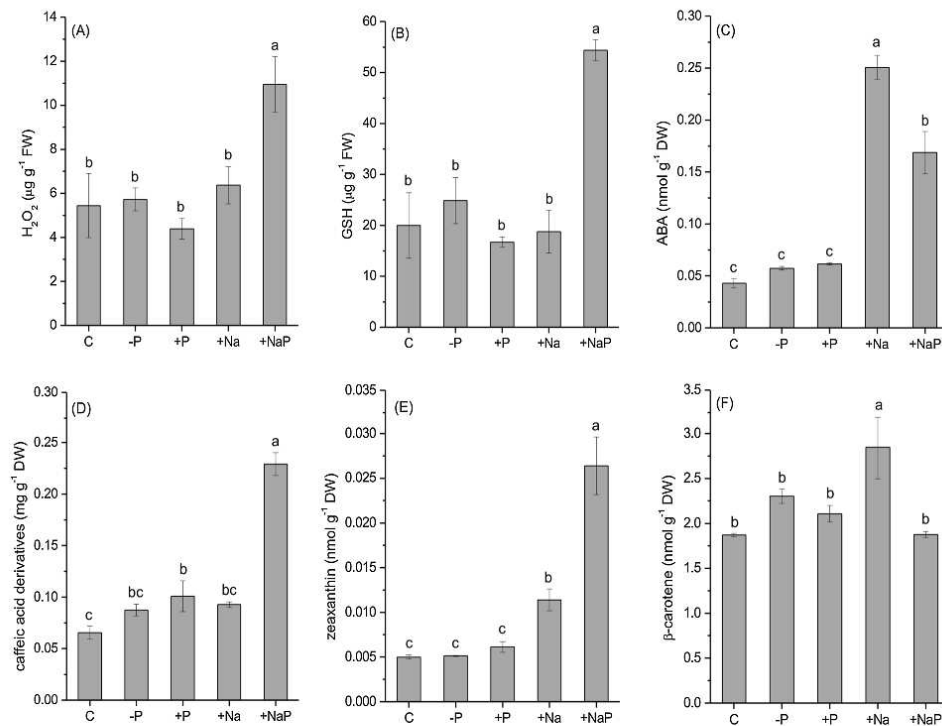
6

Fig. 2. Hydrogen peroxide (H_2O_2) (A), glutathione (GSH) (B), abscisic acid (ABA) (C), caffeic acid derivatives (D), zeaxanthin (E) and β-carotene (F) content of *A. donax* plants in control (C) conditions, without phosphorus supply (-P), with excess supply of phosphorus (+P) or of sodium chloride (+Na), and with an excess supply of both phosphorus and sodium chloride (+NaP). Data are means of 4 plants per treatment ± SE; different letters indicate statistical difference at $P < 0.05$.

symptoms of alteration of cell ultrastructure and the presence of peroxisomes (Fig. 4D), indicating initial stages of oxidation stress. However, high P concentrations did not hamper growth and photosynthesis of *A. donax* (Table 1 and 2). Tolerance of photosynthesis to + P treatment could be the result of the tight regulation of P homeostasis within the cytoplasm, due to the activation of mechanisms that transport and store the excess of P into the vacuoles [60]. However, excess P strongly decreased starch accumulation in leaves (Table 4), as confirmed by histological observations (Fig. 3C, D). Our transcriptomic results indicate that the limitation of starch metabolism in *A. donax* exposed to + P was mainly due to the transcriptional repression of ADP-glucose pyrophosphorylase, rather than to enhanced translocation of triosophosphates, eventually reducing the availability of substrates for starch synthesis in the chloroplasts [61,62]. Moreover, in + P plants there was a strong induction of few transcripts coding for cytosolic fructose-1,6-bisphosphatase, an enzyme that catalyzes the first irreversible reaction turning fructose-1,6-bisphosphate into fructose-6-phosphate and inorganic phosphate [63], and plays an important regulatory role in carbohydrates biosynthesis and metabolism [64].

Consistent with previous results [23] and a recent meta-analysis [22], leaves of + P plants emitted less isoprene than control and −P plants. Although isoprene production is a highly demanding ATP process [65], exposure to + P treatment may prompt a competition between mitochondrial respiration and the methylerythritol 4-phosphate (MEP) pathway, in turn limiting isoprene biosynthesis [66]. In particular, phosphoenolpyruvate (PEP) is a substrate for both isoprene biosynthesis and mitochondrial respiration. Mitochondrial respiration was likely increased in plants grown at high P concentration [23].

Indeed, we observed an increased transcription of genes involved in energy requiring processes associated with protein production and export (Fig. S4). Therefore, our results seem to indicate that incorporation of P into PEP, principally serving the respiratory metabolism, made it less available for isoprene production in + P leaves.

A. donax did not tolerate P starvation. Although P concentration in leaves did not significantly decrease after 43 days of −P treatment, numerous genes related to cell wall structure, chloroplast and membranes were down-regulated. This explains the alterations of cell ultrastructure occurring to the chloroplasts, system of grana, stroma lamellae (also reported by [67]) and plastoglobules [19,68], as observed in leaves of -P plants. In particular, the high sensitivity of transcriptomic analysis and ultrastructure imaging indicate that both genetic reprogramming and modifications of cell ultrastructure were induced in *A. donax* leaves following P starvation, ahead of a significant decrease in P content. In addition, despite *A. donax* rhizomes might have accumulated P during the pre-treatment period, this reserve was clearly insufficient to sustain physiological processes and growth during the long (43-days) period of our experimentation, also due to very low cation exchange capacity of the substrate (quartz sand) where P cannot accumulate. Indeed, results of this study showed that *A. donax* reduced photosynthesis (Table 2) and produced shorter culms and a lower number of leaves already 9 days since beginning of P starvation with respect to plants grown under normal P availability (Table S1). Lack of tolerance of *A. donax* to low P concentration in soil may affect the capacity to maintain functionality and growth, thus limiting the potential use of *A. donax* for biomass production in less fertile soils.
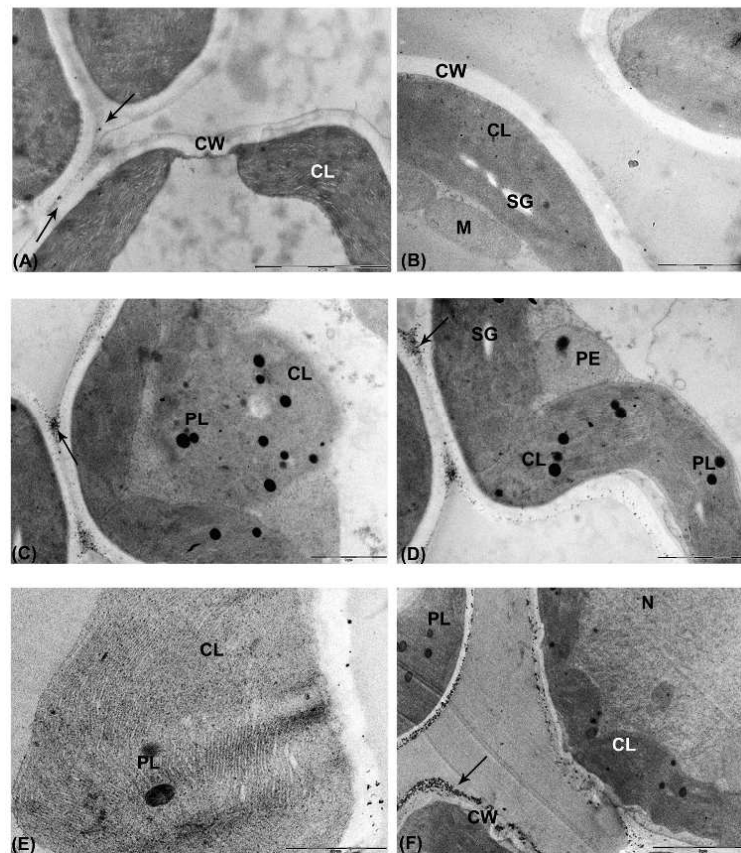
7

Fig. 3. Micrographs of leaf ultrastructure of *A. donax* in control conditions with CeCl₃ (A) and without CeCl₃ (B), with excess supply of phosphorus (C, D) and without phosphorus (E, F) supply. Legend: CL: chloroplast; CW: cell wall; L: lipid body; M: mitochondrion; N: nucleus; PE: peroxisome; PL: plastoglobule; SG: starch grain; V: vacuole. Black arrows refer to electron-dense deposits of CeCl₃, indicative of the presence of H_2O_2. A, B, C, D: bar 1 μm; E: bar 100 nm; F: bar 2 μm.

4.2. Arundo donax is sensitive to Na+ stress, and to the synergistic action of high Na+ and P

Accumulation of Na^+ in leaves affected g_s increasing, consequently, diffusive limitations to A (namely the acquisition of CO_2), as further shown by low values of Ci (Table 2). This response to + Na occurs widely across plant species [27,69]. The observed stomatal closure was likely triggered by increased synthesis of ABA upon salinity stress, as often reported [70,71]. In leaves of + Na *A. donax*, A and ETR were strongly reduced, whereas synthesis of zeaxanthin and β-carotene were enhanced. This suggests the onset of coordinated photochemical processes to counteract and reduce the accumulation of reactive oxygen species (ROS). Salinity stress also increased the biosynthesis of sucrose in *A. donax* leaves (Table 4), as confirmed by the significantly increased expression of genes of GO categories related to '*carbohydrate metabolic process*' (Table S4). Besides playing a signaling role [72], sucrose was likely able to balance the drop in osmotic potential as RLWC decreases during progressive exposure to salinity (Table 1). However, changes to the leaf ultrastructure of + Na plants, where some mesophyll cells and chloroplasts were completely destroyed (Fig. 4), confirmed that *A. donax* is moderately sensitive to high Na^+ concentration in leaves. Indeed, *A. donax* possesses more glycophytic than halophytic features [6]

and tolerates salinity through mechanisms that may prevent ROS formation despite accumulation of Na^+ in the leaves [26].

Salinity impaired photosynthesis but increased (although not significantly) isoprene emission from *A. donax* leaves. Isoprene is synthesized from carbon assimilated through photosynthesis [73], but its emission may be also sustained by extra-chloroplastic carbon sources when photosynthesis is limited under (abiotic) stress [74,75]. Overall, the simultaneous increases in the biosynthesis of isoprene and carotenoids may imply activation of the 2-C-methyl-D-erythritol 4-phosphate (MEP) pathway under salt stress [76]. Unfortunately, activation of antioxidants of the MEP pathway [14] is not maintained under + NaP stress, as discussed below.

An additive effect of the simultaneous exposure to high Na + and P concentrations (+ NaP) was clearly highlighted by a 10-fold increase in the number of both up- and down-regulated genes in leaves of these plants compared to controls. Some of the most representative transcription factors already identified in *A. donax* under drought [36] were also differentially regulated under Na^+ and P stress. Among them, one gene encoding for a NAC (No apical meristem, Arabidopsis transcription activation factor, Cupshaped cotyledon) transcription factor was strongly induced in + Na, +P and + NaP plants, whereas genes coding for WRKY 50, 53 and 41 were down-regulated only in + NaP plants
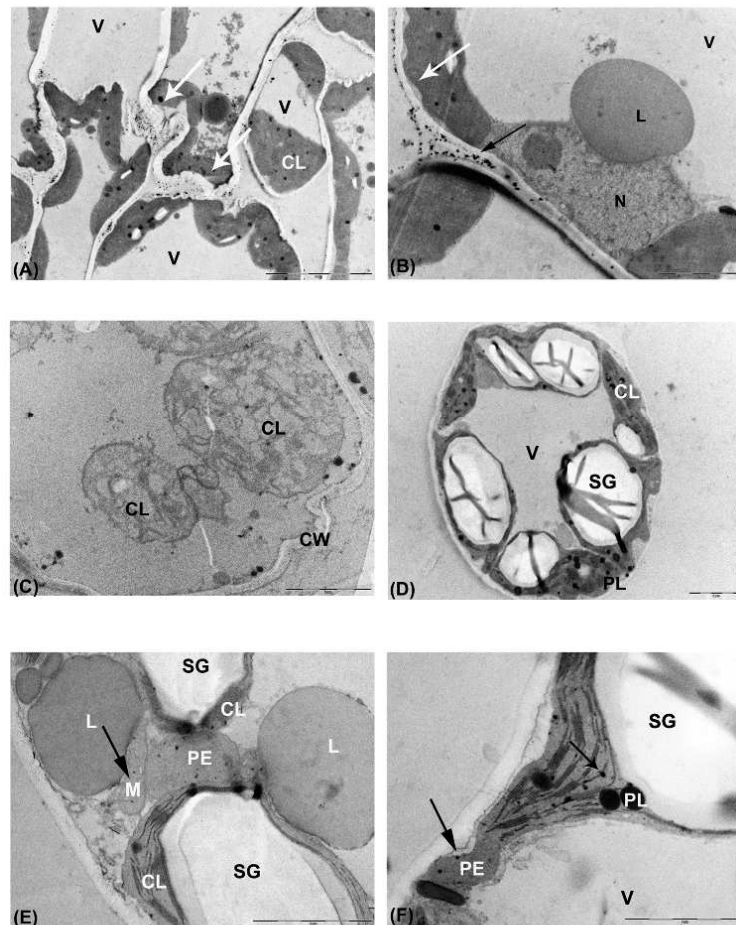
Fig. 4. Micrographs of leaf ultrastructure of *A. donax* plants supplied with an excess of sodium chloride (A, B, C), with both excess supply of phosphorus and sodium chloride (D, E, F). Legend: CL: chloroplast; CW: cell wall; L: lipid body; M: mitochondrion; N: nucleus; PE: peroxisome; PL: plastoglobule; SG: starch grain; V: vacuole. White arrows refer to wavy structure; black arrows refer to electron-dense deposits of CeCl$_3$, indicative of the presence of H$_2$O$_2$. A: bar 5 μm; B, C, D: bar 2 μm; E, F: bar 1 μm.

(Table S3). NAC and WRKY genes family are known to mediate water-[77] and Na$^+$ - stress responses, as well as the ABA-signaling pathway in plants [78]. Genes coding for stress-associated proteins (SAPs) are important regulators of tolerance to multiple abiotic stresses [79] and were found to be induced in water-stressed *A. donax* plants [35]. However, only two SAPs were down-regulated in + Na and + NaP plants (Table S3). Despite inducing a higher expression of genes involved in abiotic stress tolerance (e.g., NAC, WRKY and SAP genes), high P concentration exacerbated the reduction of A in Na$^+$-stressed *A. donax* plants, as also indicated by the over-expression of many genes of the GO category related to '*cellular metabolic process*' in + NaP plants (Table S4). Photosynthesis could have been limited by altered sugar metabolism, as the amount of soluble (i.e., carbohydrates, fructose, glucose) increased two-fold in + NaP plants. It is suggested that combined supply of Na$^+$ and P strongly reduced the turnover of carbohydrates and may have favored the formation of large starch grains in the chloroplasts to reduce the amount of soluble carbohydrates (Fig. 4D, E,

F). Our results show that the increase in starch biosynthesis in + NaP plants was related (as in + P plants) to the induction of ADP-glucose pyrophosphorylase, whereas translocation of triosephosphates was not significantly affected. However, in + NaP plants, A increased under low O$_2$ conditions, indicating that feedback limitation of A, typically induced by carbohydrate accumulation [80,81] did not occur. Low sugar and starch concentrations, but high photosynthetic rates were found, in three *A. donax* ecotypes grown in field conditions under low water availability, and this was attributed to high availability of sinks for photosynthate [82]. The accumulation of carbohydrates induced by P supply in Na$^+$-stressed plants may serve protective purposes, by enhancing the osmotic capacity of the plants to assimilate water [83] as confirmed by the over expression of genes of the GO category '*organic substance metabolic process*' in + NaP plants (Table S4). Carbohydrate accumulation may also help prevent damage to the cell structures [84]. Indeed, the + NaP treatment also induced a SNF1-related protein kinase coding gene (SnRK2), which responds to both ionic and non-ionic

osmotic stress conditions [34,85]. Genes coding for dehydrins (DHNs) proteins, which play cellular protection in abiotic stress tolerance [86,87], were also up-regulated in leaves of + NaP plants. Remarkably, we also observed that, while Early Responsive to Dehydration (ERD4) genes were induced as expected in *Poaceae* (see [34] for similar responses in drought-stress conditions), two ERD6 genes coding for carbohydrate transporters were down-regulated, consistent with the carbohydrate accumulation shown in the leaves of + NaP plants.

Interactions between high concentrations of Na$^+$ and P did not significantly affect isoprene emission, which was uncoupled from photosynthesis in stressed leaves [74,88]. However, the small reduction of isoprene emission with respect to + P leaves could be associated to the very large negative effect of the combined treatment (+NaP) on photosynthesis, and to the consequent reduction in photosynthetic substrate entering the MEP pathway. Transcriptomic results show up-regulation of ABA biosynthesis and down-regulation of β-carotene (both made by MEP) in + NaP compared to + Na leaves. This suggests a rearrangement of the flux of carbon into the MEP pathway towards hormones controlling stomatal movement and away from antioxidants such as carotenoids. Moreover, competition with starch for PEP could also limit isoprene synthesis in + NaP as well as in + P leaves (see above). However, starch was not a limiting factor in + NaP leaves as it was in + P leaves. The accumulation of carbohydrates in + NaP leaves was also consistent with the over-expression of genes of GO category '*organic substance metabolic process*' (Table S4), suggesting that a glucose 6-phosphate shunt might have been activated to increase the availability of precursors for the MEP pathway [89], despite the low flux of carbon fixed by photosynthesis.

In + NaP leaves, a significant increase of both H$_2$O$_2$ and glutathione (GSH) content was observed, and further confirmed in our transcriptome analysis by over-expression of genes of GO categories '*cellular metabolic process*' and '*organic substance metabolic process*' (Table S4), indicating enhanced ROS formation and activation of the antioxidant metabolism. Moreover, enhanced biogenesis of peroxisomes in + NaP leaf cells (Fig. 4E, F), most likely indicates a general increase of conditions of oxidative stress [90]. Indeed, peroxisomes contain antioxidant enzymes able to metabolize ROS and to enhance tolerance to a wide range of stresses [91]. High synthesis of GSH possibly prevents the increase of H$_2$O$_2$ to toxic levels while allowing this compound to exert signaling functions [92,93] that may further enhance the stress response of *A. donax* [94]. However, this was clearly insufficient to protect photosynthesis in + NaP leaves.

5. Conclusions

By combining in vivo plant phenotyping, quantification of metabolites and ultrastructural imaging of the leaves with transcriptome, it was found that *A. donax* growth is negatively affected by P deficiency in the soils. On the other hand, excess of P does not hamper photosynthesis of *A. donax*, although it deeply affects carbon metabolism by the reduction of starch content and isoprene production. The salinity treatments impaired *A. donax* performance by causing detrimental effects on leaf cells ultrastructure. However, Arundo plants responded to Na + stress by enhancing biosynthesis of antioxidant carotenoids, sucrose and isoprene, which probably have protective role in saline soils. Finally, we highlight that high P supply to salt-stressed *A. donax*, further enhances transcriptomic changes that induce the onset of protective physiological mechanisms on one hand but, on the other hand, strongly limits plant growth and biomass production.

Author contributions

CC and BF designed the research, analyzed the data and wrote the article with contributions of all the authors; PSa, CC, BF performed research; ML, RS, BC, GC, PSu, MM provided technical assistance; CM, AG, TR, LF supervised and complemented the writing.

Appendix A. Supplementary data

Supplementary material related to this article can be found, in the online version, at doi:https://doi.org/10.1016/j.plantsci.2019.110260.

References

[1] R. Pilu, A. Bucci, F.C. Badone, M. Landoni, Giant reed (*Arundo donax* L.): a weed plant or a promising energy crop? Afr. J. Biotechnol. 11 (2012) 163–9174.

[2] R.J. Webster, S.M. Driever, J. Kromdijk, J. McGrath, A.D.B. Leakey, K. Siebke, T. Demetriades-Shah, S. Bonnage, T. Peloe, High C3 photosynthetic capacity and high intrinsic water use efficiency underlies the high productivity of the bioenergy grass Arundo donax, Sci. Rep. 6 (2016) 20694.

[3] B. Rossa, A. Tüffers, G. Naidoo, D. Willert, *Arundo donax* L. (*Poaceae*) — a C3 species with unusually high photosynthetic capacity, Bot. Acta 111 (1998) 216–221.

[4] E. Sánchez, S. Gil, J. Azcón-Bieto, S. Nogués, The response of *Arundo donax* L. (C3) and *Panicum virgatum* (C4) to different stresses, Biomass Bioenergy 85 (2016) 335–345.

[5] C.S.C. Calheiros, P.V.B. Quiterio, G. Silva, L.F.C. Crispim, H. Brix, S.C. Moura, P.M.L. Castro, Use of constructed wetland systems with *Arundo* and *Sarcocornia* for polishing high salinity tannery wastewater, J. Environ. Manage. 95 (2012) 66–71.

[6] L. Nackley, S.H. Kim, A salt on the bioenergy and biological invasions debate: salinity tolerance of the invasive biomass feedstock Arundo donax, GCB Bioenergy 7 (2015) 752–762.

[7] M. Haworth, S. Catola, G. Marino, C. Brunetti, M. Michelozzi, E. Riggi, G. Avola, L.S. Cosentino, F. Loreto, M. Centritto, Moderate drought stress induces increased foliar dimethylsulphoniopropionate (DMSP) concentration and isoprene emission in two contrasting ecotypes of Arundo donax, Front. Plant Sci. 8 (1016) (2017), https://doi.org/10.3389/fpls.2017.01016.

[8] M. Haworth, G. Marino, L.S. Cosentino, C. Brunetti, A. De Carlo, G. Avola, E. Riggi, F. Loreto, M. Centritto, Increased free abscisic acid during drought enhances stomatal sensitivity and modifies stomatal behaviour in fast growing giant reed (*Arundo donax*), Environ. Exp. Bot. 147 (2018) 116–124.

[9] M. Haworth, M. Centritto, A. Giovannelli, G. Marino, N. Proietti, D. Capitani, A. De Carlo, F. Loreto, Xylem morphology determines the drought response of two *Arundo donax* ecotypes from contrasting habitats, GCB Bioenergy 9 (2017) 119–131.

[10] S. Pollastri, A. Savvides, M. Pesando, E. Lumini, M.G. Volpe, E.A. Ozudogru, A. Faccio, F. De Cunzo, M. Michelozzi, M. Lambardi, V. Fotopoulos, F. Loreto, M. Centritto, R. Balestrini, Impact of two arbuscular mycorrhizal fungi on *Arundo donax* L. response to salt stress, Planta 247 (2018) 573–585.

[11] V. Velikova, C. Brunetti, M. Tattini, D. Doneva, M. Ahrar, T. Tsonev, M. Stefanova, T. Ganeva, A. Gori, F. Ferrini, C. Varotto, F. Loreto, Physiological significance of isoprenoids and phenylpropanoids in drought response of *Arundinoideae* species with contrasting habitats and metabolism, Plant Cell Environ. 39 (2016) 2185–2197.

[12] F. Loreto, V. Velikova, Isoprene produced by leaves protects the photosynthetic apparatus against ozone damage, quenches ozone products, and reduces lipid peroxidation of cellular membranes, Plant Physiol. 127 (2001) 1781–1787.

[13] V. Velikova, Z. Várkonyi, M. Szabó, L. Maslenkova, I. Nogues, L. Kovács, V. Peeva, M. Busheva, G. Garab, T.D. Sharkey, F. Loreto, Increased thermostability of thylakoid membranes in isoprene-emitting leaves probed with three biophysical techniques, Plant Physiol. 157 (2011) 905–916.

[14] F. Loreto, J.P. Schnitzler, Abiotic stresses and induced BVOCs, Trends Plant Sci. 15 (2010) 154–166, https://doi.org/10.1016/j.tplants.2009.12.006.

[15] S. Fares, C. Barta, F. Brilli, M. Centritto, L. Ederli, F. Ferranti, S. Pasqualini, L. Reale, D. Tricoli, F. Loreto, Impact of high ozone on isoprene emission, photosynthesis and histology of developing Populus alba leaves directly or indirectly exposed to the pollutant, Physiol. Plant. 128 (2006) 456–465.

[16] E. Beck, P. Ziegler, Biosynthesis and degradation of starch in higher plants, Ann. Rev. Plant Physiol. Plant Mol. Biol. 40 (1989) 95–118.

[17] H. Marschner, Mineral nutrition of higher plants, Second edition, Functions of Mineral Nutrients: Macronutrient vol 8, Academic Press Inc. (Elsevier), 1995, pp. 229–312.

[18] J. Shen, L. Yuan, J. Zhang, H. Li, Z. Bai, X. Chen, W. Zhang, F. Zhang, Phosphorus dynamics: from soil to plant, Plant Physiol. 156 (2011) 997–1005.

[19] G. Hernández, M. Ramírez, O. Valdés-López, M. Tesfaye, M.A. Graham, T. Czechowski, A. Schlereth, M. Wandrey, A. Erban, F. Cheung, H.C. Wu, M. Lara, C.D. Town, J. Kopka, M.K. Udvardi, C.P. Vance, Phosphorus stress in common bean: root transcript and metabolic responses, Plant Physiol. 144 (2007) 752–767.

[20] M.J. Wassen, H.O. Venterink, E.D. Lapshina, F. Tanneberger, Endangered plants persist under phosphorus limitation, Nature 437 (2005) 547–550.

[21] A.L. Fredeen, I.M. Rao, N. Terry, Influence of phosphorus nutrition on growth and carbon partitioning in Glycine max, Plant Physiol. 89 (1989) 225–230.

[22] M. Fernández-Martínez, J. Llusià, I. Filella, Ü. Niinemets, A. Arneth, I.J. Wright, F. Loreto, J. Peñuelas, Nutrient-rich plants emit a less intense blend of volatile isoprenoids, New Phytol. (2017) doi.org/10.1111/nph.14889.

[23] S. Fares, F. Brilli, I. Nogués, V. Velikova, T. Tsonev, S. Dagli, F. Loreto, Isoprene emission and primary metabolism in Phragmites australis grown under different phosphorus levels, Plant Biol. 10 (2008) 38–43.

[24] T.W. Jr. Rufty, C.T. MacKown, D.W. Israel, Phosphorus stress effects on assimilation of nitrate, Plant Physiol. 94 (1990) 328–333.

[25] D. Cordell, J.-O. Drangert, S.B. White, The story of phosphorus: global food security and food for thought, Global Environ. Change 19 (2009) 292–305.

[26] R. Munns, M. Tester, Mechanisms of salinity tolerance, Annu. Rev. Plant Biol. 9 (2008) 651–681.

[27] M. Centritto, F. Loreto, K. Chartzoulakis, The use of low [CO_2] to estimate diffusional and non-diffusional limitations of photosynthetic capacity of salt-stressed olive saplings, Plant Cell Environ. 26 (2003) 585–594.

[28] M.M. Chaves, J. Flexas, C. Pinheiro, Photosynthesis under drought and salt stress: regulation mechanisms from whole plant to cell, Ann. Bot. 103 (2009) 551–560.

[29] R.S. Dubey, A.K. Singh, Salinity induces accumulation of soluble sugars and alters the activity of sugar metabolising enzymes in rice plants, Biol. Plant. 42 (1999) 233–239.

[30] A. Parida, A.B. Das, P. Das, NaCl stress causes changes in photosynthetic pigments, proteins and other metabolic components in the leaves of a true mangrove, Bruguiera aparviflora, in hydroponic cultures, J. Plant Biol. 45 (2002) 28–36.

[31] H. Kalaji, K. Govindjee, J. BosaKoscielniak, K. Zuk-Golaszewska, Effects of salt stress on photosystem II efficiency and CO_2 assimilation of two Syrian barley land races, Environ. Exp. Bot. 73 (2011) 64–72.

[32] H. Sobhanian, K. Aghaei, S. Komatsu, Changes in the plant proteome resulting from salt stress: toward the creation of salt-tolerant crops? J. Proteomics 74 (2011) 1323–1337.

[33] G. Sablok, Y. Fu, V. Bobbio, M. Laura, G.L. Rotino, P. Bagnaresi, A. Allavena, V. Velikova, R. Viola, F. Loreto, M. Li, C. Varotto, Fuelling genetic and metabolic exploration of C3 bioenergy crops through the first reference transcriptome of Arundo donax L, Plant Biotechnol. J. 12 (2014) 554–567.

[34] Y. Fu, M. Poli, G. Sablok, B. Wang, Y. Liang, N. La Porta, V. Velikova, F. Loreto, M. Li, C. Varotto, Dissection of early transcriptional responses to water stress in Arundo donax L. By unigene-based RNA-seq, Biotechnol. Biofuels 9 (2016) 54, https://doi.org/10.1186/s13068-016-0471-8.

[35] C. Evangelistella, A. Valentini, R. Ludovisi, A. Firrincieli, F. Fabbrini, S. Scalabrin, F. Cattonaro, M. Morgante, G. Scarascia Mugnozza, J.J.B. Keurentjes, A. Harfouche, De novo assembly, functional annotation, and analysis of the giant reed (Arundo donax L.) leaf transcriptome provide tools for the development of a biofuel feedstock, Biotechnol. Biofuels 10 (2017) 138.

[36] D.R. Hoagland, D.I. Arnon, The water-culture method for growing plants without soil, Cal Agr Exp Stat Circular 347 (1950) 1–39.

[37] H.D. Barrs, P.E. Weathercley, A re-examination of the relative turgidity techniques for estimating water deficits in leaves, Aust. J. Biol. Sci. 15 (1962) 413–428.

[38] K.S. Smith, M.S. Cresser, Soil and Environmental Analysis: Modern Instrumental Techniques, CRC Press, 2003 pages 53-74.

[39] V. Sreenivasulu, N.S. Kumar, V. Dharmendra, M. Asif, V. Balaram, H. Zhengxu, Z. Zhen, Determination of boron, phosphorus, and molybdenum content in biosludge samples by microwave plasma atomic emission spectrometry (MP-AES), Appl. Sci. Basel 7 (2017) 264, https://doi.org/10.3390/app7030264.

[40] S. von Caemmerer, G.D. Farquhar, Some relationships between the biochemistry of photosynthesis and the gas exchange of Phaseolus vulgaris cultivar Hawkesbury Wonder leaves, Planta 153 (1981) 376–387.

[41] B. Genty, J.M. Briantis, N.R. Baker, The relationship between the quantum yield of photosynthetic electron transport and quenching of chlorophyll fluorescence, Biochim. Biophys. Acta 990 (1989) 87–92.

[42] Z.S. Zhang, M.J. Liu, R. Scheibe, J. Selinski, L.T. Zhang, C. Yang, X.L. Meng, H.Y. Gao, Contribution of the alternative respiratory pathway to PSII photoprotection in C3 and C4 Plants, Mol. Plant 10 (2017) 131–142.

[43] F. Brilli, B. Gioli, D. Zona, E. Pallozzi, T. Zenone, G. Fratini, C. Calfapietra, F. Loreto, I.A. Janssens, R. Ceulemans, Simultaneous leaf and ecosystem-level fluxes of volatile organic Compounds from a poplar-based SRC plantation, Agr. For. Met. 187 (2014) 22–35.

[44] A.M. Bolger, M. Lohse, B. Usadel, Trimmomatic: A flexible trimmer for Illumina Sequence Data, Bioinformatics 30 (2014) 2114–2120.

[45] K.D. Hansen, S.E. Brenner, S. Dudoit, Biases in Illumina transcriptome sequencing caused by random hexamer priming, Nucleic Acids Res. 38 (2010) 131.

[46] B.J. Haas, A. Papanicolaou, M. Yassour, M. Grabherr, P.D. Blood, J. Bowden, M.B. Couger, D. Eccles, B. Li, M. Lieber, M.D. Macmanes, M. Ott, J. Orvis, N. Pochet, F. Strozzi, N. Weeks, R. Westerman, T. William, C.N. Dewey, R. Henschel, R.D. Leduc, N. Friedman, A. Regev, De novo transcript sequence reconstruction from RNA-seq using the Trinity platform for reference generation and analysis, Nat. Protoc. 8 (2013) 1494–1512.

[47] W. Li, A. Godzik, Cd-hit: a fast program for clustering and comparing large sets of protein or nucleotide sequences, Bioinformatics 22 (2006) 1658–1659.

[48] B. Li, C.N. Dewey, RSEM: accurate transcript quantification from RNA-Seq data with or without a reference genome, BMC Bioinformatics 12 (2011) 323.

[49] A. Conesa, S. Götz, Blast2GO: A Comprehensive Suite for Functional Analysis in Plant Genomics, Int. J. Plant Genom. (2008), https://doi.org/10.1155/2008/619832.

[50] A. Kuhn, R. Luthi-Carter, M. Delorenzi, Cross-species and cross-platform gene expression studies with the Bioconductor-compliant R package annotation Tools, BMC Bioinformatics 9 (2008) 26.

[51] C. Xie, X. Mao, J. Huang, Y. Ding, J. Wu, S. Dong, L. Kong, G. Gao, C.H. Li, L. Wei, KOBAS 2.0: a web server for annotation and identification of enriched pathways and diseases, Nucleic Acids Res. 39 (2011) W316–W322.

[52] M. Kanehisa, Y. Sato, M. Kawashima, M. Furumichi, M. Tanabe, KEGG as a reference resource for gene and protein annotation, Nucleic Acids Res. 44 (2016) D457–D462.

[53] M. Tattini, C. Galardi, P. Pinelli, R. Massai, D. Remorini, G. Agati, Differential accumulation of flavonoids and hydroxycinnamates in leaves of Ligustrum vulgare under excess light and drought stress, New Phytol. 163 (2004) 547–561.

[54] P.S. Chow, S.M. Landhäusser, A method for routine measurements of total sugar and starch content in woody plant tissues, Tree Physiol. 24 (2004) 1129–1136.

[55] V. Alexieva, I. Sergiev, S. Mapelli, E. Karanov, The effect of drought and ultraviolet radiation on growth and stress markers in pea and wheat, Plant Cell Environ. 24 (2001) 1337–1344.

[56] J. Sedlak, R.H. Lindsay, Estimation of total, protein-bound, and nonprotein sulfhydryl groups in tissue with Ellman's reagent, Anal. Biochem. 25 (1968) 192–205.

[57] M. López-Carbonell, M. Gabasa, O. Jáuregui, Enhanced determination of abscisic acid (ABA) and abscisic acid glucose ester (ABA-GE) in Cistus albidus plants by liquid chromatography-mass spectrometry in tandem mode, Plant Physiol. Biochem. 47 (2009) 256–261.

[58] C.S. Bestwick, I.R. Brown, M.H.R. Bennett, J.W. Mansfield, Localization of hydrogen peroxide accumulation during the hypersensitive reaction of lettuce cells to Pseudomonas syringae pv phaseolicola, Plant Cell 9 (1997) 209–221.

[59] A. Ranieri, A. Castagna, J. Pacini, B. Baldan, A. Mensuali Sodi, G.F. Soldatini, Early production and scavenging of hydrogen peroxide in the apoplast of sunflower plants exposed to ozone, J. Exp. Bot. 54 (2003) 2529–2540.

[60] T. Mimura, K. Dietz, W. Kaiser, M. Schramm, G. Kaiser, U. Heber, Phosphate transport across biomembranes and cytosolic phosphate homeostasis in barley leaves, Planta 180 (1990) 139–146.

[61] J. Pozueta-Romero, M. Frehner, A.M. Viale, T. Akazawa, Direct transport of ADP glucose by an adenylate translocator is linked to starch biosynthesis in amyloplasts, Proc. Natl. Ac. Sci. 88 (1991) 5769–5773.

[62] H.W. Heldt, U.I. Flügge, S. Borchert, Diversity of specificity and function of phosphate translocators in various plastids, Plant Physiol. 95 (1991) 341–343.

[63] U.S. Ladror, S.P. Latshaw, F. Marcus, Spinach cytosolic fructose1,6-bisphosphatase. Purification, enzyme properties, and structural comparisons, Eur. J. Biochem. 189 (1990) 89–94.

[64] J. Daie, Cytosolic fructose-1,6-bisphosphatase: a key enzyme in the sucrose biosynthetic pathway, Photosynth. Res. 38 (1993) 5–14.

[65] F. Loreto, T.D. Sharkey, A gas exchange study of photosynthesis and isoprene emission in red oak, Planta 182 (1990) 523–531.

[66] F. Loreto, M. Centritto, C. Barta, C. Calfapietra, S. Fares, R.K. Monson, The relationship between isoprene emission rate and dark respiration rate in white poplar (Populus alba L.) leaves, Plant Cell Environ. 30 (2007) 662–669.

[67] J.D. Hall, R. Barr, A.H. Al-Abbas, F.L. Crane, The ultrastructure of chloroplasts in mineral-deficient maize leaves, Plant Physiol. 50 (1972) 404–409.

[68] R. Müller, M. Morant, H. Jarmer, L. Nilsson, T.H. Nielsen, Genome-wide analysis of the Arabidopsis leaf transcriptome reveals interaction of phosphate and sugar metabolism, Plant Physiol. 143 (2007) 156–171.

[69] S. Delfine, A. Alvino, M.C. Villani, F. Loreto, Restrictions to CO_2 conductance and photosynthesis in spinach leaves recovering from salt stress, Plant Physiol. 119 (1999) 1101–1106.

[70] S. Wilkinson, W.J. Davies, ABA-based chemical signalling: the coordination of responses to stress in plants, Plant Cell Environ. 25 (2002) 195–210.

[71] C. Seiler, V.T. Harshavardhan, K. Rajesh, P.S. Reddy, M. Strickert, H. Rolletschek, U. Scholz, U. Wobus, N. Sreenivasulu, ABA biosynthesis and degradation contributing to ABA homeostasis during barley seed development under control and terminal drought-stress conditions, J. Exp. Bot. 62 (2011) 2615–2632.

[72] H.J. Park, W.Y. Kim, D.J. Yun, A new insight of salt stress signaling in plant, Mol. Cells 39 (2016) 447–459.

[73] C. Delwiche, T. Sharkey, Rapid appearance of ^{13}C in biogenic isoprene when $^{13}CO_2$ is fed to intact leaves, Plant Cell Environ. 16 (1993) 587–591.

[74] F. Brilli, C. Barta, A. Fortunati, M. Lerdau, F. Loreto, M. Centritto, Response of isoprene emission and carbon metabolism to drought in white poplar (Populus alba) saplings, New Phytol. 175 (2007) 244–254.

[75] A. Fortunati, C. Barta, F. Brilli, M. Centritto, I. Zimmer, J.P. Schnitzler, F. Loreto,

11

Isoprene emission is not temperature-dependent during and after severe drought-stress: a physiological and biochemical analysis, Plant J. 55 (2008) 687–697.

[76] F. Loreto, S. Pollastri, S. Fineschi, V. Velikova, Volatile isoprenoids and their importance for protection against environmental constraints in the Mediterranean area, Environ. Exp. Bot. 103 (2014) 99–106.

[77] T. Hadiarto, L.S.P. Tran, Progress studies of drought-responsive genes in rice, Plant Cell Rep. 30 (2011) 297–310.

[78] J. Jiang, S. Ma, N. Ye, M. Jiang, J. Cao, J. Zhang, WRKY transcription factors in plant responses to stresses, J. Int. Plant Biol. 2 (2017) 86–101.

[79] J. Giri, P.K. Dansana, K.S. Kothari, G. Sharma, S. Vij, A.K. Tyagi, SAPs as novel regulators of abiotic stress response in plants, BioEssays 35 (2013) 639–648.

[80] T.D. Sharkey, Feedback limitation of photosynthesis and the physiological role of ribulose bisphosphate carboxylase carbamylation, Bot Mag, Tokyo 2 (1990) 87–105.

[81] Z. Xu, Y. Jiang, G. Zhou, Response and adaptation of photosynthesis, respiration, and antioxidant systems to elevated CO_2 with environmental stress in plants, Front. Plant Sci. 6 (2015) 701.

[82] M. Haworth, G. Marino, E. Riggi, G. Avola, C. Brunetti, D. Scordia, G. Testa, M.T.G. Gomes, F. Loreto, S.L. Cosentino, M. Centritto, The effect of summer drought on the yield of *Arundo donax* is reduced by the retention of photosynthetic capacity and leaf growth later in the growing season, Ann. Bot. (2018) doi.org/10.1093/aob/mcy223.

[83] H. Lambers, I.I.I. Chapin, F.S.T.L. Pons, Plant Physiological Ecology, 2nd edition, Springer, New York, 2008 pages 151.

[84] Y. Yang, Y. Guo, Elucidating the molecular mechanisms mediating plant salt-stress responses, New Phytol. 217 (2017) 523–539.

[85] L. Virlouvet, M. Fromm, Physiological and transcriptional memory in guard cells during repetitive dehydration stress, New Phytol. 205 (2015) 596–607.

[86] J. Gao, T. Lan, Functional characterization of the late embryogenesis abundant (LEA) protein gene family from *Pinus tabuliformis* (Pinaceae) in *Escherichia coli*, Sci. Rep. 6 (2016) 19467.

[87] G. Verma, Y.V. Dhar, D. Srivastava, M. Kidwai, P.S. Chauhan, S.K. Bag, M.H. Asif, D. Chakrabarty, Genome-wide analysis of rice dehydrin gene family: its evolutionary conservedness and expression pattern in response to PEG induced dehydration stress, PLoS One 12 (2017) e0176399.

[88] C.E. Vickers, J. Gershenzon, M.T. Lerdau, F. Loreto, A unified mechanism of action for volatile isoprenoids in plant abiotic stress, Nat. Chem. Biol. 5 (2009) 283–291.

[89] T. Sharkey, S.E. Weise, The glucose 6-phosphate shunt around the Calvin-Benson cycle, J. Exp. Bot. 68 (2017) 4067–4077.

[90] E. Lopez-Huertas, W. Charlton, B. Johnson, I. Graham, A. Baker, Stress induces peroxisome biogenesis genes, EMBO J. 19 (2000) 6770–6777.

[91] Y. Nyathi, A. Baker, Plant peroxisomes as a source of signalling molecules, Biochim. Biophys. Acta 1763 (12) (2006) 1478–1495.

[92] R. Mittler, Oxidative stress, antioxidants and stress tolerance, Trends Plant Sci. 7 (2002) 405–410.

[93] A. Baxter, R. Mittler, N. Suzuki, ROS as key players in plant stress signalling, J. Exp. Bot. 65 (2014) 1229–1240.

[94] H. Knight, M.R. Knight, Abiotic stress signalling pathways: specificity and cross-talk, Trends Plant Sci. 6 (2001) 262–267.

48

PAPER II

Identification of abiotic stress responsive microRNAs and their targets in the bioenergy crop Arundo donax L. by using high-throughput sequencing

Silvia Rotunno[1,2], Claudia Cocozza[3], Vitantonio Pantaleo[4], Paola Leonetti[4], Loris Bertoldi[5], Giorgio Valle[5,6], Gian Paolo Accotto[2], Francesco Loreto[6], Gabriella Stefania Scippa[4], Laura Miozzi[2]

[1] Department of Biosciences and Territory, University of Molise, Contrada Fonte Lappone, 86090 Pesche, Italy

[2] National Research Council of Italy, Institute for the Sustainable Plant Protection (CNR-IPSP), Strada delle Cacce 73, 10135 Torino, Italy

[3] Department of Agriculture, Food, Environment and Forestry (DAGRI), University of Florence, Via San Bonaventura 13, 50145 Florence, Italy

[4] National Research Council of Italy, Institute for Sustainable Plant Protection (CNR-IPSP), Research Unit of Bari, CNR, 70126 Bari, Italy

[5] BMR Genomics S.r.l, via Redipuglia 22, 35131 Padova, Italy

[6] Department of Biology, University of Padua, via Ugo Bassi 58/B 35131 Padua, Italy

[7] Department of Biology, University of Naples Federico II, Naples, Italy

* Corresponding author, email: laura.miozzi@ipsp.cnr.it

In preparation

ABSTRACT

MicroRNAs (miRNAs) are a class of non-coding molecules involved in the regulation of a variety of biological processes. MiRNAs have been identified and characterized in several plant species, but not in *Arundo donax L.*, one of the most promising bioenergy crops. Here we identified, for the first time, *A. donax* conserved and novel miRNAs together with their targets, through a combined analysis of high-throughput sequencing of small RNAs and degradome libraries, in plants grown in control conditions and under stress induced by accumulation of phosphorous and sodium, alone or in combination. A total of 134 conserved miRNAs, belonging to 33 families, and 27 novel miRNA candidates were identified. Integration of miRNAs and degradome data identified conserved miRNAs that play a role in the response to abiotic stress (belonging to miR169, miR399, miR528 and miR827, families); candidate novel miRNAs possibly involved in *A. donax* stress response were also proposed.

The identified set of conserved and novel stress-related miRNAs, together with their targets, extends our knowledge about miRNAs in monocots and pave the way to understand miRNAs-mediated regulatory processes, particularly abiotic stress tolerance, in *A. donax* and other bioenergy crops.

keywords: Giant reed, miRNAs, small RNAs, degradome, salt stress, phosphorus excess, abiotic stress

1. INTRODUCTION

Improving clean energy production and ensuring universal access to affordable and sustainable energy resources are the main objectives of goal 7 of the seventeen Sustainable Development Goals (SDGs) promoted by the United Nations to end poverty, protect the planet and ensure peace and prosperity to all people by 2030 (https://www.un.org/sustainabledevelopment/). The 2019 Global report from The Food and Land Use Coalition (FOLU) (https://www.foodandlandusecoalition.org/global-report/) claims the need to "focus on bioenergy that do not (or only minimally) increase the pression on land use", cultivating energy crops that do not compete with food production, forest or degraded land restoration. In this context, second-generation biofuels, defined as fuels that can be manufactured from various types of non-food biomass, including plant materials and animal waste, represent a promising alternative.

Arundo donax L., commonly called giant reed, is a perennial rhizomatous invasive grass elonging to the Poaceae family, often cultivated as energy crop for second generation biofuels production (Corno et al., 2018). One of the advantages of *A. donax* cultivation resides in its potential to grow in very low nutrient availability conditions (Ren et al., 2019) and to be employed for restoration of marginal lands (Corno et al., 2016) and phytoremediation (Cano-Ruiz et al., 2020; Cristaldi et al., 2020).

Indeed, the ability of this plant to cope with different biotic and abiotic stresses and survive in degraded and marginal areas has been widely demonstrated (Cocozza et al., 2019; Cocozza et al., 2020; Docimo et al., 2019; Haworth et al., 2019; Shaheen et al., 2018). Previously, we observed that, in response to salt or phosphorus excess as well as in combination of both stresses, *A. donax* can activate its transcriptomic machinery in order to induce the onset of protective physiological mechanisms. It was sensitive to constraints conditions by showing a progressive decline in stomatal conductance and consequently in photosynthesis (Cocozza et al., 2019). However, the prolonged exposure to salt and phosphorous excess stimulated in *A. donax* the production of metabolites, such as H_2O_2, carbohydrates, phenylpropanoids, zeaxanthin and increased the de-epoxidation state of the xanthophylls, that resulted in a high stress tolerance and a fast and full recovery following stress relief (Cocozza et al., 2020). MicroRNAs (miRNAs) are a class of small RNA (sRNA) molecules of 20-24 bp involved in the post-transcriptional regulation of a variety of fundamental biological aspects in eukaryotic organisms, including plants (Bartel, 2004). MiRNAs are transcribed by

RNA polymerase II from MIR genes.

These sequences, called primary miRNAs (pri-miRNAs), contain a self-complementary region that is processed by Dicer complex; the first cleavage removes the non-complementary part, originating the miRNAs precursor (pre-miRNA), while the second cleavage originates a small double-stranded RNA molecule, known as miRNA/miRNA* duplex, with 2-nt 3' overhang. AGO1/HSP90 complex binds the duplex and free the miRNA guide strand, originating a mature RISC complex, that is transported into the cytoplasm, where it can perform its function: cleaving the target transcript or inhibiting its translation (Manavella et al., 2019; Pegler et al., 2019). Several studies have shown that miRNAs are strongly involved in the response to abiotic and biotic stress (Li et al., 2017) and that, plants can activate their physiological responses by expressing some miRNAs that act on stress-related target genes (Sun et al., 2019).

Despite the economic importance of *A. donax*, its genome has not been sequenced so far, probably due to its complexity (Danelli et al., 2020) and only transcriptomic studies were performed to investigate its gene content and its molecular responses to the environment (Barrero et al., 2015; Cocozza et al., 2019; Docimo et al., 2019; Evangelistella et al., 2017; Y. Fu et al., 2016; Sablok et al., 2014; Sicilia et al., 2020). As far as we know, only one study on *in-silico* prediction of *A. donax* miRNAs was conducted, based on the available transcriptomic data from different tissues (root, bud, culm and leaf), and resulting in the prediction of 141 conserved miRNAs distributed into 14 miRNA families and 462 *in silico* predicted target transcripts (Jike et al., 2018).

In the present study, we carried out for the first time a high-throughput sequencing approach to identify known miRNAs and putative candidate novel miRNAs of the bioenergy crop *A. donax* under different abiotic stress conditions characterized by salt accumulation in the soil. Furthermore, we investigated, by the high-throughput sequencing of RNA ends (degradome analysis) (German et al., 2008), the targets of both known and candidate novel miRNAs and conducted a functional pathway enrichment analysis in order to explore the miRNA putative functions and gain new insights into the mechanisms of *A. donax* response to abiotic stresses. Overall, this study advances our knowledge of *A. donax* miRNAs and provide an inventory of miRNAs and related targets useful for further studies, aiming to clarify and improve the management of *A. donax* in unfavorable environments.

2. MATERIALS AND METHODS

2.1 Plant material

A. donax plants were propagated from rhizomes collected in Sesto Fiorentino, (43°81′75″ N, 11°18′88″ E) (Italy), and grown in a climatic chamber under controlled environmental conditions for two months before the beginning of the experiment. Four different nutrient solutions were supplied: 1) Hoagland solution (Control, C); 2) Hoagland solution complemented with 8.0 mM KH_2PO4 (excess of phosphorus, +P); 3) Hoagland solution complemented with 200 mM NaCl (excess of salt, +Na); and 4) Hoagland solution complemented with both 200 mM NaCl and 8.0 mM KH_2PO_4 (excess of phosphorus and salt, +NaP). These solutions were supplied twice a week for the entire duration of the experiment (43 days). For each plant, the third fully expanded leaf was collected at the end of the experiment and stored at -80°C until RNA extraction was performed. Three individual biological replicas for each treatment were collected. More experimental details on plant's growth conditions, stress treatments and samples collection are reported in the cognate paper Cocozza et al. (2019).

2.2 sRNAs and degradome sequencing

Total RNA extraction was performed with TRIzol® Reagent (Thermo Fisher Scientific®, Wilmington, USA), according to the manufacturer's instructions. DNA contamination was removed using TURBO DNA-free[TM] kit (Thermo Fisher Scientific®, Wilmington, USA). RNA concentration was determined by Nanodrop spectrophotometer (Thermo Fisher Scientific®, Wilmington, USA). For sRNAs sequencing, for each treatment, three samples were pooled together, while, for degradome sequencing, a pool from samples of all the treatments was prepared. Samples were sent to LCSciences (https://www.lcsciences.com/; Houston, Texas, USA) for library preparation and sequencing with Illumina technology (single-end reads, 50bp). Raw data have been deposited in the Sequence Read Archive (https://www.ncbi.nlm.nih.gov/sra) with SRA accession PRJNA774159.

2.3 Data analysis

Quality reads assessment of sequencing data was carried out with FastQC (http://www.bioinformatics.babraham.ac.uk/projects/fastqc/ v. 0.11.5).

In order to identify known miRNAs, after adapter removal with Trimmomatic (v 0.39)

(Bolger et al., 2014), clean reads were aligned to mature monocotyledons miRNAs (downloaded from miRBase v 22.1) with PASS software (v. 2.30) (Campagna et al., 2009) using the following parameters: read trimming with a quality threshold of 15 in a window of 6 nt, local alignment with ungapped seed structure, 89.9% as identity percentage (i.e. 2 mismatches) and 18 nt as minimal alignment size.

Identical mapped reads were collapsed with the tool fastx_collapser belonging to the FASTX toolkit (v. 0.0.13) and renamed according to the corresponding miRNAs. The reads that did not align were saved to be further explored. Primary miRNA sequences (pri-miRNA) were searched in the *A. donax* transcriptome (Cocozza et al., 2019) using the Perl script SumirFind.pl (v. 1.1) (Alptekin et al., 2016; Lucas & Budak, 2012) allowing two mismatches. MIReNA tool (v. 2.0) (Mathelier & Carbone, 2010) was then used for precursors (pre-miRNAs) sequences identification and validation and for calculation of Minimum Folding Energy (MFE) and Minimal Folding Energy Index (MFEI). MFE values estimated the stability of the stem-loop structure of the miRNA precursor whereas MFEI values was used to distinguish pre-miRNA sequences from other coding or non-coding RNAs. Secondary structure design was carried out with RNAfold (Lorenz et al., 2011). miRNAs* sequences were defined as the strand with lower frequency between the two complementary strands.

For novel miRNAs prediction, unaligned reads were scanned with Infernal (v. 1.1.2) in order to remove rRNA, tRNA and snoRNA, and then blasted against the complete chloroplast genomes of three *Arundo* species, i.e., *A. formosana* (NC_054211.1), *A. donax* (NC_037077.1) and *A. plinii* (NC_034652.1) available in the NCBI RefSeq database, to remove chloroplastic sequences. Reads were then size selected (less than 24 nt long), then collapsed with fastx_collapser (FASTX toolkit, v. 0.0.13) and clustered using CD-HIT software (v. 4.6.6), using a word size of 5 and 85% identity in order to reduce redundancy. After checking the presence in at least two different libraries (i.e., two different treatments), reads were selected for further analyses as hypothetical novel miRNAs. Pre-miRNA, pri-miRNA and miRNA* sequences were identified as described above for known miRNAs.

The miRNA relative expression in the different treatments in comparison to control plants was estimated using the NOISeq R package (v. 2.30.0; R v. 3.6.1) (Tarazona et al., 2015) using the functionality of pairwise differential expression analysis without replicates with the following parameters: nss = 5, pnr = 0.2, v = 0.02.

Normalized counts for each condition were obtained with TMM (Trimmed Mean of M values) method (Robinson & Oshlack, 2010). miRNAs with higher probability (q > 0.9) were considered as differentially expressed.

In the case of degradome-sequencing data, adapters and low-quality reads trimming was performed with BBMap (v. 38.67). Clean reads were then used to identify miRNA sliced target sites using the CleaveLand 4 pipeline (v. 4.4; (Addo-Quaye et al., 2009). According to the relative abundance of the mapping reads, sliced target sites were distributed into five categories, defined as follows. Category 0: more than one read mapping at the cleavage position, equal to the maximum on the transcript, when there is just one position at the maximum value; category 1: more than one read mapping at the cleavage position, equal to the maximum on the transcript, when there is more than one position at maximum value; category 2: more than one read mapping at the cleavage position, above the average depth, but not the maximum on the transcript; category 3: more than one read mapping at the cleavage position, but below or equal to the average depth of coverage on the transcript; category 4: just one read mapping at the cleavage position. KEGG pathway enrichment analysis of target genes was carried out with KOBAS-i, using as reference the *O. sativa* genome (Bu et al., 2021).

2.4 5' RACE for cleavage site identification of miRNA targets

Poly(A) RNA fraction from total RNA was collected using the MicroPoly(A) Purist™ kit (Thermo Fisher Scientific®, Wilmington, USA). Generation of cDNAs of poly-adenylated 5'remnants ligated to 5' adapter was carried out according to the protocol reported in German et al. (2009). PCR was performed using 5'adapter primer and 3'specific primer (denoted by the target id in Table S1). PCR conditions were: initial denaturation at 98°C for 30'' followed by 34 cycles of denaturation at 98°C for 20'', annealing at 60°C for 30'' and elongation at 72°C for 15''; final elongation was performed at 72°C for 3'. PCR products were resolved in 1X TRIS-Borate buffer, 8% acrylamide gel, eluted in sterilized water at 4°C, overnight and precipitated adding 2.5 v/v of absolute Ethanol and 1/10 of 2M NaCl. Purified PCR products were subjected to a second round of amplification with the same pairs of primers, purified using the MinElute® PCR Purification kit (Qiagen, Hilden, Germania) and cloned into the pGEM®-T Easy Vector System I (Promega, Madison, USA). Clones were sent to BMR Genomics (https://www.bmr-genomics.it/) for Sanger sequencing.

3. RESULTS

3.1 sRNA profiles of *A. donax*

In order to identify miRNAs from *A. donax*, sRNA libraries were generated from total RNA extracted for each of the following treatments: 1) control plants (C); 2) excess of phosphorus (+P); 3) excess of sodium (+Na); 4) excess of sodium and phosphorus (+NaP). Libraries were then sequenced with the high-throughput Illumina technology. After trimming of adapters, removing of low-quality sequences, rRNA, tRNA and snoRNA, and selection of reads shorter than 29 nt, a total of clean reads ranging between 2,545,750 (+Na) and 4,096,100 (+P) were retained for further analyses (Table S2).

In all the libraries, the majority of sRNA reads ranged between 20- and 24-nt in length (C, 69.1%; +P, 71.9%; +Na, 64.1%; +NaP, 59.6%); for all treatments, the most abundant sRNAs were 24-nt in length, followed by the 21-nt sRNAs (Fig. 1). As expected, being miRNAs mostly 21-nt long, in all treatments 21-nt sRNAs showed a doubled level of redundancy compared to 24nt-sRNAs (estimated by the average complexity index of 0.30 and 0.65, respectively).

3.2 Identification of conserved and novel candidate miRNAs in *A. donax*

By analyzing all the sRNA libraries, a total of 134 known miRNAs, belonging to 45 miRNA families, were identified. Among them, the family of miR395 was the most represented with 19 members, followed by the family of miR167 and miR169, both with 9 members, and the one of miR164 represented by 8 members. By contrast, several miRNA families were represented by 2 or 1 member (Fig. 2 and Table S3). As expected, the majority of conserved miRNAs were of 21-nt, followed by those of 22-nt, i.e., 67% and 20%, respectively. The overall nucleotide composition of the mature miRNA sequences was 25.89% of uracil, 23.21% of adenine, 28.17% of guanine and 22.72% of cytosine with a GC content of 50.89%, (Table S4).

Position specific nucleotide sequence analysis of the identified conserved miRNAs revealed that uracil was the most represented nucleotide at the 5' end, with a percentage of 52.99%. Considering position 10 and 11 as the two principal common cleavage sites, we observed that adenine was the most represented nucleotide at position 10, with a percentage of 34.33%, while uracil and guanine were the two most represented nucleotides at position 11, with a percentage of 37.31% and 30.60%, respectively

(Fig. 3 and Table S4). According to the last release of the miRbase database (v22.1), among the 45 miRNA families, 29 were conserved in both monocot and dicot clades, 15 were identified so far only in the Poaceae grass family and 1 in both Poaceae and Bromeliaceae (both belonging to the order of Poales).

MIReNA analysis allowed us to predict the pre-miRNA sequences of 29 known miRNAs, with a length ranging from 60- and 217-nt and an average length of 121-nt. The reliability of the pre-miRNA's prediction was supported by the highly negative MFE values, ranging from -122.3 kcal/mol to -26.0 kcal/mol. Moreover, the pre-miRNAs MFEI values, ranging between -1.48 kcal/mol and -0.85 kcal/mol, clearly indicated that they do not belong to other classes of non-coding RNAs such as tRNAs (MFEI=-0.64 kcal/mol), rRNAs (MFEI=-0.59 kcal/mol) and mRNAs (MFEI=0.62-0.66 kcal/mol) (Bonnet et al., 2004; Zhang et al., 2006).

Based on the recently revised annotation criteria (Axtell & Meyers, 2018), 27 candidate novel miRNAs (miRCs) were identified (Table S5). As expected, *A. donax* miRCs were mostly of 21 nt, and pre-miRNAs ranged from 60 to 252 nt in length, with an average length of 114 nt. Similarly to the pre-miRNAs of conserved miRNAs, the negative MFE (ranging from -124.5 kcal/mol to -19.9 kcal/mol) and MFEI values (ranging from -1.90 to -0.94) supported the reliability of predictions.

3.3. Differentially expressed miRNAs and miRCs in response to stress

The relative abundance of conserved miRNAs and miRCs was estimated as transcript per million (TPM). In the case of conserved miRNAs, the obtained TPM values widely varied among the miRNA families identified. In particular, we found that members of the conserved miRNA families miR167, miR168, miR169 and miR396 as well as members of monocots-specific miRNA families miR2275, miR5072 and miR5168 were the most highly expressed miRNAs (TPM > 10000). Among those with a TPM ranging between 10000 and 1000, we found several miRNAs families conserved in both monocots and dicots (miR156, miR159, miR160, miR162, miR164, miR168, miR169, miR171, miR172, miR393, miR394, miR827) and few members of monocots-specific miRNA families (miR444, miR9773, miR9774) (Table S3).

Using the NOISeq R package, we identified 33 miRNAs differentially expressed in at least one condition in respect to the control treatment, with a probability higher than 0.9. The global miRNA differential expression pattern in +Na clustered with that in +NaP, highlighting specific traits for +P treatment (Fig.4A). Five out of 33 miRNAs

were differentially expressed in response to all the considered stresses (Fig.4A and B). More specifically, miR169g, miR169n, miR169o, miR169q, were induced in all the stress conditions while miR169c-3p was induced in +P but repressed in +Na and +NaP (Fig.4A). The other 28 miRNAs resulted differentially expressed in only one or two of the tested conditions (Fig.4A and B). In detail, 10 miRNAs were specifically regulated only in +P; miR160a, miR160f, miR169a, miR169c-5p were induced while miR2275c, miR299a, miR399d, miR5072, miR827-3p, miR827-5p were repressed. Two miRNAs, i.e., miR164f-5p and miR164a-5p, were specifically differentially expressed (down-regulated) only in +Na condition. Finally, 9 miRNAs were differentially regulated only in +NaP treatment, and, in particular, miR156d-3p, miR167a-5p.1, miR167c-5p, miR444d and miR9773 were induced while miR2118a, miR2118d, miR5523, miR164f-5p.1 and miR164a-5p.1 were repressed (Fig.4A and Table S3).

In general, the abundance of miRC reads was lower if compared to what observed for the conserved miRNAs and varied significantly among the different treatments. Only the miRC10722-29 and miRC12006-27 had a TPM higher than 1000 in all the considered conditions, while seven miRCs (miRC45695-9, miRC22398-17, miRC76001-6, miRC1648-141, miRC71512-6, miRC19508-19, miRC2508-96) had a TPM value higher than 100 in at least two conditions.

Similarly to conserved miRNAs, miRCs differential expression profiles in +Na and +NaP clustered together and were distinguished from +P (Fig.4C). NOISeq analysis identified eight miRCs differentially expressed in at list one condition, with a probability higher than 0.9; miRC32911-12 was induced in response to all stress conditions in respect to C, miRC20665-18 and miRC35861-11 were induced in +Na and +NaP but not in +P, miRC256921-3 was repressed in +P and +NaP, miRC310360-3 was repressed in +P and +Na, miRC2107992-1 was induced only in +Na, miRC2495602-1 was induced only in +P, and miRC37052-11 was induced only in +NaP (Fig.4C).

3.4 miRNAs and miRCs targets identification and functional characterization

A. donax miRNAs and miRCs targets were identified by high-throughput degradome sequencing (German et al., 2008). A total of 5,897,713 raw reads, corresponding to 796,012 unique sequences, were obtained. After adapters and low-quality reads trimming, a total of 1,557,573 clean reads, representing 464,300 unique reads, were

retained. To identify miRNA targets, these reads were analyzed by CleaveLand 4 pipeline (v. 4.4), using the *A. donax* transcriptome previously assembled from the same samples for mapping (Cocozza et al., 2019). The 67% of degradome reads mapped to the *A. donax* transcriptome. We identified 69 targets for 49 conserved miRNAs belonging to 26 miRNA families, including 8 Poaceae-specific families. In the case of miRCs, 27 targets for nine miRCs were identified. According to the relative abundance of the mapping reads, sliced target sites were categorized into five categories, from 0 to 4 (see Material and Method for category description).

The most relevant targets (category from 0 to 3) are reported in Table 1 while the complete list of targets is reported in Table S3 and S5.

The KEGG functional analysis of miRNA targets using the tool KOBAS-I (http://kobas.cbi.pku.edu.cn/) highlighted their involvement in different biological processes that can be clustered in five functional groups as reported in Table 2, i.e., energy metabolism, RNA processing and transcription, protein metabolism, carbohydrate metabolism, secondary metabolism. In detail, targets related with the *"energy metabolism"* and *"photosynthesis"* were present among the targets of miRNAs expressed in +Na and +NaP, while *"cysteine and methionine metabolism"* related targets were found only in the case of +P. It is worth to note that targets related to the *"ascorbate and aldarate metabolism"* were overrepresented (p-value<0.05) in all the conditions. In the case on miRC targets, six main functional groups were observed, i.e., energy metabolism, energy and carbohydrate metabolism, RNA processing and transcription, signal transduction, protein metabolism and secondary metabolism. In this case, several functional categories resulted with a p-value <0.05 (Table 2)

3.5 Validation of miRNAs and miRCs cleavage sites

In order to verify the cleavage sites identified by the degradome analysis and to confirm their nucleotide position, 5'RACE experiments were conducted on selected targets, i.e., an oxygen-evolving enhancer chloroplastic protein coding transcript (TR10651) targeted by miRC174433-3 and a 32 kDa dirigent-like coding transcript (TR4471) targeted by miR156d-3p (Table 1). By 5'RACE of the transcript TR10651, we could amplify a specific fragment of ca. 120 bp in all treatments except the control (Fig. 5A). The Sanger sequencing of 13 independent clones confirmed 5' remnants found in the degradome analysis in the range of positions from 1520 to 1580 of

TR10651 (Fig. 5B, blu dots), including two cases (out of 13) of cleavage sites located two nucleotides downstream the CleaveLand predicted cleavage site (Fig.5B, blue dot downstream red dot). Possible explanations include the presence of other endonucleases cleavage sites or accumulation of a particularly stable decay intermediates (German et al., 2008). The cleavages 2-nt downstream of the red dot (Fig. 5B) could be explained by the presence of miRC174433-3 isoforms (denotes as isomiRs, i.e., miRNAs deriving from the same precursor), that have sequence offset at their 5' ends (Fig.5C and D) or other not yet identified pre-miRNA variants. Similar situation has been found in the case of osa-miR171 (Jeong & Green, 2012).

According to the degradome analysis, the miR156d-3p was identified to guide the cleavage of the transcript TR4471, coding for a 32kDa dirigent-like protein, at position 1,749. The results obtained with 5' RACE showed a double fragment in +NaP sample. Re-exanining the CleaveLand pipeline steps, we found the presence in the degradome library of 5' remnants confirming the existence of a double cleavage site for miR156d-3p, located at position 1,749 and 1,830 and compatible with 5'RACE results; however, due to stringent set up, only the first one was reported in the final CleaveLand output (Fig. S1).

4. DISCUSSION

4.1 miRNAs and miRCs in *A. donax*

A growing body of evidence (Li et al., 2017; Sun et al., 2019) indicates that miRNAs are involved in response to stresses, helping the plant to cope with adverse environmental conditions or pathogen attack and to activate adequate physiological responses including hormone-mediated responses, ubiquitin-mediated proteolysis, antioxidant production and modulation of energy metabolism (Sun et al., 2019). Therefore, investigating the role of miRNAs in the regulation of stress responses becomes of primary importance to elucidate how plants react and adapt themselves to environmental adversities. Identification and characterization of miRNAs in response to stress may be particularly relevant for *A. donax*, a promising biomass species, with relatively high yields and low agronomic inputs requirement, and also able to tolerate adverse environmental conditions and to resist to most pests (Fernando et al., 2016; Jámbor & Török, 2019). With the development of high-throughput sequencing, miRNAs have been identified from various plant species. However, for *A. donax*, for which a fully sequenced genome still lacks, only an *in-silico*

miRNA prediction, based on transcriptomic data, has been performed so far (Jike et al., 2018).In the present study, small RNAs from *A. donax* plants were sequenced and known as well as candidate novel miRNAs were identified. The obtained sRNA profiles were consistent with the typical ones reported for rice, wheat and other monocots (Chen et al., 2016; Fu et al., 2017; Morin et al.,2008; Zhao et al., 2020), where the 24-nt sRNAs are the most abundant and heterogeneous class of small non-coding RNAs in the sRNAs libraries, while the 21-nt sRNAs, being mostly miRNA sequences, show a low level of redundancy. Consistently with the general characteristic of miRNAs (Axtell & Meyers, 2018) and with previous reports on *A. donax* (Jike et al., 2018) and other plants (Chen et al., 2016; Huang et al., 2020), we observed a miRNA length distribution with a prevalence of 21-nt sequences followed by those of 20-nt in length. Furthermore, the observed 5' enrichment of uracil as well as the overall nucleotide composition of the mature miRNA sequences (Table S4) are comparable with the values reported previously for *in silico* predicted *A. donax* mature miRNAs and for *O. sativa* (Jike et al., 2018) and are in line with the known preference of the AGO1 protein for harboring miRNAs with a 5' terminal uracil (Mi et al., 2008). Finally, the reliability of predictions is supported by the length of precursors beneath 300-nt (Mi et al., 2008) as well as by the negative MFE and MFEI values obtained for both miRNAs and miRCs (Bonnet et al., 2004; Zhang et al., 2006).

In order to identify the *A. donax* miRNA targets, a degradome high-throughput sequencing approach was performed and 5'RACE experiments were conducted to confirm the 5' cleavage remnants for specific cases. This approach allowed us to identify the miRC174433-3 and its isomiRs, possibly originated from the pre-miRC174433-3 or from other not yet identified pre-miRNA genes. The length of miRC174433-3 and its variants ranged from 23- to 24-nt. Previous studies have shown that precursors representing most conserved miRNA families are also independently processed by DCL3 (in addition or in alternative to the canonical DCL1 cleavage) to generate miRNAs that are 23–25-nt in length, called long miRNAs (Vazquez et al., 2008). This evidence has been confirmed in several plants (Achkar et al., 2016; Pantaleo et al., 2010). Moreover, the accumulation of miRNAs longer than 21-nt in *A. thaliana* was shown to be inversely correlated with the level of miRNA conservation (Vazquez et al., 2008). Such evidences prompted us to hypothesize the existence of additional isomiR genes, besides the novel candidate miRNA gene pre-

miRC174433-3 (Fig. 5C-D) and highlights the importance of specific miming of the transcriptome assembly in order to unravel more isomiRs.

Interestingly, pre-miRC174433-3 shows a structure with a "minimal" loop (Fig. 5D). Similarly, osa-miR531, sbi-miR5383 and bdi-miR1135 deriving from precursors with minimal loops, are 23- to 24-nt long (Calviño et al., 2011; Liu et al., 2005; Unver & Budak, 2009). The function of 23-24-nt miRNAs has not been determined yet, however, they look to be dependent on the organ-specific expression of DCL3 and the hierarchical action of other DCLs, upon biotic or abiotic stresses (Pantaleo et al., 2010); the fact that we were able to identify cleavage remnants only in $Na+$ or $P+$ or $NaP+$ conditions and not in the control (Fig. 5A), would confirm the importance to further explore the role of miRC174433-3 and its isomiRs during stress conditions.

4.2 Stress-responsive miRNAs in *A. donax*

Among the differentially expressed miRNAs, we found several conserved miRNAs families known to be responsive to stress in other plants, i.e., miR156, miR160, miR164, miR167, miR169, miR396, miR399, miR528, miR827 (Sun et al., 2019). Five members of the family miR169 were responsive to all the tested stress conditions (+P, +Na, +NaP), and, indeed, this family has been reported to be involved in stress tolerance and response to abiotic stresses (Pegler et al., 2019; Sun et al., 2019). Interestingly, the same members that we found induced in response to excess of salt, phosphorus or both stresses (miR169g, miR169n, miR169o) were reported to be high salinity-responsive miRNAs in rice (B. Zhao et al., 2009). Our results extend their involvement in salt stress response also in *A. donax* and suggest a role in the case of phosphorus-related stress. The same miRNA family includes miR169l and miR169m, induced in +P and +Na, and miR169a and miR169c-5p that were specifically induced only in +P. The targets of these two last miRNAs, identified by the degradome analysis, were respectively an mRNA cleavage and polyadenylation factor (CLP1) homolog and a Vascular Plant One-Zinc-Finger (VOZ) 1-like transcription factor. The first one is involved in the 3′-end cleavage and polyadenylation of eukaryotic mRNAs, a critical step of gene expression, that has been recently related also to the regulation of stress responses (Hunt, 2020). Vascular Plant One-Zinc-Finger (VOZ) Transcription Factors are involved in regulating numerous biological processes such as floral induction and development, defense against pathogens, and response to multiple types of abiotic stress (Ganie et al., 2020; Rehman et al., 2021). In particular, VOZ

transcription factors positively affect salt stress tolerance through the regulation of many stress-responsive genes (Li et al., 2020; Prasad et al., 2018) and may be considered a promising target for the generation of salt-tolerant crops. Among the stress responsive miRNAs, miR827 and miR399, consistently with their role in regulating cellular phosphate homeostasis (Hackenberg et al., 2013; Lin et al., 2018), were both repressed specifically in +P, thus suggesting that their role is conserved in *A. donax*. Particular attention should also be paid to miR528, a miRNA previously established as multistress regulator, that has been shown to positively regulates rice salt tolerance by down-regulating a gene encoding an L-ascorbate oxidase (AO), thereby bolstering up the AO-mediated abscisic acid synthesis and ROS scavenging (Wang et al., 2021). In *A. donax*, we highlighted that miR528-5p is slightly induced in both +Na and +NaP conditions and targets an L-ascorbate oxidase coding transcript, thus suggesting that this regulatory mechanism is conserved in this species. The ascorbate plays multiple roles in the plant response to abiotic stresses (Xiao et al., 2021) and, indeed, the ascorbate and aldarate metabolism was overrepresented among the functional categories of the miRNA targets we identified (Table 2).

4.3 Stress-responsive miRCs in A. donax

As already reported in previous studies (Chen et al., 2016; Mao et al., 2012; Song et al., 2010), the newly identified miRCs were generally weakly expressed in respect to the conserved miRNAs, a characteristic possibly explained by the recent evolutionary origin of species-specific novel miRNAs (Cuperus et al., 2011). Among the miRCs, it is worth to mention miRC35861-11 and miRC37052-11.

The first one was induced in both +Na and +NaP, but not in +P, and, by the degradome analysis, it was found to target a geranylgeranyl pyrophosphate synthase coding transcript. It is interesting to note that, in sweet potato, this enzyme is involved in the biosynthesis of carotenoids and is likely associated with tolerance to osmotic stress (Chen et al., 2015), and that, in *A. donax*, the excess of salt do enhance the biosynthesis of carotenoids (Cocozza et al., 2019). Therefore, it is plausible to hypothesize that miRC35861-11 may be involved in the *A. donax* response to osmotic stress through the regulation of the carotenoid biosynthesis pathway. miRC37052-11 is induced specifically in +NaP and targets a PAD4 lipase-like coding transcript. In Arabidopsis this enzyme is important for the activation of defense responses dependent from salicylic acid (Jirage et al., 1999), a phytohormone increasingly recognized for its

significance in improving plant abiotic stress-tolerance (Khan et al., 2015). Therefore, miRC37052-11 could be involved in a salicylic acid-mediated response of *A. donax* to stress conditions.

5. CONCLUSION

To conclude, despite the complexity of the *A. donax* genome (Bucci et al., 2013; Hardion et al., 2015) and the lack of its full sequence, we identified several known miRNAs and associated pre-mirRNAs, expanding the list of species hosting conserved miRNAs in their genome. We also highlighted the existence of conserved miRNA-based responsive patterns, selecting stress-responsive miRNAs that can be considered promising targets for crop tolerance improving. As mining of species-specific miRNAs has still not been carried out in *A. donax*, we proceeded with a high-throughput sequencing based annotation of novel candidate miRNAs and their targets and identified new species-specific miRNAs expressed under salt and/or phosphorus stress conditions. Far to be exhaustive, our results constitute a first step towards a more extensive understanding of the microRNA-based mechanisms adopted by this economically important crop to cope with environmental adversities, and point out the need to improve *A. donax* genome and transcriptome data resolution.

Data availability statement

The data that support the findings of this study are included in the manuscript/supplementary files. Raw sequencing data are openly available in the Sequence Read Archive (https://www.ncbi.nlm.nih.gov/sra) at SRA accession PRJNA774159.

References

Achkar, N. P., Cambiagno, D. A., & Manavella, P. A. (2016). miRNA Biogenesis: A Dynamic Pathway. *Trends Plant Sci, 21*(12), 1034-1044. doi:10.1016/j.tplants.2016.09.003

Addo-Quaye, C., Miller, W., & Axtell, M. J. (2009). CleaveLand: a pipeline for using degradome data to find cleaved small RNA targets. *Bioinformatics, 25*(1), 130-131. doi:10.1093/bioinformatics/btn604

Alptekin, B., Akpinar, B. A., & Budak, H. (2016). A Comprehensive Prescription for Plant miRNA Identification. *Front Plant Sci, 7*, 2058. doi:10.3389/fpls.2016.02058

Axtell, M. J., & Meyers, B. C. (2018). Revisiting Criteria for Plant MicroRNA Annotation in the Era of Big Data. *Plant Cell, 30*(2), 272-284. doi:10.1105/tpc.17.00851

Barrero, R. A., Guerrero, F. D., Moolhuijzen, P., Goolsby, J. A., Tidwell, J., Bellgard, S. E., & Bellgard, M. I. (2015). Shoot transcriptome of the giant reed, Arundo donax. *Data Brief, 3*, 1-6. doi:10.1016/j.dib.2014.12.007

Bartel, D. P. (2004). MicroRNAs: genomics, biogenesis, mechanism, and function. *Cell, 116*(2), 281-297. doi:10.1016/s0092-8674(04)00045-5

Bolger, A. M., Lohse, M., & Usadel, B. (2014). Trimmomatic: a flexible trimmer

for Illumina sequence data. *Bioinformatics, 30*(15), 2114-2120. doi:10.1093/bioinformatics/btu170

Bonnet, E., Wuyts, J., Rouzé, P., & Van de Peer, Y. (2004). Evidence that microRNA precursors, unlike other non-coding RNAs, have lower folding free energies than random sequences. *Bioinformatics, 20*(17), 2911-2917. doi:10.1093/bioinformatics/bth374

Bu, D., Luo, H., Huo, P., Wang, Z., Zhang, S., He, Z., . . . Kong, L. (2021). KOBAS-i: intelligent prioritization and exploratory visualization of biological functions for gene enrichment analysis. *Nucleic Acids Res*. doi:10.1093/nar/gkab447

Bucci, A., Cassani, E., Landoni, M., Cantaluppi, E., & Pilu, R. (2013). Analysis of chromosome number and speculations on the origin of Arundo donax L. (Giant Reed). *Cytology and Genetics, 47*(4), 237-241. doi:10.3103/S0095452713040038

Calviño, M., Bruggmann, R., & Messing, J. (2011). Characterization of the small RNA component of the transcriptome from grain and sweet sorghum stems. *BMC Genomics, 12*(1), 356. doi:10.1186/1471-2164-12-356

Campagna, D., Albiero, A., Bilardi, A., Caniato, E., Forcato, C., Manavski, S., . . . Valle, G. (2009). PASS: a program to align short sequences. *Bioinformatics, 25*(7), 967-968. doi:10.1093/bioinformatics/btp087

Cano-Ruiz, J., Ruiz Galea, M., Amorós, M. C., Alonso, J., Mauri, P. V., & Lobo, M. C. (2020). Assessing Arundo donax L. in vitro-tolerance for phytoremediation purposes. *Chemosphere, 252*, 126576. doi:10.1016/j.chemosphere.2020.126576

Chen, J. L., Zheng, Y., Qin, L., Wang, Y., Chen, L. F., He, Y. J., . . . Lu, G. (2016). Identification of miRNAs and their targets through high-throughput sequencing and degradome analysis in male and female Asparagus officinalis. *Bmc Plant Biology, 16*, 19. doi:10.1186/s12870-016-0770-z

Chen, W., He, S., Liu, D., Patil, G. B., Zhai, H., Wang, F., . . . Liu, Q. (2015). A Sweetpotato Geranylgeranyl Pyrophosphate Synthase Gene, IbGGPS, Increases Carotenoid Content and Enhances Osmotic Stress Tolerance in Arabidopsis thaliana. *PLoS One, 10*(9), e0137623. doi:10.1371/journal.pone.0137623

Cocozza, C., Brilli, F., Miozzi, L., Pignattelli, S., Rotunno, S., Brunetti, C., . . . Loreto, F. (2019). Impact of high or low levels of phosphorus and high sodium in soils on productivity and stress tolerance of Arundo donax plants. *Plant Sci, 289*, 110260. doi:10.1016/j.plantsci.2019.110260

Cocozza, C., Brilli, F., Pignattelli, S., Pollastri, S., Brunetti, C., Gonnelli, C., . . . Loreto, F. (2020). The excess of phosphorus in soil reduces physiological performances over time but enhances prompt recovery of salt-stressed Arundo donax plants. *Plant Physiol Biochem, 151,* 556-565. doi:10.1016/j.plaphy.2020.04.011

Corno, L., Lonati, S., Riva, C., Pilu, R., & Adani, F. (2016). Giant cane (Arundo donax L.) can substitute traditional energy crops in producing energy by anaerobic digestion, reducing surface area and costs: A full-scale approach. *Bioresour Technol, 218,* 826-832. doi:10.1016/j.biortech.2016.07.050

Corno, L., Pilu, R., & Adani, F. (2014). Arundo donax L.: a non-food crop for bioenergy and bio-compound production. *Biotechnol Adv, 32*(8), 1535-1549. doi:10.1016/j.biotechadv.2014.10.006

Cristaldi, A., Oliveri Conti, G., Cosentino, S. L., Mauromicale, G., Copat, C., Grasso, A., . . . Ferrante, M. (2020). Phytoremediation potential of Arundo donax (Giant Reed) in contaminated soil by heavy metals. *Environ Res, 185,* 109427. doi:10.1016/j.envres.2020.109427

Cuperus, J. T., Fahlgren, N., & Carrington, J. C. (2011). Evolution and functional diversification of MIRNA genes. *Plant Cell, 23*(2), 431-442. doi:10.1105/tpc.110.082784

D'Imporzano, G., Pilu, R., Corno, L., & Adani, F. (2018). Arundo donax L. can substitute traditional energy crops for more efficient, environmentally-friendly production of biogas: A Life Cycle Assessment approach. *Bioresource Technology, 267,* 249-256. doi:10.1016/j.biortech.2018.07.053

Danelli, T., Laura, M., Savona, M., Landoni, M., Adani, F., & Pilu, R. (2020). Genetic Improvement of. *Plants (Basel), 9*(11). doi:10.3390/plants9111584

Docimo, T., De Stefano, R., De Palma, M., Cappetta, E., Villano, C., Aversano, R., & Tucci, M. (2019). Transcriptional, metabolic and DNA methylation changes underpinning the response of Arundo donax ecotypes to NaCl excess. *Planta, 251*(1), 34. doi:10.1007/s00425-019-03325-w

Evangelistella, C., Valentini, A., Ludovisi, R., Firrincieli, A., Fabbrini, F., Scalabrin, S., . . .Harfouche, A. (2017). De novo assembly, functional annotation, and analysis of the giant reed (Arundo donax L.) leaf transcriptome provide tools for the development of a biofuel feedstock. *Biotechnology for Biofuels, 10*(1), 138.

doi:10.1186/s13068-017-0828-7

Fernando, A. L., Barbosa, B., Costa, J., & Papazoglou, E. G. (2016). Chapter 4 - Giant Reed (Arundo donax L.): A Multipurpose Crop Bridging Phytoremediation with Sustainable Bioeconomy. In M. N. V. Prasad (Ed.), *Bioremediation and Bioeconomy* (pp. 77-95): Elsevier.

Fu, R., Zhang, M., Zhao, Y. C., He, X. C., Ding, C. Y., Wang, S. K., . . . Wang, B. H. (2017). Identification of Salt Tolerance-related microRNAs and Their Targets in Maize (Zea mays L.) Using High-throughput Sequencing and Degradome Analysis. *Frontiers in Plant Science, 8*, 13. doi:10.3389/fpls.2017.00864

Fu, Y., Poli, M., Sablok, G., Wang, B., Liang, Y. C., La Porta, N., . . . Varotto, C. (2016). Dissection of early transcriptional responses to water stress in Arundo donax L. by unigene-based RNA-seq. *Biotechnology for Biofuels, 9*. doi:10.1186/s13068-016-0471-8

Ganie, S. A., Ahammed, G. J., & Wani, S. H. (2020). Vascular plant one zinc-finger (VOZ) transcription factors: novel regulators of abiotic stress tolerance in rice (Oryza sativa L.). *Genetic Resources and Crop Evolution, 67*(4), 799-807. doi:10.1007/s10722-020-00904-9

German, M. A., Pillay, M., Jeong, D. H., Hetawal, A., Luo, S. J., Janardhanan, P., . . .Green, P. J. (2008). Global identification of microRNA-target RNA pairs by parallel analysis of RNA ends. *Nature* 53 *Biotechnology, 26*(8), 941-946. doi:10.1038/nbt1417

Hackenberg, M., Shi, B. J., Gustafson, P., & Langridge, P. (2013). Characterization of phosphorus-regulated miR399 and miR827 and their isomirs in barley under phosphorus-sufficient and phosphorus-deficient conditions. *BMC Plant Biol, 13*, 214. doi:10.1186/1471-2229-13-214

Hardion, L., Verlaque, R., Rosato, M., Rosselló, J. A., & Vila, B. (2015). Impact of polyploidy on fertility variation of Mediterranean Arundo L. (Poaceae). *C R Biol, 338*(5),298-306. doi:10.1016/j.crvi.2015.03.013

Haworth, M., Marino, G., Riggi, E., Avola, G., Brunetti, C., Scordia, D., . . . Centritto, M. (2019). The effect of summer drought on the yield of Arundo donax is reduced by the retention of photosynthetic capacity and leaf growth later in the growing season. *Ann Bot, 124*(4),567-580. doi:10.1093/aob/mcy223

Huang, B. S., Gan, L., Chen, D. J., Zhang, Y. C., Zhang, Y. J., Liu, X. L., . . . He, Y. C. (2020). Integration of small RNA, degradome and proteome sequencing in

Oryza sativa reveals a delayed senescence network in tetraploid rice seed. *Plos One, 15*(11), 21. doi:10.1371/journal.pone.0242260

Hunt, A. G. (2020). mRNA 3' end formation in plants: Novel connections to growth, development and environmental responses. *Wiley Interdiscip Rev RNA, 11*(3), e1575. doi:10.1002/wrna.1575

Jeong, D. H., & Green, P. J. (2012). Methods for validation of miRNA sequence variants and the cleavage of their targets. *Methods, 58*(2), 135-143. doi:10.1016/j.ymeth.2012.08.005

Jike, W., Sablok, G., Bertorelle, G., Li, M., & Varotto, C. (2018a). In silico identification and characterization of a diverse subset of conserved microRNAs in bioenergy crop Arundo donax L. *Sci Rep, 8*(1), 16667. doi:10.1038/s41598-018-34982-8

Jike, W., Sablok, G., Bertorelle, G., Li, M. G., & Varotto, C. (2018b). In silico identification and characterization of a diverse subset of conserved microRNAs in bioenergy crop Arundo donax L. *Scientific Reports, 8*. doi:10.1038/s41598-018-34982-8

Jirage, D., Tootle, T. L., Reuber, T. L., Frost, L. N., Feys, B. J., Parker, J. E., . . . Glazebrook, J.(1999). Arabidopsis thaliana PAD4 encodes a lipase-like gene that is important for salicylic acid signaling. *Proc Natl Acad Sci U S A, 96*(23), 13583-13588. doi:10.1073/pnas.96.23.13583

Jámbor, A., & Török, Á. (2019). The Economics of Arundo donax—A Systematic Literature Review. *Sustainability, 11*(15), 4225.

Fhan, M. I., Fatma, M., Per, T. S., Anjum, N. A., & Khan, N. A. (2015). Salicylic acid-induced abiotic stress tolerance and underlying mechanisms in plants. *Front Plant Sci, 6,* 462. doi:10.3389/fpls.2015.00462

Li, B., Zheng, J. C., Wang, T. T., Min, D. H., Wei, W. L., Chen, J., . . . Ma, Y. Z. (2020). Expression Analyses of Soybean VOZ Transcription Factors and the Role of. *Int J Mol Sci, 21*(6). doi:10.3390/ijms21062177

Li, S., Castillo-González, C., Yu, B., & Zhang, X. (2017). The functions of plant small RNAs in development and in stress responses. *Plant J, 90*(4), 654-670. doi:10.1111/tpj.13444

Lin, W. Y., Lin, Y. Y., Chiang, S. F., Syu, C., Hsieh, L. C., & Chiou, T. J. (2018). Evolution of microRNA827 targeting in the plant kingdom. *New*

Phytol,   *217*(4), 1712-1725. doi:10.1111/nph.14938

Liu, B., Li, P., Li, X., Liu, C., Cao, S., Chu, C., & Cao, X. (2005). Loss of function of OsDCL1 affects microRNA accumulation and causes developmental defects in rice. *Plant Physiol, 139*(1), 296-305. doi:10.1104/pp.105.063420

Lorenz, R., Bernhart, S. H., Höner Zu Siederdissen, C., Tafer, H., Flamm, C., Stadler, P. F., & Hofacker, I. L. (2011). ViennaRNA Package 2.0. *Algorithms Mol Biol, 6*, 26. doi:10.1186/1748-7188-6-26

Lucas, S. J., & Budak, H. (2012). Sorting the wheat from the chaff: identifying miRNAs in genomic survey sequences of Triticum aestivum chromosome 1AL.   *PLoS One, 7*(7), e40859. doi:10.1371/journal.pone.0040859

Manavella, P. A., Yang, S. W., & Palatnik, J. (2019). Keep calm and carry on: miRNA biogenesis under stress. *Plant J, 99*(5), 832-843. doi:10.1111/tpj.14369

Mao, W., Li, Z., Xia, X., Li, Y., & Yu, J. (2012). A combined approach of high-throughput sequencing and degradome analysis reveals tissue specific expression of microRNAs and their targets in cucumber. *PLoS One, 7*(3), e33040. doi:10.1371/journal.pone.0033040

Mathelier, A., & Carbone, A. (2010). MIReNA: finding microRNAs with high accuracy and no learning at genome scale and from deep sequencing data. *Bioinformatics, 26*(18), 2226-2234. doi:10.1093/bioinformatics/btq329

Mi, S., Cai, T., Hu, Y., Chen, Y., Hodges, E., Ni, F.,   Qi, Y. (2008). Sorting of small RNAs into Arabidopsis argonaute complexes is directed by the 5' terminal nucleotide. *Cell, 133*(1), 116-127. doi:10.1016/j.cell.2008.02.034

Morin, R. D., Aksay, G., Dolgosheina, E., Ebhardt, H. A., Magrini, V., Mardis, E. R., Unrau, P. J. (2008). Comparative analysis of the small RNA transcriptomes of Pinus contorta and Oryza sativa. *Genome Research, 18*(4), 571-584. doi:10.1101/gr.6897308

Pantaleo, V., Szittya, G., Moxon, S., Miozzi, L., Moulton, V., Dalmay, T., & Burgyan, J. (2010). Identification of grapevine microRNAs and their targets using   high-throughput sequencing and degradome analysis. *Plant J, 62*(6), 960-976. doi:10.1111/j.0960-7412.2010.04208.x

Pegler, J. L., Grof, C. P. L., & Eamens, A. L. (2019). The Plant microRNA Pathway: The Production and Action Stages. *Methods Mol Biol, 1932*, 15-39. doi:10.1007/978-1-4939-9042-9_2

Prasad, K. V. S. K., Xing, D., & Reddy, A. S. N. (2018). Vascular Plant One-Zinc-

Finger (VOZ) Transcription Factors Are Positive Regulators of Salt Tolerance in Arabidopsis. *International journal of molecular sciences, 19*(12), 3731. doi:10.3390/ijms19123731

Rehman, S. U., Qanmber, G., Tahir, M. H. N., Irshad, A., Fiaz, S., Ahmad, F., Geng, Z. (2021). Characterization of Vascular plant One-Zinc finger (VOZ) in soybean (Glycine max and Glycine soja) and their expression analyses under drought condition. *PLOS ONE, 16*(7), e0253836. doi:10.1371/journal.pone.0253836

Ren, L., Eller, F., Lambertini, C., Guo, W. Y., Brix, H., & Sorrell, B. K. (2019). Assessing nutrient responses and biomass quality for selection of appropriate paludiculture crops. *Sci Total Environ, 664*, 1150-1161. doi:10.1016/j.scitotenv.2019.01.419

Robinson, M. D., & Oshlack, A. (2010). A scaling normalization method for differential expression analysis of RNA-seq data. *Genome Biol, 11*(3), R25. doi:10.1186/gb-2010-11-3-r25

Sablok, G., Fu, Y., Bobbio, V., Laura, M., Rotino, G., Bagnaresi, P., . . . Varotto, C. (2014). Fuelling genetic and metabolic exploration of C-3 bioenergy crops through the first reference transcriptome of Arundo donax L. *Plant Biotechnology Journal, 12*(5), 554-567. doi:10.1111/pbi.12159

Shaheen, S., Ahmad, R., Mahmood, Q., Mubarak, H., Mirza, N., & Hayat, M. T. (2018). Physiology and selected genes expression under cadmium stress in Arundo donax L. *International Journal of Phytoremediation, 20*(11), 1162-1167. doi:10.1080/15226514.2018.1460312

Sicilia, A., Santoro, D. F., Testa, G., Cosentino, S. L., & Lo Piero, A. R. (2020). Transcriptional response of giant reed (Arundo donax L.) low ecotype to long-term salt stress by unigene-based RNAseq. *Phytochemistry, 177*, 112436. doi:10.1016/j.phytochem.2020.112436

Song, C., Wang, C., Zhang, C., Korir, N. K., Yu, H., Ma, Z., & Fang, J. (2010). Deep sequencing discovery of novel and conserved microRNAs in trifoliate orange (Citrus trifoliata). *BMC Genomics, 11*, 431. doi:10.1186/1471-2164-11-431

Sun, X., Lin, L., & Sui, N. (2019). Regulation mechanism of microRNA in plant response to abiotic stress and breeding. *Mol Biol Rep, 46*(1), 1447-1457. doi:10.1007/s11033-018-4511-2

Tarazona, S., Furió-Tarí, P., Turrà, D., Pietro, A. D., Nueda, M. J., Ferrer, A., & Conesa,

A. (2015). Data quality aware analysis of differential expression in RNA-seq with NOISeq R/Bioc package. *Nucleic Acids Res, 43*(21), e140. doi:10.1093/nar/gkv711

Unver, T., & Budak, H. (2009). Conserved microRNAs and their targets in model grass species Brachypodium distachyon. *Planta, 230*(4), 659-669. doi:10.1007/s00425-009-0974-7

Vazquez, F., Blevins, T., Ailhas, J., Boller, T., & Meins, F. (2008). Evolution of Arabidopsis MIR genes generates novel microRNA classes. *Nucleic Acids Res, 36*(20),6429-6438. doi:10.1093/nar/gkn670

Wang, M., Guo, W., Li, J., Pan, X., Pan, L., Zhao, J., . . . Liu, Q. (2021). The miR528-AO Module Confers Enhanced Salt Tolerance in Rice by Modulating the Ascorbic Acid and Abscisic Acid Metabolism and ROS Scavenging. *Journal of Agricultural and Food Chemistry, 69*(31), 8634-8648. doi:10.1021/acs.jafc.1c01096

Xiao, M., Li, Z., Zhu, L., Wang, J., Zhang, B., Zheng, F., . . . Zhang, Z. (2021). The Multiple Roles of Ascorbate in the Abiotic Stress Response of Plants: Antioxidant, Cofactor, and Regulator. *Front Plant Sci, 12*, 598173. doi:10.3389/fpls.2021.598173

Zhang, B. H., Pan, X. P., Cox, S. B., Cobb, G. P., & Anderson, T. A. (2006). Evidence that miRNAs are different from other RNAs. *Cell Mol Life Sci, 63*(2), 246-254. doi:10.1007/s00018-005-5467-7

Zhao, B., Ge, L., Liang, R., Li, W., Ruan, K., Lin, H., & Jin, Y. (2009). Members of miR-169 family are induced by high salinity and transiently inhibit the NF-YA transcription factor. *BMC Mol Biol, 10*, 29. doi:10.1186/1471-2199-10-29

Zhao, Y., Xu, K., Liu, G. R., Li, S. S., Zhao, S. H., Liu, X. W., . . . Xiao, K. (2020). Global identification and characterization of miRNA family members responsive to potassium deprivation in wheat (*Triticum aestivum* L.). *Scientific Reports, 10*(1), 13. doi:10.1038/s41598-020-72642-y

Supporting information

Name	Sequence	Melting temperature
5' adapter_fw	5'-GTTCAGAGTTCTACAGTCCGAC-3'	47°C
TR10651_rev	5'-CCTTGAACCACCTCTTGTCGC-3'	56°C
TR4471_rev	5'-TCCCTCACCTCTCTGCTCATG-3'	54°C

Table S1. Primer sequences and melting temperature used for PCRs in 5' RACE

pool	raw reads (redundant)	raw reads (non-redundant)	clean reads (redundant)	clean reads (non-redundant)
C	12,616,870	2,008,550	2,766,570	1,105,041
+P	14,180,274	2,751,532	4,096,100	1,704,026
+Na	11,403,618	1,963,790	2,545,750	983,071
+NaP	9,813,447	1,741,065	2,683,450	880,357

Table S2. Reads statistics of small RNAs high-throughput sequencing

Table S3. *A.donax* conserved miRNAs with their expression values and identified targets

Position	Adenine		Cytosine		Guanine		Uracil	
	No.	Percentage (%)	No.	Percentage (%)	No.	Percentage (%)	No.	Percentage (%)
1	16	11.94	11	8.21	36	26.87	71	52.99
2	20	14.93	18	13.43	47	35.07	49	36.57
3	29	21.64	28	20.90	55	41.04	22	16.42
4	54	40.30	37	27.61	31	23.13	12	8.96
5	57	42.54	22	16.42	31	23.13	24	17.91
6	44	32.84	28	20.90	39	29.10	23	17.16
7	36	26.87	17	12.69	28	20.90	53	39.55
8	20	14.93	19	14.18	76	56.72	19	14.18
9	24	17.91	33	24.63	36	26.87	41	30.60
10	46	34.33	26	19.40	21	15.67	41	30.60
11	15	11.19	28	20.90	41	30.60	50	37.31
12	19	14.18	26	19.40	60	44.78	29	21.64
13	25	18.66	34	25.37	50	37.31	25	18.66
14	28	20.90	37	27.61	44	32.84	25	18.66
15	34	25.37	26	19.40	36	26.87	38	28.36
16	25	18.66	27	20.15	42	31.34	40	29.85
17	42	31.34	25	18.66	32	23.88	35	26.12
18	34	25.37	38	28.36	32	23.88	30	22.39
19	28	20.90	78	58.21	21	15.67	7	5.22
20	25	18.66	35	26.12	12	8.96	62	46.27
21	20	16.39	44	36.07	28	22.95	30	24.59
22	14	43.75	8	25.00	3	9.38	7	21.88
23	3	60.00	1	20.00	0	0.00	1	20.00
24	2	50.00	0	0.00	0	0.00	2	50.00
Overall	660	23.21	646	22.72	801	28.17	736	25.89

Table S4. Base composition of *A. donax* conserved miRNAs and comparison with Jike et al. (2018)

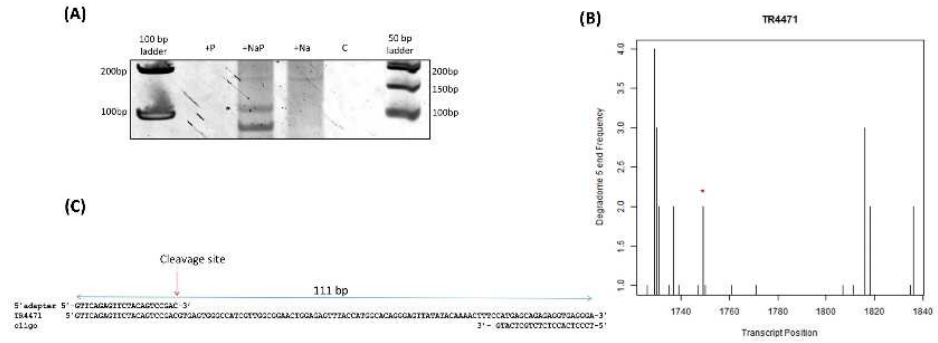**Table S5.** *A.donax* miRCs with their expression values and identified targets

Fig. S1. 5' RACE on transcript TR4471, coding for a 32kDa dirigent-like protein targeted by miR156d-3p
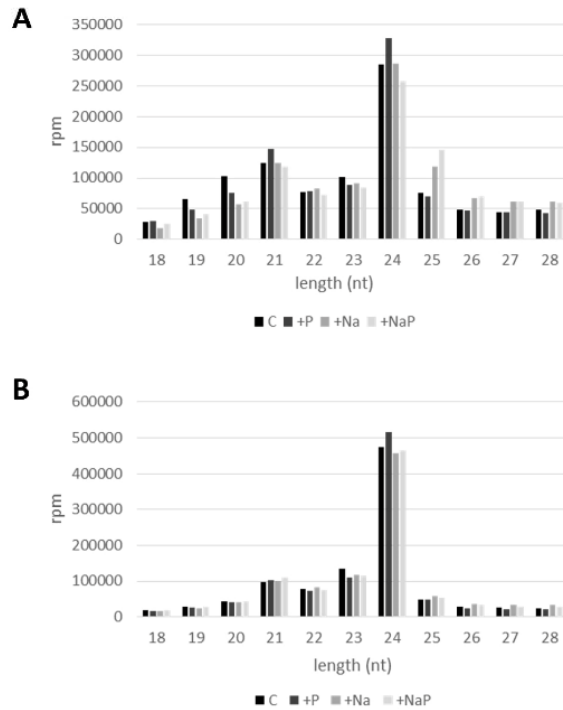
Figure and table legends

Fig. 1. Length distribution of A) redundant and B) non-redundant reads in C, +P, +Na, +NaP libraries; rpm: reads per million.
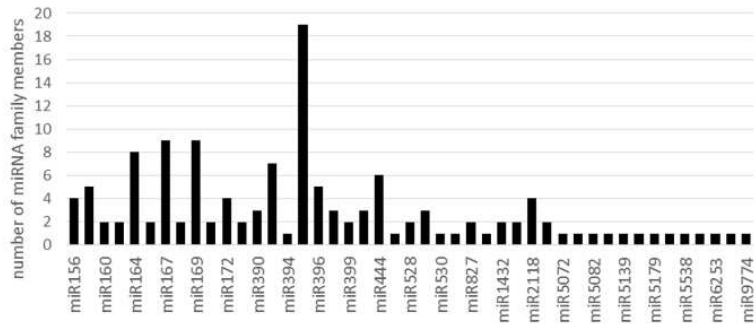
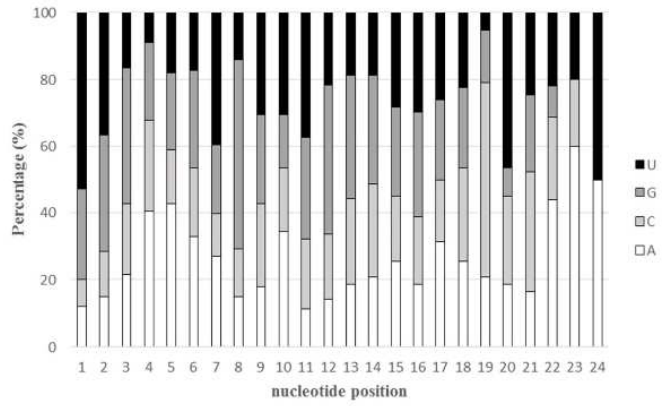**Fig. 2.** Number of miRNA members for each conserved miRNA family identified in *A.donax* L.

Fig. 3. Nucleotide composition of A. donax L. mature conserved miRNAs.

Fig. 4 – A) Heatmap of the conserved miRNA relative expression in response to stress; B) Ven Diagram reporting the number of conserved miRNAs differentially expressed in response to stress; C) Heatmap of the novel candidate miRNA relative expression in response to stress. +P, excess of phosphorus; +Na, excess of NaCl; +NaP, excess of phosphorus and NaCl; M values indicate the log2(FoldChange) in each stress condition in respect to control treatment; asterisk indicates high confident expression values (NOISeq probability>0.9); dark green arrows indicate miRNAs found only in the poaceae family; light green arrows indicate miRNAs found only in poaceae and bromeliaceae;
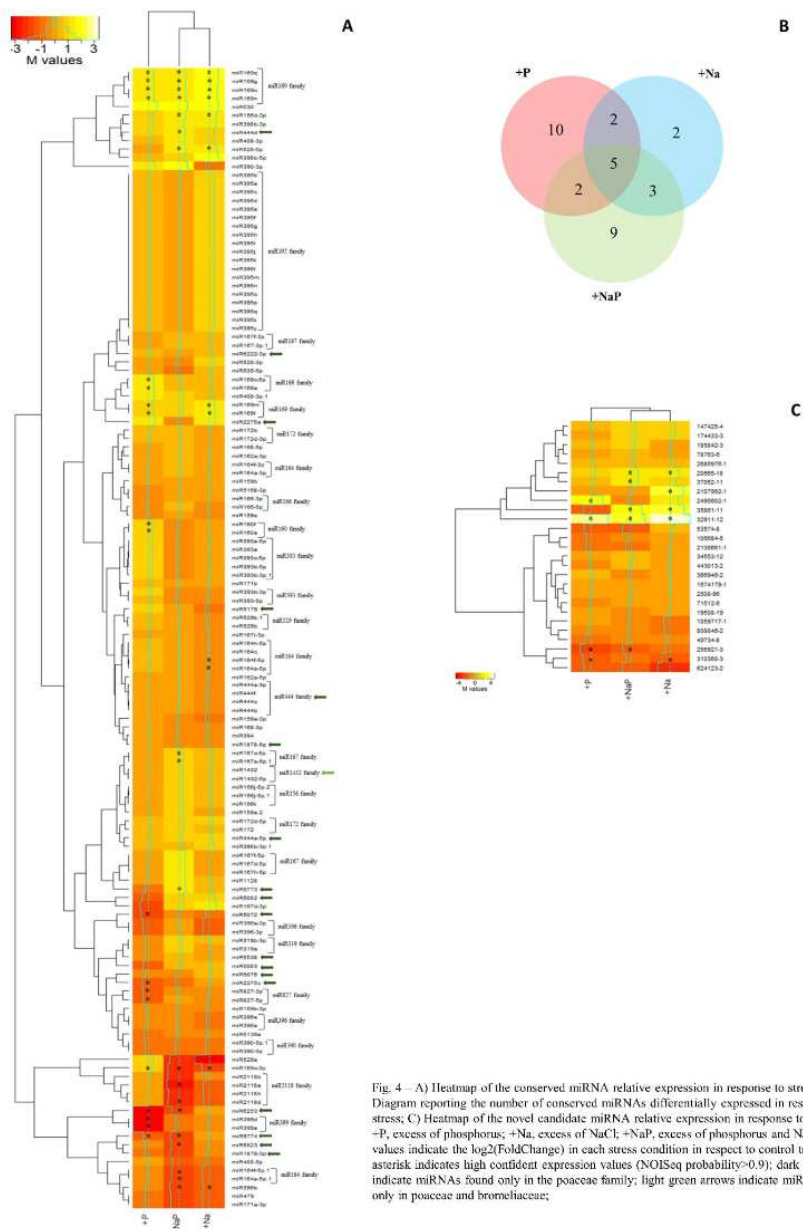
Fig. 4. A) Heatmap of the conserved miRNA relative expression in response to stress; B) Ven Diagram reporting the number of conserved miRNAs differentially expressed in response to stress; C) Heatmap of the novel candidate miRNA relative expression in response to stress. +P, excess of phosphorus; +Na, excess of NaCl; +NaP, excess of phosphorus and NaCl; M values indicate the log2(FoldChange) in

each stress condition in respect to control treatment; asterisk indicates high confident expression values (NOISeq probability>0.9); dark green arrows indicate miRNAs found only in the poaceae family; light green arrows indicate miRNAs found only in poaceae and bromeliaceae.
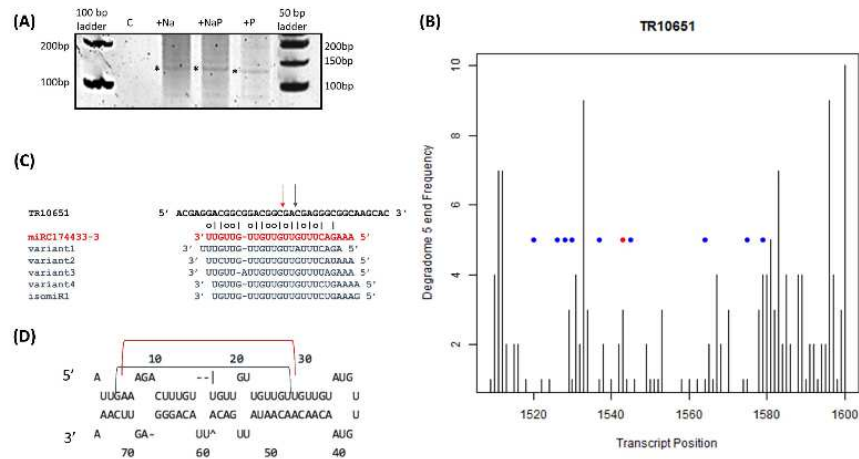

Fig. 5. 5' RACE on transcript TR10651 coding for an oxygen-evolving enhancer chloroplastic protein targeted by miRC174433-3. A) Fragment of 120 bp amplified by 5'RACE in all treatments, except the control treatment, (*) indicates the eluted band; B) CleaveLand plot for TR10651 in the range of 1500-1600 nt, red dot indicates the slicing site found by CleaveLand, blue dots indicate sites derived from Sanger sequencing of clones obtained by 5'RACE; C) Schematic representation of miRC174433-3 cleavage site. Red arrow indicates the cleavage site confirmed by CleaveLand; blue arrow indicates the cleavage sites found by 5' RACE analysis. Possible isomiRs are reported in blue; D) pre-miRNA hairpin, the red bracket represent the position of miRC174433-3 and the blue bracket represents the position of miRC174433-3 variants.

	Name	Target Id	Target Annotation	Category	p-value
Known miRNAs	miR1128	TR24300	Senescence-associated partial	2	0.082
	miR156d-3p	**TR4471**	**32 kDa dirigent-like**	**2**	**0.037**
	miR156j-5p.2	TR14474	Hypothetical protein SETIT_036744mg	0	0.007
	miR159a-3p	TR5918	n/a	3	0.055
	miR159b	TR24324	n/a	3	0.058
	miR159b	TR30640	n/a	0	0.059
	miR159e	TR11309	BEL1-like homeodomain 4	2	0.025
	miR159e	TR4218	Uncharacterized protein LOC101753284 isoform X1	3	0.046
	miR159e	TR6528	Ankyrin repeat domain-containing 13B	0	0.066
	miR167c-5p	TR29148	ATP synthase delta chloroplastic	2	0.005

	miRNA	TR	Annotation	Cat.	p-value
	miR169c-3p	TR24300	Senescence-associated partial	2	0.051
	miR172b	TR25857	Hypothetical protein SETIT_019819mg	3	0.086
	miR172d-5p	TR29998	Pentatricopeptide repeat-containing At1g18485	3	0.036
	miR319a	TR1733	Calcineurin B 1	3	0.034
	miR319b-3p	TR24557	n/a	0	0.026
	miR396b	TR20898	Chlorophyll a-b binding chloroplastic-like	2	0.062
	miR528-3p	TR1686	n/a	3	0.266
	miR528-3p	TR8922	Peptidyl-prolyl cis-trans isomerase-like 3	0	0.313
	miR529a	TR20898	n/a	3	0.163
	miR6253	TR13145	Serine carboxypeptidase II-3	3	0.066
	miR9774	TR9615	F-box SKIP22	3	0.022
Candidate miRNAs	**miRC174433-3**	**TR10651**	**Oxygen-evolving enhancer chloroplastic**	**3**	**0.553**
	miRC174433-3	TR27080	Gamma-glutamyl peptidase 5-like	2	0.063
	miRC174433-3	TR8896	Hypothetical protein SORBI_004G242300	0	0.141
	miRC366946-2	TR28663	Cytochrome P450 89A2	2	0.005
	miRC71512-6	TR24307	B-box zinc finger 24	2	0.064
	miRC808846-2	TR19738	n/a	3	0.083

Table 1. List of miRNA and miRC targets with the corresponding CleaveLand category and p-value (only targets with CleaveLand category below or equal to 3 are reported; targets selected for confirmation by 5'RACE are in bold; n/a, not annotated.

	Group	Term	+P	+Na	+NaP
Targets of miRNAs	Energy metabolism	Oxidative phosphorylation	-	0.1207	0.129035
		Photosynthesis	-	0.063847	0.068409
	RNA processing and transcription	Spliceosome	0.157475	0.157475	0.168096
		mRNA surveillance pathway	0.091913	0.091913	0.098372
	Protein metabolism	Ubiquitin mediated proteolysis	0.112235	0.112235	0.120026
		Cysteine and methionine metabolism	0.098997	-	-
		Protein processing in endoplasmic reticulum	0.176382	0.176382	0.18813
	Carbohydrate metabolism	Starch and sucrose metabolism	0.131362	0.131362	-
	Secondary metabolism	Ascorbate and aldarate metabolism	**0.044951**	**0.044951**	**0.048198**
		Biosynthesis of secondary metabolites	0.646972	0.646972	-
		Term	**+P**	**+Na**	**+NaP**
Targets of miRCs	Energy metabolism	Carbon fixation in photosynthetic organisms	**0.012466**	**0.036928**	**0.036928**
		Photosynthesis	-	**0.035997**	**0.035997**
	Energy and carbohydrate metabolism	Carbon metabolism	**0.042932**	0.123328	0.123328
		Inositol phosphate metabolism	-	**0.029458**	**0.029458**
		Pentose phosphate pathway	**0.009281**	**0.027582**	**0.027582**
	RNA processing and transcription	RNA polymerase	**0.007526**	**0.022406**	**0.022406**
		Spliceosome	-	0.090822	0.090822
	Signal transduction	Phosphatidylinositol signaling system	-	**0.030863**	**0.030863**
	Protein metabolism	Biosynthesis of amino acids	**0.037804**	0.109161	0.109161
		Biosynthesis of secondary metabolites	0.175424	0.108634	0.108634

| | Secondary metabolism | Terpenoid backbone biosynthesis | - | **0.026173** | **0.026173** |

Table 2. KEGG functional analysis of miRNA and miRCs targets; p-value <0.05 are in bold.

PAPER III

Modulation of class III peroxidase pathways and phenylpropanoids in *Arundo donax* under salt and phosphorus stress

Cocozza Claudia[1], Bartolini Paola[2], Brunetti Cecilia[2], Miozzi Laura[3], Pignattelli Sara[4], Podda Alessandra[3], Scippa Gabriella Stefania[4], Trupiano Dalila[4], Rotunno Silvia[2,4], Brilli Federico[2], Maserti Bianca Elena[2]

[1] Department of Agriculture, Food, Environment and Forestry, University of Florence, 50145 Florence, Italy

[2] CNR-IPSP- National Research Council, Institute for Sustainable Plant Protection, Strada delle Cacce 73, 10135 Torino, Italy

[3] Univerza v Novi Gorici, SI-5000 Nova Gorica, Slovenija

[4] Department of Biosciences and Territory, University of Molise, 86090 Pesche, Italy

Corresponding author: claudia.cocozza@unifi.it

Present address: Department of Agriculture, Food, Environment and Forestry, University of Florence, 50145 Florence, Italy

In preparation

ABSTRACT

Arundo donax L. is an invasive species that has been recently employed for biomass production due to its well-known ability to colonize harsh environment. The present study investigated the modulation of class III peroxidases and their substrates phenylpropanoids, through biochemical and transcriptomic analysis in *A. donax* after Na^+ and P excess supply, both in single stress and in combination, and after growth at low P level. The levels of hydrogen peroxide, flavonoids (i.e., quercetin, apigenin and kaempferol) and the activity of class III peroxidases, as well as the expression of several genes encoding for their enzymes involved in their biosynthesis, increased when Na^+ was supplied in combination with P. These results suggest that those biomolecules are involved in the response of *A. donax*, to the presence of +Na and P in the soil. Moreover, even though at the sampling time no significant accumulation of lignin has been determined, the trend of accumulation of such metabolite and most of all the increase of several transcripts involved in its synthesis was found. This work for the first time indicates the need of further investigation devoted to elucidate whether the strengthening of cell walls via lignin synthesis is one of the mechanisms used by *A. donax* to adapt to harsh environments.

Keywords

Arundo donax, stress tolerance, salt stress, phosphorus stress, peroxidase, transcriptome

1. Introduction

Soil salinity affects more than 1 billion of hectares worldwide and this global threat is gradually increasing. Soil salinization reduces soil quality and limits plant growth thus leading to the abandonment of agricultural soils. Salinity stress, as excess of sodium (Na^+), affects plant development and reproduction by reducing water uptake from soil, and induces to both ion toxicity and nutrient deficiency through the induction of osmotic and oxidative stress (Siddiqui et al., 2008; Almeida Machado and Serralheiro, 2017). Even though many researches have been performed to elucidate salinity stress, my questions should be answered yet (Isayenkov and Maathuis, 2019). Moreover, salinity stress significantly reduces phosphorus (P) uptake in plants because phosphate ions precipitate with calcium (Ca) ions (Grattan and Grieve, 1998). Therefore, high salinity and low levels of P are concomitant in calcareous and alkaline soils typical of Mediterranean area (Zribi et al., 2012). When a P excess occurs in soil, this element becomes toxic, thus causing eutrophication (Smith and Schindler, 2009) and reducing plant performances by interfering with the biosynthesis of starch (Cocozza et al., 2020), secondary metabolites (e.g. isoprenoids) (Cocozza et al., 2020), nitrate assimilation, and plant's nutrients absorption (Crouse, 2018). A direct result of these effects is the enhanced accumulation of reactive oxygen species (ROS) which can have a role both as signaling molecules (Foyer 2018) and cause oxidative stress leading to programmed cell death (Van Breusegem and Dat, 2006). As direct consequence of ROS accumulation, plant metabolism is directed toward the activation of a complex antioxidant machinery including enzymatic and non-enzymatic compounds. Among the non-enzymatic compounds, the biosynthesis of specific secondary metabolites, phenylpropanoids, in particular flavonoids, results rapidly activated in response to changes in redox state of the cell (Deng and Fu, 2017; Sharma et al., 2019). Indeed, flavonoids are mainly located in the vacuoles where they may scavenge high doses of H_2O_2 by forming a co-operative regenerating cycle with ascorbic acid and vacuolar peroxidase (Yamasaki et al., 1997;

3

Takahama and Oniki, 2000; Takahama, 2004). In particular, this model, corroborated by the study conducted by Ferreres et al. (2011), suggests that H_2O_2 is scavenged by peroxidases using flavonols as substrates, and then flavonoid radicals are recycled back by ascorbic acid to their reduced forms.

Class III peroxidases are secretory enzymes which play role in a broad range of physiological and developmental processes (Lüthje and Martinez-Cortes, 2018). Peroxidases are responsible either for cell elongation or cell wall stiffening, affecting carbon allocation, auxin level and redox homeostasis, which implicates their key role as being in the regulation of growth and defense under stress condition (Kidwai et al., 2020). Class III peroxidases act through three different cycles, namely peroxidative cycle, oxidative and hydroxylic cycles. In their main peroxidative cycle, class III plant peroxidases act as antioxidant molecules involved in detoxification or generation of hydrogen peroxide (H_2O_2), catalysing the reduction of H_2O_2 by taking electrons from various donor molecules such as phenolic compounds, lignin precursors (i.e. caffeic acid), auxin, or secondary metabolites (Ferreres et al., 2011; Lüthje and Martinez-Cortes, 2018). Moreover their role in the plant lignification has also been reported (Almagro et al., 2009; Marjamaa et al., 2009).

The cultivation of marginal lands using tolerant crops has been proposed to reverse non-sustainable management and land degradation (Schröder et al., 2018). Among non-food and bioenergy crops that represent valid solutions for land recovery, one of the most promising is the giant reed (*Arundo donax L.*) (Corno et al., 2014). It is a perennial and herbaceous plant, occurring over a wide range of climatic habitats and growing spontaneously and abundantly all over the Mediterranean region (Sánchez et al., 2016), due to its high performance. Despite being a C3 plant, *A. donax* shows very high photosynthetic rate (37 µmol m^{-2} s^{-1}) and productivity like C4 species, with an average biomass yield ranging between 21 and 51 t ha^{-1} under medium-low supply of nitrogen and water (Angelini et al., 2009). *A. donax* is

4

known to be growing in all types of soil, from clay to sand, with presence of rocks or not, with soil pH ranging from 5 to 8.7, and in conditions of high salinity (De Stefano et al., 2017).

Several investigations have been conducted to elucidate the mechanisms underlying the ability of *A. donax* to colonize harsh environments. The transcriptional response of *A. donax* to long-term salt stress was elucidated by Sicilia et al. (2020). Furthermore, Docimo et al. (2020) observed increased proline, ABA and leaf antioxidants and paralleled up-regulation of antioxidant genes in different genotypes of *A. donax* exposed to salinity stress. Negative effects on the physiological parameters and increase of hydrogen peroxide and secondary compounds have been reported in *A. donax* under salinity stress (Cocozza et al 2019; 2020). However, despite in wheat a member of Class III peroxidase was reported to enhance salinity tolerance (Su et al., 2020), and class III peroxidases are well known to act in abiotic and biotic mechanisms (Kidwai et al., 2020) no information on the involvement of these classes of enzymes has been reported in *A. donax* yet. Unravelling the involvement of class III PRXs in this plant species plants might help to better understanding the response mechanism of such non-food crop plants and their ability to colonize harsh environments.

In this work the modulation of antioxidant scavengers, class III peroxidases and phenylpropanoids, and their encoding genes were determined in *A. donax* after Na$^+$ and P excess supply, both in single stress and in combination, and after growth at low P level. The long-term experimental treatment (43 days) allowed to elucidate how class III peroxidases and phenylpropanoids, as well as their potential substrates act into the mechanisms conferring plasticity to environmental stress to *A. donax.*

2. Materials and Methods

2.1. Plant material and growth conditions

5

Arundo donax (L.) plants were obtained by rhizomes collected in Sesto Fiorentino (Italy). Rhizomes were hydrated in tap water for one day and then planted in 6 L pots in quartz sand. The experiment was carried out in a conditioned climatic chamber, where temperature ranged between 24°C and 26°C, relative air humidity between 40% and 60%, photosynthetic photon flux density (PPFD) was 700 μmol m^{-2} s^{-1} for 14 h per day. Plants were watered twice per week with half strength Hoagland solution for two months before the beginning of the experiment. The experiment was performed for 43 days by applying four different nutrient conditions: Hoagland solution (control); Hoagland solution deprived of phosphorus (-P); Hoagland solution complemented with 8.0 mM KH_2PO_4 (+P), very high phosphorus levels, as commonly observed in water (Neal et al., 2003); Hoagland solution complemented with 200 mM NaCl (+Na), 100 mM NaCl in Hoagland solution causes electrical conductivity of 13 dS m^{-1} (Carrasco-Ríos et al. 2013); and Hoagland solution complemented with both 200 mM NaCl and 8.0 mM KH_2PO_4 (+NaP). All different nutrient conditions were supplied twice a week by causing an "acute" stress to plants, as found in Cocozza et al. (2020). Four replicates (plants) per treatments were sampled for the following analyses. Fully expanded young leaves of *A. donax* plants were sampled after 43 days of treatment (stress point, St), and after a recovery period, after stopping the treatments, lasting 14 days (Re). In the companion study, plant phenotyping (biometrics and gas-exchange) of *A. donax* in response to Na and P high supply dropped at 43 days and it was restored after 14 days of suspension of stress conditions (Cocozza et al. 2020).

2.2 Determination of hydrogen peroxide and ascorbic acid and dehydroascorbate

Endogenous H_2O_2 content was determined according to the method of Velikova et al. (2000), with slight modifications. Briefly, leaves (0.25 g) were ground to a powder by mortar and pestle in liquid nitrogen and then, homogenated with 3 mL of 5 % (w/v) trichloroacetic acid (TCA) at 4 °C. The homogenate was centrifuged at 12,000g for 215 min. To 0.5 mL aliquot of the supernatant, 0.5 mL of 10 mM potassium

6

phosphate buffer (pH 7.0) and 0.75 ml of 1 M KI were added, and the absorbance was measured at 390 nm (EasySpec UV-Vis spectrophotometer, SAFAS). The relative absorbance (sample absorbance minus the absorbance of the same supernatant aliquot without KI) was used to determine the H_2O_2 content against a H_2O_2 standard curve. Data were expressed as $\mu mol\ g^{-1}$ DW.

Ascorbic acid (AS) and dehydroascorbate (DHA) were quantified following the method of Law et al., (1983). Briefly, leaves (0.5 g) were crushed with liquid nitrogen and then homogenized in 400 μL of 10% (w/v) trichloroacetic acid (TCA). After vortexing, the homogenate was kept in ice for 5 min and 10 μL of 5M NaOH solution was added. Then, samples were vortexed and centrifuged for 2 min at room temperature (RT). Two hundred microliters of 150 mM-NaH_2PO_4 buffer (pH 7.4) and 200 μL of distilled water were added to 200μL of homogenate sample. To another homogenate sample aliquot (200μL), 200 μL of 150 mM-NaH_2PO_4 buffer and 100μL of 10 mM-dithiothreitol were added. The solution was vortex-mixed and incubated at RT for 15 min, then 100 μL of 0.5 (w/v) N-ethylmaleimide was added. Both samples were vortex-mixed, incubated for 2 min at RT, and then 400 μL of 10% (w/v) TCA, 400 μL of 44% (w/v) H_3PO_4, 400 μL of bypiridyl in 70% (v/v) ethanol and 200 μL of 3% (w/v) $FeCl_3$ were added. Samples were vortex-mixing and incubated at 37°C for 60 min. The absorbance was measured at 525 nm and a standard curve with AS and DHA was used for the calibration. AS and DHA content was expressed as $\mu g\ g^{-1}$.

2.3 Class III peroxidase assay

Stored leaves samples at -80°C were grounded to a powder by mortar and pestle in liquid nitrogen. Then, 100 mg of leaf samples were solubilised in 500 μl of 50 mM Tris-HCl pH 7.5 and 1% (3-((3-cholamidopropyl) dimethylammonio)-1-propanesulfonate) (CHAPS) for enzyme assay for 2h and then centrifuged at 14 g for 30 min at 4°C. The protein concentration was determined by using Bradford assay (Bradford, 1976).

7

The activity of class III peroxidases of *A. donax* (AdPrx) was determined using three different substrates, guaiacol, syringaldazine and coniferyl alcohol, as described in Cesarino et al. (2012), and adding to the assay solution a volume of leaf homogenate corresponding to 10 mg of protein. Briefly the activity of AdPrx using guaiacol was determined measuring the increase of absorbance at 470 nm for 2 min relative to guaiacol oxidation to tetraguaiacol (ϵ = 26.6 m M^{-1} cm^{-1}). The assay (1 mL) contained leaf homogenate, 8.26 mM guaiacol and 0.03% H_2O_2 (v/v) in 50 mM Na-acetate buffer (pH 5.0) and the Guaiacol activity was expressed as µmol tetraguaiacol min^{-1} mg^{-1} total protein.

The AdPrx activity using syringaldazine as substrate was measured by following the increase of absorbance at 530 nm (ϵ = 27.1 $mM^{-1}cm^{-1}$) for 2 min in 1 mL reaction mixture containing 50 mM of syringaldazine, 0.03% H_2O_2 and a volume of leaf homogenate in 20 mM Tris HCl buffer (pH 7.5). Syr activity was expressed as µmol SYR oxidized min^{-1} mg^{-1} total protein. The AdPrx activity when coniferyl alcohol was used as substrate was determined by following the decrease of absorbance at 262 nm (ϵ= 9.6 $mM^{-1}cm^{-1}$) for 2 min in a 1 mL reaction mixture containing 50 mM coniferyl alcohol, 0.03% H_2O_2 and a volume of leaf homogenate corresponding to 10 mg of protein in 50 mM Na-acetate buffer (pH 5.0). Ca activity was expressed as µmol coniferyl alcohol oxidized min^{-1} mg^{-1} total protein.

2.4 Quantification of flavonoids

Individual phenylpropanoids were analysed following the protocol previously reported in Cocozza *et al*., 2020. In brief, 300 mg of leaf tissue was grounded with liquid nitrogen, placed in a centrifuge tube and extracted three times with 4 mL of 75% EtOH/H_2O adjusted to pH 2.5 with formic acid. The supernatant was partitioned with *n*-hexane to remove chlorophyll and carotenoids, reduced to dryness, and finally rinsed with 2 mL of CH_3OH/H_2O (8:2). The extracts were injected (5 µL) into a Perkin Elmer liquid chromatograph equipped with a quaternary 200Q/410 pump and a LC 200 diode array detector (DAD)

8

89

(all from Perkin Elmer, Bradford, CT, USA). Phenylpropanoids were separated using a 250 x 4.6 mm Zorbax SB-C18 column (5 μm) operating at 40 °C with a flow rate of 1 mL min^{-1}. The mobile phases were (A) H_2O/CH_3CN (9:1, added with 0.1% of HCOOH) and (B) CH_3CN/H_2O (9:1, added with CH_3CN 0.1% of HCOOH). Phenylpropanoids were separated using a linear gradient elution from A to B over a 45 min run and chromatograms recorded at 330 nm and 350 nm. Individual phenylpropanoids were identified using retention times and comparison of UV spectral characteristics of those of authentic standards (caffeic acid, apigenin-7-*O*-glucoside, quercetin-3-*O*-glucoside and kaempferol-3-*O*-glucoside, all from Extrasynthese, Lyon-Nord, Genay, France). The phenylpropanoids consisted of three apigenin derivatives, one quercetin derivative and three kaempferol derivatives, all quantified with the external standard method and reported as mg g^{-1} DW.

2.5 Quantification of total lignin content

Lignin content was determined using a protocol based on the extraction of lignothioglycolic acid with minor modifications (Trupiano et al., 2012). Briefly, 0.5 g of lyophilized leaf tissue was pulverized and homogenized in 10 mL of extraction buffer (50 mM Tris–HCl, 0.01% Triton X-100, 1 M NaCl, pH 8.3). The suspension was stirred, centrifuged at 10000 g for 10 min, washed twice with 4 mL of extraction buffer, 4 mL of 80% (v/v) acetone, 4 mL of acetone and then dried in a concentrator. Each pellet was then treated with 0.2 ml of thioglycolic acid and 1 mL of 2 M HCl, for 4 h, at 100 °C, centrifuged at 15000 g for 10 min and washed three times with distilled water. Lignothioglycolic acid from each pellet was then extracted with 1.5 mL of 0.5 M NaOH, under stirring for 16 h, at 25 °C. The supernatant was acidified with 0.2 mL of 37% (v/v) HCl. Lignothioglycolic acid was precipitated at 4°C, for 4 h, recovered by centrifugation at 15000 g for 15 min, and dissolved in 1 mL of 0.5 M NaOH. Lignin content

9

was obtained by absorbance measurement at 280 nm, using a specific absorbance coefficient of 6.0 g^{-1} L cm (Doster and Bostock, 1988).

2.6 RNA extraction, sequencing and differential expression analysis

RNA extraction was performed using TRIzol® Reagent (Ambion). A total of 15 RNA samples, 3 biological replicates for each of the 5 treatments, were sent to HuGeF sequencing service (http://www.hugef-torino.org, Human Genetics Foundation, Turin, Italy), for paired-end libraries (2 x 75bp) construction and sequencing with Illumina NextSeq 500. Raw data have been deposited in the Sequence Read Archive (https://www.ncbi.nlm.nih.gov/sra) with SRA accession SRP145569. After low-quality filtering and adapters removal, *de novo* transcriptome assembly was performed through Trinity software (version 2.0.6). A total of 184,849 transcripts were assembled, reduced to 120,553 after redundancy removal. Analysis of differential expression of transcripts was performed with edgeR (version 3.16.5, R version 3.3.2), using a false discovery rate cut off 0.05 (5% FDR). The differential expression is reported as fold change (FC), i.e. the ratio between the expression value in the treatment and the expression value in the control of a transcript. A detailed description of the protocol can be found in Cocozza et al. (2019).

2.7 Statistical analyses

Descriptive statistics (means, standard errors) of all the measured parameters were calculated. To account for variability in the samples, a pooled standard deviation was computed from the four replicated plants from each experimental condition. Normality of the population distribution was tested using the Shapiro–Wilk test. The homogeneity of variances was performed with the Levene's test. One-way ANOVA with post-hoc Tukey HSD Test was applied to test the effect of Na+ and P supply in *A. donax* plants, and two-way ANOVA was performed to define the effects of treatments in the experimental points, stress point

10

91

and recovery. An LSD post-hoc test was applied to assess significantly different means among treatments ($P < 0.05$ level). Statistical analyses were performed using OriginPro 8 program (OriginLab Corporation, Northampton, UK). For transcriptomic analysis, the false discovery rate (FDR) represents an adjusted p-value, obtained applying a multiple testing correction (method of Benjamini and Hockberg, 1995). Indeed, when a large number of genes/transcripts are tested, a certain number of false positives is expected. In these cases, the FDR is used to lower the number of false positives. The FDR calculation is done by edgeR analysis according to Benjamini and Hockberg (1995). An FDR under 0.05 is usually used and means that we accept that 5 out of 100 measures (differential expression) can be false positive. The lower the FDR, the lower is the probability that the differential expression observed is a false positive.

3. Results

3.1 Hydrogen peroxide, ascorbic acid and dehydroascorbate content in A. donax under stress conditions

The H_2O_2 concentration was increased of 2-fold by +NaP respect to the levels measured in control plant. Under recovery, the H_2O_2 concentration decreased in plants deprived of P respect to the levels measured in the other stress conditions and in control plants (Fig. 1).

Ascorbate (AS) and dehydroascorbate (DHA) concentrations did not changes among the treatments (C, -P, +P, +Na, +NaP) after 43 days (stress point, St) or after 14 days from the end of treatments (Recovery, Re) (Table S1).

3.2 Content of phenylpropanoids and related biosynthetic pathway in A. donax under stress conditions

At the end of stress, the apigenin derivatives increased in plants treated with +NaP, and decreased in –P and +P treatments compared to control plants (Fig. 2A). After recovery, the apigenin derivatives significantly increased in +NaP and –P plants, whereas +P plants showed lower content of these

11

metabolites compared to control ones (Fig. 2A). The quercetin derivatives increased in Na+ and +NaP plants at the end of stress treatment and after recovery. No significant change was induced by the other treatments (Fig. 2B). The content of kaempferol derivatives was significantly increased only in +NaP plants , both at stress and recovery, while in −P plants an increment in these metabolites was observed only at recovery (Fig. 2C). Transcriptomic analysis showed that in +NaP plants, the synthesis of flavonoids was stimulated, as shown by the upregulation of the transcripts of the gene coding for the chalcone synthase (isoforms TR30713|c0_g1_i2 and TR30713|c0_g1_i3, FC=12.1 and FC=8.2, respectively), the first enzyme of the flavonoid biosynthetic pathway. No increased or decreased expression of the genes related to flavonoid biosynthesis was found in −P, +P or +Na treatment with respect to C plants (Fig. S1; Table 1). In plants grown under excessive content of both Na and P in soil (+NaP), the transcripts of genes involved in caffeic acid synthesis and its derivatives, i.e. the trans-cinnamate 4-monooxygenase (TR12947|c1_g1_i1 FC=3.8, TR22013|c1_g1_i1 FC=2.9, and TR22013|c1_g1_i3 FC=4.9) and shikimate O-hydroxycinnamoyl transferase (TR5007|c0_g1_i1 FC=2.8, TR3575|c0_g1_i1 FC=3.9), were up-regulated. No increased or decreased expression of these genes was observed in −P, +P or +Na treatment. Transcripts coding for Chalcone-flavanone isomerase (TR14275|c1_g1_i4 FC=3.9, TR15117|c1_g1_i2 FC=9.2 and TR15117|c1_g1_i3 FC=7.9), involved in the synthesis of apigenin, were up-regulated in +NaP treatments. Transcripts coding for the anthocyanidin 3-O-glucosyltransferase 2, involved in apigenin derivatives, were up-regulated in +NaP (five transcripts with FC between 4.2 and 12.6), +Na (TR136|c4_g3_i3 FC=2.9) and −P (TR12985|c2_g1_i1 FC=6.8) treatments. The transcriptomic data agreed with the levels of apigenin measured in +NaP plants, whereas there was no correlation between the induction of the anthocyanidin 3-O-glucosyltransferase 2 transcript (Table 1) and the decrease of apigenin derivatives measured in −P plants (Fig. 2B).

12

93

A transcript coding for a flavonoid 3–hydroxylase, one of the enzymes involved in the synthesis of quercetine, as well as one coding for a flavonol sulfotransferase, involved in quercetine derivatives synthesis, were up-regulated in +NaP treatment (TR18107|c0_g2_i1 FC=11.2 and TR24551|c3_g2_i3 FC=7.7, respectively) (Fig. S1). The same flavonol sulfotransferase transcript was induced in +Na treatment (FC=4.3) (Table 1). On the other hand, one other transcript coding for flavonol sulfotransferase and two isoforms of a transcript coding for an anthocyanidin 5,3-O-glucosyltransferase, also involved in the biosynthesis of quercetine derivatives, were down-regulated in +NaP (TR24226|c1_g1_i1 FC=0.1, TR5705|c4_g3_i2 FC=0.25, TR5705|c4_g3_i3 FC=0.07) (Table 1). No up- or down-regulation was observed in –P or +P with respect to C plants (Table 1).

In +NaP treatment, the transcripts coding for enzymes involved in the synthesis of kaempferol and its derivatives, i.e. flavonol synthase flavanone 3-hydroxylase-like and anthocyanidin 5,3-O-glucosyltransferase, were either up-regulated (TR296|c0_g3_i1 FC=34.5) or down-regulated (five transcripts with FC between 0.1 and 0.5), respectively. No up- or down- regulation of these transcripts was measured in the other treatments (Table 1).

3.3 Peroxidase activities and related transcript content in A. donax under stress conditions

The activity of Arundo peroxidases when coniferyl alcohol (Fig. 3A) or siryngaldazine (Fig. 3B) were used as substrates increased in the plants exposed to high concentrations of Na+ and +P, both in single stress and in combination. The lower increment was observed in the plants deprived of P (-P plants), whereas the same plants presented high levels of Prx at recovery when siryngaldazine was provided. The activity of peroxidases in presence of guaiacol increased quite 2-fold in +NaP plants respect to the control at the end of treatment, and more moderately as consequence of all the other treatments (Fig. 3C). At

recovery, increased activity was also observed in all treatments compared to control plants, with the highest values recorded in -P plants.

Transcriptomic analysis showed that in +NaP treatment, four peroxidase encoding genes were up-regulated, and 8 were down-regulated (Table 2). Among these, four transcripts were of particular interest: peroxidase 17, known to be involved in lignin deposition (Cosio et al., 2016), was up-regulated (isoforms TR19645|c0_g1_i5 FC=2.4 and TR19645|c0_g1_i6 FC=2.7), while peroxidase P7-like (TR482|c0_g1_i4) and peroxidase 66 (TR5652|c2_g2_i1), involved in the deposition of syringal monomers (GO:1901430, positive regulation of syringal lignin biosynthetic process), were down-regulated (FC=0.14 and FC=0.12, respectively) (Table 1). A transcript coding for a peroxidase 5-like was down-regulated in −P and in +P (TR23604|c5_g1_i4 FC=0.08, in both) treated plants. In +Na treated plants, no differential expression among peroxidase genes was found (Table 2).

3.4 Lignin content and related biosynthetic pathway in A. donax under stress conditions

Total lignin content in leaves did not change significantly among plant treatments, even though a tendence through lignin accumulation was evident when *A. donax* in all the treatment respect to the control (Table S2). Data obtained from transcriptomic analysis showed that the expression of several genes encoding the enzymes involved in the lignin biosynthetic pathway, part of the phenylpropanoid biosynthetic pathway, were induced by the +NaP treatment, while slightly impaired by the other treatments (Fig. S2; Table 2) respect to control. In detail, in +NaP plants, the transcripts of phenylalanine ammonia-lyase, the first enzyme of the lignin biosynthetic pathway, was down-regulated (TR3072|c2_g2_i4 FC=0.19) (Fig. S2, Table 2). Among 6 transcripts coding for 4-coumarate-CoA ligase, two were down-regulated (TR19035|c0_g1_i1 FC=0.24 and TR3027|c2_g2_i1 FC=0.25) and four were up-regulated (TR22604|c3_g2_i1 FC=4.2, TR5718|c1_g1_i5 FC=3.1, TR7497|c3_g2_i3 FC=6.7

14

and TR7497|c3_g2_i7 FC=4.2). Three transcripts for cinnamoyl-CoA reductase, the first key enzyme for monolignol biosynthesis, were up-regulated (TR6509|c1_g1_i1 FC=4.3, TR6509|c1_g1_i6 FC=2.7 and TR9597|c1_g4_i1 FC=2.3) and 2 transcripts codifying for caffeoyl-O-methyltransferase 1 show opposite regulation (TR18821|c1_g3_i8 FC=0.07 and TR30139|c0_g1_i3 FC=7.1); 2 transcripts codifying for caffeoylshikimate esterase were down-regulated (TR1036|c1_g1_i10 FC=0.11 and TR11203|c3_g1_i3 FC=0.35) and one was up-regulated (TR1036|c1_g1_i12 FC=2.41). Finally, 4 transcripts for laccase genes, involved in the polymerization of monolignol subunit, were up-regulated (TR18961|c2_g1_i1 FC=2.9, TR18961|c2_g1_i4 FC=2.2, TR6554|c0_g1_i2 FC=41.3 and TR7969|c1_g1_i3 FC=37.8) and 2 were down-regulated (TR6546|c1_g1_i2 FC=0.15 and TR6546|c1_g1_i3 FC=0.08) (Fig. S2, Table 2). In +Na treated plants, transcript coding for cinnamoyl-CoA reductase 1-like (TR6509|c1_g1_i7 FC=3) and for cinnamyl alcohol dehydrogenase (TR24767|c0_g1_i4 FC=7.6), involved in the last step of monolignol biosynthesis, were up-regulated, while a laccase gene (TR6546|c1_g1_i3 FC=11.2) was down-regulated (Fig. S2, Table 2). In -P treated plants, a cinnamoyl-CoA reductase, a caffeoylshikimate esterase and a peroxidase were down-regulated (TR9597|c1_g4_i1 FC=0.3, TR11203|c3_g1_i6 FC=0.44, TR23604|c5_g1_i4 FC=0.08, respectively). In +P treated plants, genes involved in lignin biosynthesis were not regulated, except for one transcript codifying for a peroxidase (TR23604|c5_g1_i4 FC=0.08) (Table 2).

4. Discussion

The present study showed the effects of exposure of +Na and P in the soil, in single and combined stress conditions, on the modulation of class III peroxidase and their substrates phenylpropanoids in *A. donax*. Companion papers (Cocozza et al., 2019, 2020) showed negative effects of salt and phosphorous supply on the physiological parameters, by highlighting that the exposure to high P increased the negative effects of salt stress on plant photosynthetic performances.

15

96

The increase of ROS levels (i.e. H_2O_2) in *A. donax* treated with a combination of +Na and P might be due to the observed photosynthetic imbalance (Cocozza et al., 2019, 2020). H_2O_2 can diffuse across biological membranes and be harmful for plant membranes and organelles (Groß et al., 2013), and, on the other hand, it can play a role as secondary messenger. Therefore a fine-tuning regulation of its levels is of relevance for cell adaptation to stress condition. In the same treatment (+NaP) the accumulation of higher amount of leaf phenylpropanoids (quercetin, apigenin, kaempferol derivatives, Fig. S3) is in line with the reported role of these metabolites in regulating and supporting the acclimatation to environmental changes (Isah, 2019). Quercetin derivatives, which possess a higher antioxidant activity than kaempferol derivatives (Nakabayashi et al., 2014), may play a direct ROS scavenging activity in *A. donax* exposed only to excess of salinity (Na+). Indeed, a specific increment of these compounds under Na+ treatment was found in *A. donax*, in accordance with the suggested role of this molecule against photo-oxidative damages and its distribution in mesophyll cells (Agati et al., 2011).

Moreover, Ferreres et al. (2011) proposed that the vacuolar class III peroxidases were involved in the homeostasis of H_2O_2 cellular concentrations, using secondary organic compounds as substrates. The increased activity of *A. donax* class III peroxidases (AdPrx) when guaiacol was used as substrate in *A. donax* under combined exposition to +Na and P (+NaP), might suggest the involvement of these enzymes in scavenging H_2O_2 utilizing glycosylated quercetin derivatives, which structure is similar to that of guaiacol, as substrates (Ferreres et al., 2011). Indeed, previous *in vitro* and *in vivo* studies demonstrated that these forms also act as substrates of class III plant peroxidases in addition to the aglycone (Yamasaki et al., 1997; Rácz et al., 2008). However, *in A. donax* experienced with P starvation or excess, the increase of AdPrx activity was also determined without accumulation of apigenin, quercetin and kaemferol derivatives and H_2O_2 when guaiacol and syringaldazine were used as substrates. Nevertheless in those treatments, high levels of caffeic acid derivatives, which structure reminds to that of guaiacol, were found

16

97

(Cocozza et al., 2019). Indeed, caffeic acid derivatives (e.g. chlorogenic acid) have been found to act as optimal substrate for POX (Takahama et al., 1999).

In addition, caffeic acid, is known as primary precursor for lignin biosynthesis. Although in *A. donax* under all the treatment, no significant change in lignin was observed at the sampling time, data showed a trend of lignin accumulation suggesting that enhanced lignin accumulation might be occurred under the studied stress. Alternatively, as recently reported for maize plants, *A. donax* under stress might be undergoing only subtle alterations in lignin composition without significant changes in its content (Oliveira et al., 2020).

The hypothesis of lignin synthesis as one of the adaptation mechanisms used by *A. donax* under stress seems corroborated by the increase of several Prx, lignin and flavonoid transcripts increase at least when +Na in single stress and in combination with P was supplied. In this regard, it is worth to remember that lignin and flavonoids biosynthesis partially overlap. In particular, the p-coumaroyl CoA is an important intermediate in the metabolic pathways of flavonoid or phenylpropanoid compounds *sensu stricto* and is the common substrate of two specific enzymes: (1) chalcone synthase, which catalyzes the formation of the flavonoid skeleton, and (2) hydroxycinnamoyl transferase, which leads to the biosynthesis of the two major lignin building units (guaiacyl and syringyl units) (Vogt et al., 2010). The cynnamyl alcohol dehydrogenase is involved in the biosynthesis of lignin and lignans, catalysing the final step of monolignol biosynthesis, where NADPH is a cofactor (Sibout et al., 2005), and the transcript coding for this enzyme was up-regulated only in +Na plants. Conversely, the trans-cinnamate 4-monooxygenase and shikimate O-hydroxycinnamoyl transferase may be directed towards flavonoids biosynthesis rather than lignin biosynthesis.

Both flavonoids and lignin are important in counteracting environmental stresses due to their ability to neutralize ROS by donating electrons to hydrogen atoms (Rice-Evans et al., 1996; Kieffer et al., 2008). Furthermore, besides the well-studied role of flavonoids as effective antioxidants, they are also

17

98

considered natural regulators of auxin gradients (by inhibiting polar auxin transport), local auxin concentrations (inhibiting peroxidase-mediated IAA oxidation), and thus could be also potentially involved in the modulation of "stress-induced morphogenic responses" and in the regulation of cell expansion (Agati et al., 2012).

A. donax has been proposed among the non-food crop for energy and biofuel production. Nevertheless the presence of lignin is still a major bottleneck for the utilization of plant biomass as a source for biofuels and bio-based materials (Vanholme et al., 2010). Therefore, our data underline for the first time, the need of performing further investigation to the possible role of lignification in the response mechanisms of A. *donax* to adaptation to harsh environment.

5. Conclusion

The data reported in this work suggest that under excess of +Na in single stress and in combination with P, class III peroxidases might scavenge ROS (i.e., H_2O_2) using hydrogen peroxide and phenylpropanoids, such as quercetin, apigenin and kaempferol concurring to the adaptation of *A. donax* to harsh environments. One the other hand, the results present in this work open the way to hypothesizing a possible accumulation of lignin and consequently the strengthening of the mechanical properties of cell wall when the plants is under +Na and/or P stress a mechanism that on one hand may *A. donax* to face the stressful conditions and on the other hand might limit its potential use in energy and biofuel production.

18

benificiary of PhD fellowship: Silvia Rotunno) of the Italian Ministry of University and Research (MIUR).

Author contributions

Conceptualization, C.C. and M.B.E.; methodology, M.B.E., B.P., B.C., M.L., P.S., P.A., T.D., R.S.; data curation, C.C., M.B.E., B.C.; writing—original draft preparation, C.C. and M.B.E.; writing—review and editing, C.C., B.C., M.L., T.D., B.F., M.B.E., G.S.S.; project administration, C.C.; funding acquisition, C.C.. All authors have read and agreed to the published version of the manuscript.

References

Agati, G., Azzarello, E., Pollastri, S., Tattini, M., 2012. Flavonoids as antioxidants in plants: location and functional significance. Plant Sci. 196, 67-76.

Agati, G., Biricolti, S., Guidi, L., Ferrini, F., Fini, A., Tattini, M., 2011. The biosynthesis of flavonoids is enhanced similarly by UV radiation and root zone salinity in *L. vulgare* leaves. J. Plant Physiol. 168, 204-212.

Almagro, L., Gómez Ros, L.V., Belchi-Navarro, S., Bru, R., Ros Barceló, A., Pedreño, M.A., 2009. Class III peroxidases in plant defence reactions. J Exp Bot., 60(2), 377-90. doi:10.1093/jxb/ern277.

Almeida Machado, R.M., Serralheiro, R.P., 2017. Soil salinity: effect on vegetable crop growth. management practices to prevent and mitigate soil salinization. Horticulturae 3(2), 30. https://doi.org/10.3390/horticulturae3020030.

Angelini, L.G., Ceccarini, L., Nassi o Di Nasso, N., Bonari, E., 2009. Comparison of *Arundo donax* L. and *Miscanthus × giganteus* in a long-term field experiment in Central Italy: analysis of productive characteristics and energy balance. Biomass Bioen. 33, 635-43.

Benjamini, Y., Hochberg, Y., 1995. Controlling the false discovery rate: a practical and powerful approach to multiple testing. J. R. Stat. Soc. Series B 57, 289–300.

Bradford, M.M., 1976. A rapid and sensitive method for the quantitation of microgram quantities of protein utilizing the principle of protein-dye binding. Analyt. Biochem. 72, 248–254.

Carrasco-Ríos, L., Rojas, C., Pinto, M., 2013. Contrasting physiological responses to high salinity between two varieties of corn 'Lluteño' (salt tolerant) and 'Jubilee' (salt sensitive). Chilean J. Agric. Res. 73, 3.

Cesarino, I., Araújo, P., Mayer, J.L.S., Leme, A.F.P., Mazzafera, P., 2012. Enzymatic activity and proteomic profile of class III peroxidases during sugar cane stem development. Plant Physiol. Biochem. 55, 66–76. doi: 10.1016/j.plaphy.2012.03.014

Cocozza, C., Brilli, F., Miozzi, L., Pignattelli, S., Rotunno, S., Brunetti, C., Giordano, C., Pollastri, S., Centritto, M., Accotto, G. P., Tognetti, R., Loreto, F., 2019. Impact of high or low levels of phosphorus and high sodium in soils on productivity and stress tolerance of *Arundo donax* plants. Plant Sci. 289, 110260. doi: 10.1016/j.plantsci.2019.110260.

Cocozza, C., Brilli, F., Pignattelli, S., Pollastri, S., Brunetti, C., Gonnelli, C., Tognetti, R., Centritto, M., Loreto, F., 2020. The excess of phosphorus in soil reduces physiological performances over time but enhances prompt recovery of salt-stressed *Arundo donax* plants. Plant Phys. Biochem. 151, 556–565.

Corno, L., Pilu, R., Adani, F., 2014. *Arundo donax* L.: a non-food crop for bioenergy and bio-compound production. Biotechnol Adv. 32(8), 1535-49. doi: 10.1016/j.biotechadv.2014.10.006.

Cosio, C., Ranocha, P., Francoz, E., Burlat, V., Zheng, Y., Perry, S. E., Ripoll, J. J., Yanofsky, M., Dunand, C., 2016. The class III peroxidase PRX17 is a direct target of the MADS-box transcription factor AGAMOUS-LIKE15 (AGL15) and participates in lignified tissue formation. New Phytol. 213(1), 250–263. https://doi.org/10.1111/nph.14127.

20

Crouse, D.A., 2018. Soils and Plant Nutrients, Chapter 1. In: K.A. Moore, and. L.K. Bradley (eds). North Carolina Extension Gardener Handbook. NC State Extension, Raleigh, NC. https://content.ces.ncsu.edu/extension-gardener-handbook/1-soils-and-plant-nutrients.

Deng, Y., Fu, S., 2017. Biosynthesis and Regulation of Phenylpropanoids in Plants. Crit. Rev. Plant Sci., 36 (4), 257-290. https://doi.org/10.1080/07352689.2017.1402852.

De Stefano, R., Cappetta, E., Guida, G., Mistretta, C., Caruso, G., Giorio, P., Albrizio, R., Tucci, M., 2017. Screening of giant reed (*Arundo donax* L.) ecotypes for biomass production under salt stress. Plant Biosystems 152, 911–917. https://doi.org/10.1080/11263504.2017.1362059.

Docimo, T., De Stefano, R., De Palma, M. et al., 2020. Transcriptional, metabolic and DNA methylation changes underpinning the response of *Arundo donax* ecotypes to NaCl excess. Planta 251, 34. https://doi.org/10.1007/s00425-019-03325-w.

Doster, M.A., Bostock, R.M., 1988. Quantification of lignin formation in almond bark in response to wounding and infection by *Phytophthora* species. Phytopathol. 78, 473–477.

Ferreres, F., Figueiredo, R., Bettencourt, S., Carqueijeiro, I., Oliveira, J., Gil-Izquierdo, A., Pereira, D.M., Valentão, P., Andrade, P.B., Duarte, P., Ros Barceló, A., Sottomayor, M., 2011. Identification of phenolic compounds in isolated vacuoles of the medicinal plant *Catharanthus roseus* and their interaction with vacuolar class III peroxidase: an H_2O_2 affair?, J. Exp. Bot., 62(8), 2841–2854.

Foyer, C. H., 2018. Reactive oxygen species, oxidative signaling and the regulation of photosynthesis. Env. Exp. Bot. 154, 134–142.

Grattan, S. R., Grieve, C.M., 1998. Salinity–mineral nutrient relations in horticultural crops. Sci. Hortic. 78 (1-4), 127-157.

Groß, J., Durner, and F. Gaupels, 2013. Nitric oxide, antioxidants and prooxidants in plant defence responses. Front. Plant Sci. 4, 419.

21

Isah, T., 2019. Stress and defense responses in plant secondary metabolites production. Biol. Res. 52, 39. doi: 10.1186/s40659-019-0246-3.

Isayenkov, S.V., Maathuis, F.J.M., 2019. Plant Salinity Stress: Many Unanswered Questions Remain. Front Plant Sci., 10, 80. doi: 10.3389/fpls.2019.00080.

Kidwai, M., Ahmad, I.Z., Chakrabarty, D., 2020. Class III peroxidase: an indispensable enzyme for biotic/abiotic stress tolerance and a potent candidate for crop improvement. Plant Cell Rep. 39, 1381–1393. https://doi.org/10.1007/s00299-020-02588-y.

Kieffer, P., Dommes, J., Hoffmann, L., Hausman, J.F., Renaut, J., 2008. Quantitative changes in protein expression of cadmium-exposed poplar plants. Proteomics 8, 2514–2530.

Law, M.Y., S.A. Charles, Halliwell, B., 1983. Glutathione and ascorbic acid in spinach (*Spinacia oleracea* L.) chloroplasts: The effect of hydrogen peroxide and of paraquat. Biochem. J. 210, 899–903.

Lüthje, S., Martinez-Cortes, T., 2018. Membrane-Bound Class III Peroxidases: Unexpected Enzymes with Exciting Functions. Int. J. Mol. Sci. 19, 2876; doi:10.3390/ijms19102876.

Marjamaa, K., Kukkola, E.M., Fagerstedt, K.V., 2009. The role of xylem class III peroxidases in lignification. J. Exp. Bot., 60(2), 367-76. doi: 10.1093/jxb/ern278. PMID: 19264758.

Nakabayashi, R., Yonekura- Sakakibara, K., Urano, K., Suzuki, M., Yamada, Y., Nishizawa, T., Saito, K., 2014. Enhancement of oxidative and drought tolerance in *Arabidopsis* by overaccumulation of antioxidant flavonoids. Plant J. 77(3), 367-379.

Neal, C., Reynolds, B., Neal, M., Hughes, S., Wickham, H., Hill, L., Rowland, P., Pugh, B., 2003. Soluble reactive phosphorus levels in rainfall, cloud water, throughfall, stemflow, soil waters, stream waters and groundwaters for the Upper River Severn area, Plynlimon, mid Wales. Sci. Tot. Environ. 1, 99–120.

22

Oliveira, D.M., Mota, T.R., Salatta, F.V., Sinzker, R.C., Končitíková, R., Kopečný, D., Dos Santos, W.D., 2020. Cell wall remodeling under salt stress: Insights into changes in polysaccharides, feruloylation, lignification, and phenolic metabolism in maize. Plant Cell Environ. 43(9), 2172-2191.

Rácz, A., Hideg, É., & Czégény, G., 2018. Selective responses of class III plant peroxidase isoforms to environmentally relevant UV-B doses. J. Plant Physiol. 221, 101-106.

Rice-Evans, C.A., Miller, N.J., Paganga, G., 1996. Structure-antioxidant activity relationships of flavonoids and phenolic acids. Free Radic Biol. Med. 20(7), 933–56.

Sánchez, E., Gil, S., Azcón-Bieto, J., Nogués, S., 2016. The response of *Arundo donax* L. (C3) and *Panicum virgatum* (C4) to different stresses. Biomass Bioenergy 85, 335-345.

Schröder, P., Beckers, B., Daniels, S., Gnädinger, F., Maestri, E., Marmiroli, N., Mench, M., Millan, R., Obermeier, M.M., Oustriere, N., Persson, T., Poschenrieder, C., Rineau, F., Rutkowska, B., Schmid, T., Szulc, W., Witters, N., Sæbø, A., 2018. Intensify production, transform biomass to energy and novel goods and protect soils in Europe — A vision how to mobilize marginal lands. Sci. Total Environ. 616–617, 1101-1123.

Sharma, A., Shahzad, B., Rehman, A., Bhardwaj, R., Landi, M., Zheng, B., 2019 Response of Phenylpropanoid Pathway and the Role of Polyphenols in Plants under Abiotic Stress. Molecules. 24(13), 2452. doi: 10.3390/molecules24132452.

Sibout, R., Eudes, A., Mouille, G., Pollet, B., Lapierre, C., Jouanin, L., Séguin, A., 2005. Cinnamyl alcohol dehydrogenase -C and -D are the primary genes involved in lignin biosynthesis in the floral stem of *Arabidopsis*. Plant Cell. 17(7), 2059-76.

Sicilia, A., Santoro, D.F., Testa, G., Cosentino, S.L., Lo Piero, A.R., 2020. Transcriptional response of giant reed (*Arundo donax* L.) low ecotype to long-term salt stress by unigene-based RNAseq. Phytochem. 177, 112436. doi: 10.1016/j.phytochem.2020.112436.

23

Siddiqui, M. H., Khan, M.N., Mohammad, F., Khan M.M.A., 2008. Role of Nitrogen and Gibberellin (GA$_3$) in the Regulation of Enzyme Activities and in Osmoprotectant Accumulation in *Brassica juncea* L. under Salt Stress. J. Agr. Sci. https://doi.org/10.1111/j.1439-037X.2008.00308.x.

Smith, V.H., Schindler, D.W., 2009. Eutrophication science: where do we go from here? Trends Ecol. Evol. 24, 201–207.

Su, P., Yan, J., Li, W., Wang, L., Zhao, J., Ma, X., Li, A., Wang, H., Kong, L., 2020. A member of wheat class III peroxidase gene family, TaPRX-2A, enhanced the tolerance of salt stress. BMC Plant Biol. 20, 392. https://doi.org/10.1186/s12870-020-02602-1.

Takahama, U., 2004. Oxidation of vacuolar and apoplastic phenolic substrates by peroxidase: Physiological significance of the oxidation reactions. Phytochem. Rev. 3(1), 207-219.

Takahama, U., Hirotsu, M., Oniki, T., 1999. Age-dependent changes in levels of ascorbic acid and chlorogenic acid, and activities of peroxidase and superoxide dismutase in the apoplast of tobacco leaves: mechanism of the oxidation of chlorogenic acid in the apoplast. Plant Cell Physiol., 40(7), 716-724.

Takahama, U., Oniki, T., 2000. Flavonoids and some other phenolics as substrates of peroxidase: physiological significance of the redox reactions. J. Plant Res. 113(3), 301-309.

Trupiano, D., Di Iorio, A., Montagnoli, A., Lasserre, B., Rocco, M., Grosso, A., Scaloni, A., Marra, M., Chiatante, D., Scippa, G.S., 2012. Involvement of lignin and hormones in the response of woody poplar taproots to mechanical stress. Physiol. Plant. 146, 39–52.

Van Breusegem, F., Dat, J.F., 2006. Reactive oxygen species in plant cell death. Plant Physiol. 141(2), 384-390.

Vanholme, R., Van Acker, R., Boerjan, W., 2010. Potential of Arabidopsis systems biology to advance the biofuel field Trends Biotechnol., 28, 543-547.

24

Velikova, V., Yordanov, I., Edreva, A., 2000. Oxidative stress and some antioxidant systems in acid rain-treated bean plants. Protective role of exogenous polyamines. Plant Sci.151, 59–66.

Vogt, T., 2010. Phenylpropanoid biosynthesis. Mol. Plant 3 (1), 2–20. https://doi.org/10.1093/mp/ssp106.

Yamasaki, H., Sakihama, Y., Ikehara, N., 1997. Flavonoid-peroxidase reaction as a detoxification mechanism of plant cells against H_2O_2. Physiol. Plant., 115, 1405-1412.

Zribi, O.T, Labidi, N, Slama, I., Debez, A., Ksouri, R., Rabhi, M., et al., 2012. Alleviation of phosphorus deficiency stress by moderate salinity in the halophyte *Hordeum maritimum* L. Plant Growth Regul. 66, 75–85. doi: 10.1007/s10725-011-9631-9.

25

Captions of figures

Figure 1. H_2O_2 content of *A. donax* plants in control conditions (C), phosphorous-deprived (-P), phosphorous-enriched (+P), sodium chloride-enriched (+Na), and phosphorous and sodium-enriched (+NaP) soil measured after 43 days by applying different solutions (St) and following a recovery period of 14 days (Re). Data are means of 4 plants per treatment ± SE; different letters indicate statistical difference between treatments at $P < 0.05$ - lowercase letters in stress point (St); capital letters in recovery (Re); two-way ANOVA defines the significance of effects of treatments in time, the experimental points, at $P < 0.05$.

Fig. 2 Apigenin (A), quercetin (B) and kaempferol (C) derivatives contents of *A. donax* plants in control conditions (C), phosphorous-deprived (-P), phosphorous-enriched (+P), sodium chloride-enriched (+Na), and phosphorous and sodium-enriched (+NaP) soil measured after 43 days (St) by applying different solutions and following a recovery period of 14 days (Re). Data are means of 4 plants per treatment ± SE; different letters indicate statistical difference between treatments at $P < 0.05$ - lowercase letters in stress point (St); capital letters in recovery (Re); two-way ANOVA defines the significance of effects of treatments in time, the experimental points, at $P < 0.05$.

Figure 3. Coniferyl alcohol peroxidase (B), syringaldazine peroxidase (C) and guaiacol peroxidase (D) activity of *A. donax* plants in control conditions (C), phosphorous-deprived (-P), phosphorous-enriched (+P), sodium chloride-enriched (+Na), and phosphorous and sodium-enriched (+NaP) soil measured after 43 days by applying different solutions (St) and following a recovery period of 14 days (Re). Data are means of 4 plants per treatment ± SE; different letters indicate statistical difference between treatments at $P < 0.05$ - lowercase letters in stress point (St); capital letters in recovery (Re); two-way ANOVA defines the significance of effects of treatments in time, the experimental points, at $P < 0.05$.

26

Captions of tables

Table 1. List of differentially expressed genes (DEGs) of flavonoids biosynthesis pathway in each treatment at false discovery rate (FDR) of 5%; FC=Fold Change relative to control.

Table 2. List of differentially expressed genes (DEGs) in each treatment at false discovery rate (FDR) of 5%; FC=Fold Change relative to control.

Captions of supplementary materials

Figure S1. Expression of genes related to phenylpropanoid biosynthesis in A) +NaP (excess of salt and phosphorus) plants, B) +Na (excess of salt), C) +P (excess of phosphorus), D) –P (lack of phosphorus); dark grey: up-regulated genes, light grey: down-regulated genes. EC:1.1.1.195 cinnamyl-alcohol dehydrogenase, EC:1.11.1.7 peroxidase, EC:1.14.14.91 trans-cinnamate 4-monooxygenase, EC:1.2.1.44 cinnamoyl-CoA reductase, EC:2.3.1.133 shikimate O-hydroxycinnamoyltransferase, EC:3.1.1.- caffeoylshikimate esterase, EC:3.2.1.21 beta-glucosidase, EC:4.3.1.24 phenylalanine ammonia-lyase, EC:6.2.1.12 4-coumarate--CoA ligase.

Table S1. Ascorbic acid (AS), dehydroascorbate (DHA) and total ascorbate in *A. donax* plants in control conditions (C), phosphorous-deprived (-P), phosphorous-enriched (+P), sodium chloride-enriched (+Na), and phosphorous and sodium-enriched (+NaP) soil after 43 days by applying different solutions (St) and following a recovery period of 14 days (Re). Data are means of 4 plants per treatment ± SE; two-way ANOVA defines the significance of effects of treatments in time, the experimental points, at $P < 0.05$; one-way ANOVA defines the significance of effects of treatments in St and Re, at $P < 0.05$.

27

Table S2. Lignin content (mg/ml) in leaves of *A. donax* in control conditions (C), phosphorous-deprived (-P), phosphorous-enriched (+P), sodium chloride-enriched (+Na), and phosphorous and sodium-enriched (+NaP) soil measured after 43 days by applying different solutions (St). Data are means of 3 plants per treatment ± SE. ANOVA defines no effects of treatments in lignin content at $P < 0.05$.

28

Modulation of class III peroxidase pathways and phenylpropanoids in *Arundo donax* under salt and phosphorus stress

Cocozza C., Bartolini P., Brunetti C., Miozzi L., Pignattelli S., Podda A., Scippa G.S., Trupiano D., Rotunno S., Brilli F., Maserti B.E.

Author contributions

Conceptualization, C.C. and M.B.E.; methodology, M.B.E., B.P., B.C., M.L., P.S., P.A., T.D., R.S.; data curation, C.C., M.B.E., B.C.; writing—original draft preparation, C.C. and M.B.E.; writing—review and editing, C.C., B.C., M.L., T.D., B.F., M.B.E., G.S.S.; project administration, C.C.; funding acquisition, C.C.. All authors have read and agreed to the published version of the manuscript.

Table 1. List of differentially expressed genes (DEGs) of flavonoids biosynthesis pathway in each treatment at false discovery rate (FDR) of 5%; FC=Fold Change relative to control.

Transcript	Description	FC(-P)*	FDR(-P)	FC(+P)*	FDR(+P)	FC(+Na)*	FDR(+Na)	FC(+NaP)*	FDR(+NaP)	E.C.
TR1141|c1_g1_i1	anthocyanidin reductase-like							-2.75	0.042	1.3.1.77
TR1141|c5_g1_i1	anthocyanidin reductase-like							-1.20	0.005	1.3.1.77
TR1141|c5_g1_i5	anthocyanidin reductase-like	-2.26	0.019					1.85	4.76E-05	1.3.1.77
TR1141|c5_g1_i8	anthocyanidin reductase-like							-1.10	0.019	1.3.1.77
TR12883|c0_g1_i1	Bifunctional dihydroflavonol 4-reductase flavanone 4-reductase							1.82	0.032	1.1.1.219
TR12947|c1_g1_i_i	trans-cinnamate 4-monooxygenase							1.93	0.009	1.14.14.91
TR12985|c2_g1_i1	anthocyanidin 3-O-glucosyltransferase 2	2.76	0.032							2.4.1.115
TR136|c4_g3_i10	anthocyanidin 3-O-glucosyltransferase 2-like							2.07	4.014E-04	2.4.1.115
TR136|c4_g3_i3	anthocyanidin 3-O-glucosyltransferase 2-like					1.53	0.022	2.15	2.537E-05	2.4.1.115
TR136|c4_g3_i7	anthocyanidin 3-O-glucosyltransferase 2-like							2.24	1.661E-05	2.4.1.115
TR14275|c1_g1_i4	chalcone-flavanone isomerase							1.97	0.029	5.5.1.6
TR15117|c1_g1_i2	Chalcone--flavonone isomerase							3.20	0.001	5.5.1.6
TR15117|c1_g1_i3	Chalcone--flavonone isomerase							2.99	0.040	5.5.1.6
TR1752|c3_g1_i1	Isoflavone reductase							1.15	0.035	1.3.1.45
TR1752|c3_g2_i3	isoflavone reductase							1.07	0.037	1.3.1.45
TR18107|c0_g2_i1	flavonoid 3 -hydroxylase							3.49	1.059E-06	1.14.14.82
TR20686|c1_g1_i1	Isoflavone reductase							-1.19	0.019	1.3.1.45
TR21372|c2_g1_i1	anthocyanidin 3-O-glucosyltransferase 2-like							3.53	0.002	2.4.1.115
TR22013|c1_g1_i1	Trans-cinnamate 4-monooxygenase							1.51	0.044	1.14.14.91
TR22013|c1_g1_i3	trans-cinnamate 4-monooxygenase							2.28	0.003	1.14.14.91
TR22581|c5_g1_i2	Bifunctional dihydroflavonol 4-reductase flavanone 4-reductase							2.47	0.018	1.1.1.219
TR23110|c1_g1_i2	anthocyanidin 5,3-O-glucosyltransferase-like							-0.96	0.048	2.4.1.-
TR24226|c1_g1_i1	Flavonol 3-sulfotransferase							-3.29	0.007	2.8.2.25
TR24551|c3_g2_i2	flavonol sulfotransferase-like							1.38	0.014	2.8.2.25
TR24551|c3_g2_i3	flavonol sulfotransferase-like					2.11	0.008	2.94	1.032E-07	2.8.2.25
TR28815|c0_g1_i8	crocetin chloroplastic-like			1.25	0.047					2.4.1.271
TR28997|c0_g2_i1	anthocyanidin 3-O-glucosyltransferase 2-like							3.65	7.447E-05	2.4.1.115
TR296|c0_g1_i1	flavonol synthase							1.44	0.008	1.14.20.6
TR296|c0_g3_i1	flavonol synthase flavanone 3-hydroxylase-like							5.11	2.049E-10	1.14.20.6 1.14.11.9
TR30713|c0_g1_i2	chalcone synthase							3.60	5.986E-07	2.3.1.74
TR30713|c0_g1_i3	chalcone synthase							3.04	1.391E-07	2.3.1.74
TR3575|c0_g1_i1	shikimate O-hydroxycinnamoyltransferase-like							1.98	0.006	2.3.1.133
TR416|c3_g5_i2	crocetin chloroplastic-like					-2.14	0.009	-2.49	3.029E-05	2.4.1.271
TR416|c3_g5_i8	crocetin chloroplastic-like					-1.52	0.040	-1.61	0.003	2.4.1.271
TR4573|c2_g2_i5	anthocyanidin 5,3-O-glucosyltransferase-like							-2.57	0.004	2.4.1.-
TR5007|c0_g1_i1	Shikimate O-hydroxycinnamoyltransferase							1.50	0.015	2.3.1.133
TR5024|c1_g1_i2	isoflavone reductase homolog IRL-like							-1.33	0.035	1.3.1.45
TR5024|c1_g1_i3	isoflavone reductase							-3.79	0.004	1.3.1.45
TR5070|c0_g1_i3	Isoflavone reductase	-4.74	4.963E-04			2.12	0.006	3.10	0.001	1.3.1.45
TR5070|c0_g1_i4	Isoflavone reductase					2.38	0.026	3.28	0.002	1.3.1.45
TR5705|c4_g2_i1	anthocyanidin 5,3-O-glucosyltransferase-like							-1.38	0.003	2.4.1.-

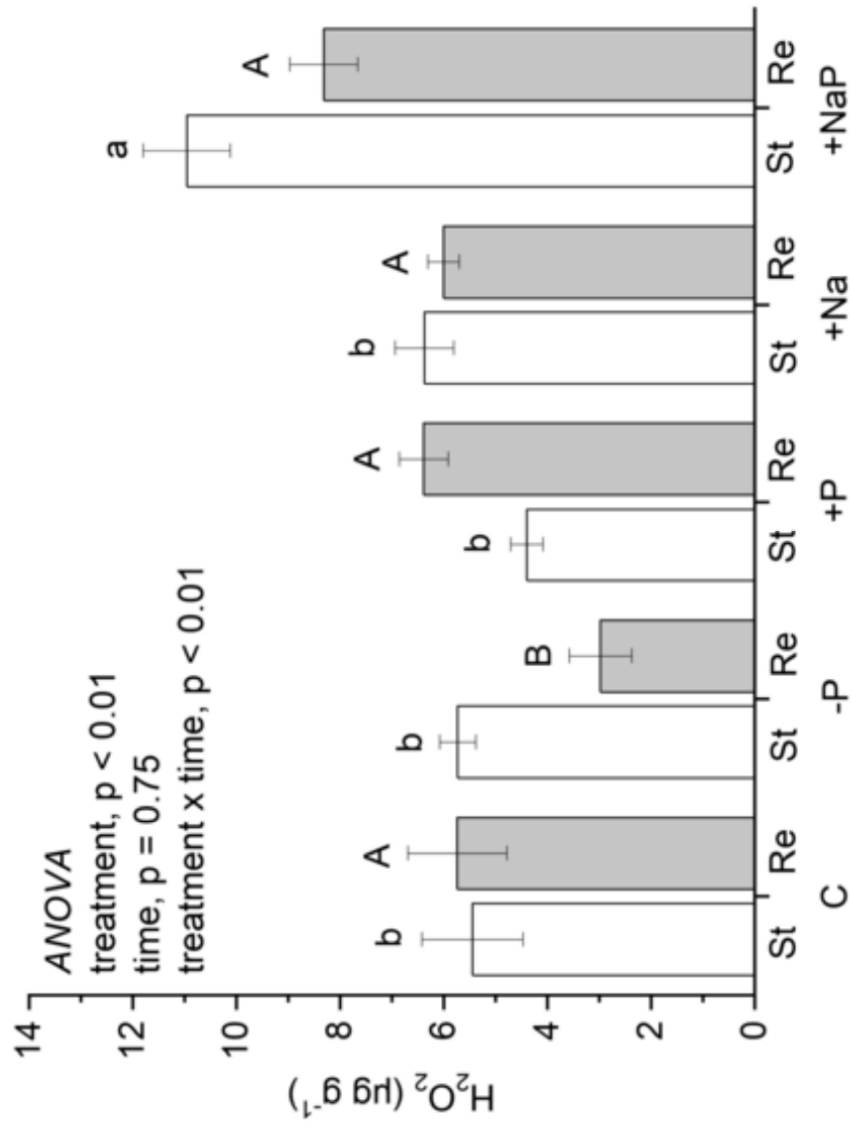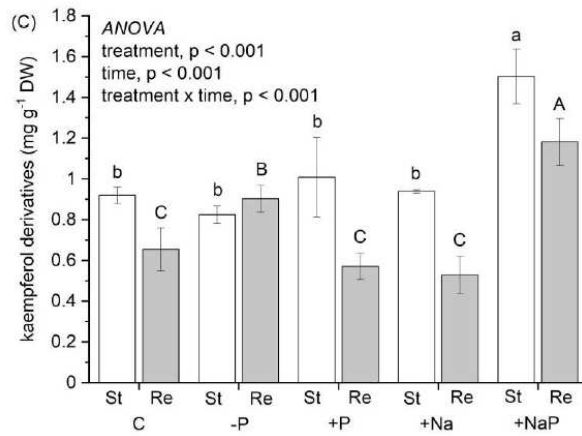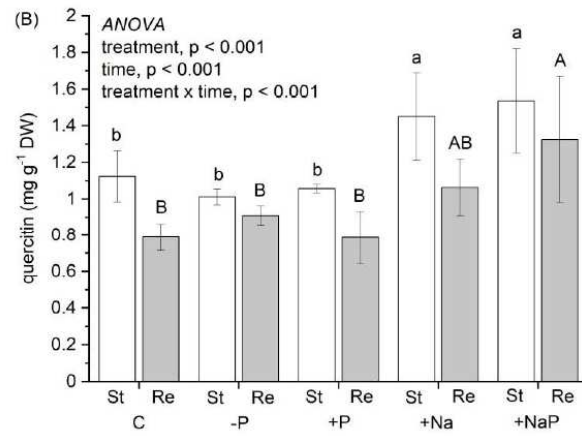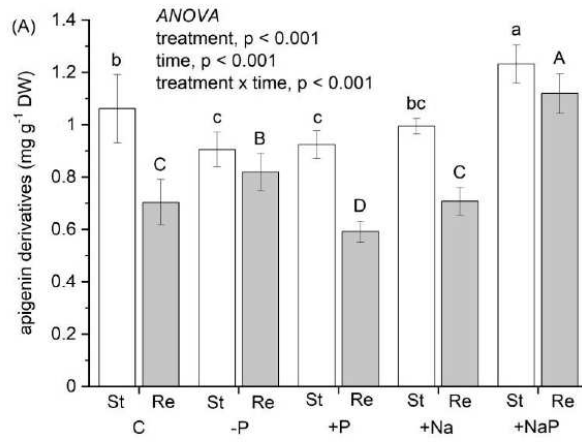| TR5705|c4_g3_i2	anthocyanidin 5,3-O-glucosyltransferase							-1.95	0.018	2.4.1.-
TR5705|c4_g3_i3	anthocyanidin 5,3-O-glucosyltransferase							-3.83	0.001	2.4.1.-

* Binary logarithm of FC

Table 2. List of differentially expressed genes (DEGs) in each treatment at false discovery rate (FDR) of 5%; FC=Fold Change relative to control.
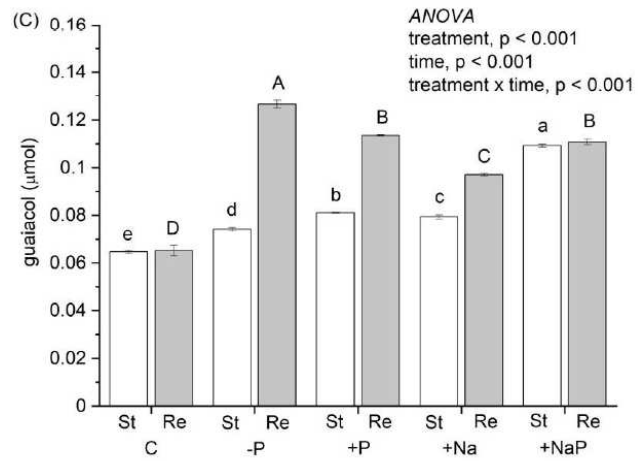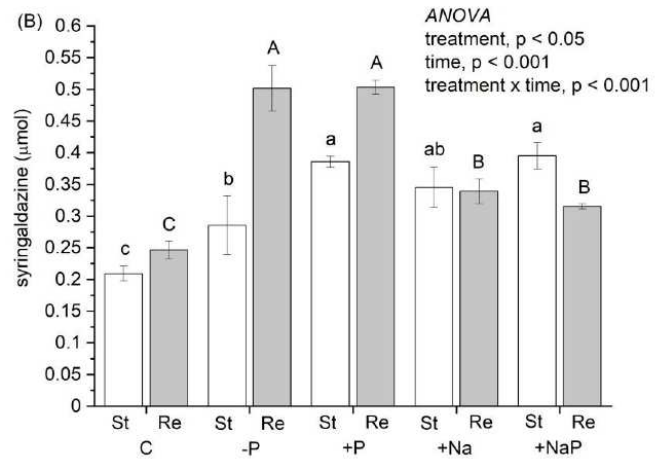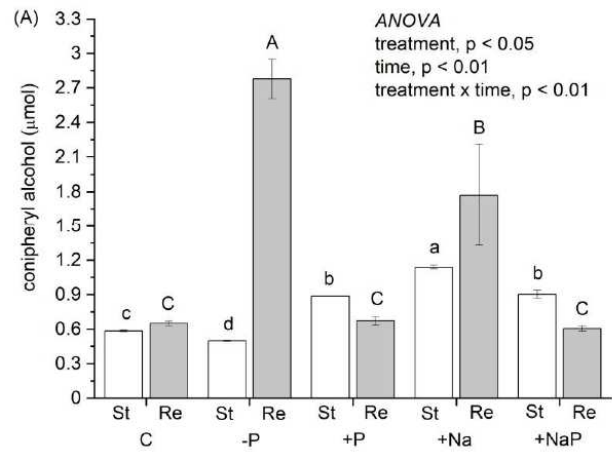
Gene Name	Transcript	Description	FC(-P)*	FDR(-P)	FC(+P)*	FDR(+P)	FC(+Na)*	FDR(+Na)	FC(+NaP)*	FDR(+NaP)	E.C.
PAL	TR30721|c2_g2_i4	phenylalanine ammonia-lyase							-2.37	0.040	4.3.1.24
C4H	TR12947|c1_g1_i1	trans-cinnamate 4-monooxygenase							1.93	0.009	1.14.14.91
C4H	TR12947|c1_g2_i2	trans-cinnamate 4-monooxygenase							1.89	0.039	1.14.14.91
C4H	TR12947|c1_g2_i4	trans-cinnamate 4-monooxygenase							1.70	0.004	1.14.14.91
C4H	TR22013|c1_g1_i1	Trans-cinnamate 4-monooxygenase							1.51	0.044	1.14.14.91
C4H	TR22013|c1_g1_i3	trans-cinnamate 4-monooxygenase							2.28	0.003	1.14.14.91
4CL	TR19035|c0_g1_i1	4-coumarate-- ligase-like 7							-2.05	0.031	6.2.1.12
4CL	TR22604|c3_g2_i1	4-coumarate-- ligase-like 1							2.06	0.036	6.2.1.12
4CL	TR3027|c2_g2_i1	4-coumarate-- ligase-like 3							-2.00	0.047	6.2.1.12
4CL	TR5718|c1_g1_i5	4-coumarate-- ligase-like 5							1.62	0.028	6.2.1.12
4CL	TR7497|c3_g2_i3	probable 4-coumarate-- ligase 2							2.75	0.029	6.2.1.12
4CL	TR7497|c3_g2_i7	probable 4-coumarate-- ligase 2							2.07	1.427E-05	6.2.1.12
CCR	TR6509|c1_g1_i1	cinnamoyl- reductase 1-like							2.11	4.733E-04	1.2.1.44
CCR	TR6509|c1_g1_i6	cinnamoyl- reductase 1-like							1.43	0.011	1.2.1.44
CCR	TR6509|c1_g1_i7	cinnamoyl- reductase 1-like					1.57	0.041			1.2.1.44
CCR	TR9597|c1_g4_i1	cinnamoyl- reductase 1	-1.73	0.004					1.20	0.049	1.2.1.44
HCT	TR3575|c0_g1_i1	shikimate O-hydroxycinnamoyltransferase-like							1.98	0.006	2.3.1.133
HCT	TR5007|c0_g1_i1	Shikimate O-hydroxycinnamoyltransferase							1.50	0.015	2.3.1.133
CCoAOMT	TR18821|c1_g3_i8	caffeoyl- O-methyltransferase At1g67980							-3.87	0.001	2.1.1.104
CCoAOMT	TR30139|c0_g1_i3	caffeoyl- O-methyltransferase 1							2.83	0.002	2.1.1.104
CSE	TR1036|c1_g1_i10	caffeoylshikimate esterase-like							-3.22	6.628E-09	3.1.1.-
CSE	TR1036|c1_g1_i12	caffeoylshikimate esterase-like							1.27	0.033	3.1.1.-
CSE	TR11203|c3_g1_i3	caffeoylshikimate esterase-like isoform X1							-1.51	0.004	3.1.1.-
CSE	TR11203|c3_g1_i6	caffeoylshikimate esterase-like isoform X1	-1.20	0.038							3.1.1.-
CAD	TR24767|c0_g1_i4	probable cinnamyl alcohol dehydrogenase 6					2.93	0.040			1.1.1.195
POX	TR11699|c3_g2_i1	peroxidase 51-like							-1.81	0.032	1.11.1.7
POX	TR11699|c3_g2_i2	peroxidase 51-like							-2.67	1.440E-04	1.11.1.7
POX	TR19645|c0_g1_i5	Peroxidase 17							1.24	0.032	1.11.1.7
POX	TR19645|c0_g1_i6	Peroxidase 17							1.44	0.009	1.11.1.7
POX	TR23604|c5_g1_i2	peroxidase 5-like	-3.60	0.002	-3.64	0.003					1.11.1.7
POX	TR23967|c3_g1_i1	peroxidase 51-like							-1.24	0.015	1.11.1.7
POX	TR23967|c3_g1_i4	peroxidase 51-like							-2.53	0.012	1.11.1.7
POX	TR23967|c4_g2_i1	peroxidase 51-like							-2.78	0.001	1.11.1.7
POX	TR482|c0_g1_i4	peroxidase P7-like							-2.79	0.007	1.11.1.7
POX	TR5593|c3_g1_i4	peroxidase 21							1.15	0.049	1.11.1.7
POX	TR5652|c2_g2_i1	Peroxidase 66							-3.04	0.010	1.11.1.7
POX	TR9608|c4_g1_i1	Peroxidase 12							2.02	4.444E-04	1.11.1.7
POX	TR9751|c0_g1_i3	polygalacturonase ADPG1-like							-3.34	1.738E-04	1.11.1.7
LAC	TR18961|c2_g1_i1	laccase-15-like							1.51	0.007	1.10.3.2
LAC	TR18961|c2_g1_i4	laccase-15-like							1.15	0.039	1.10.3.2
LAC	TR6546|c1_g1_i2	TPA: laccase family							-2.71	0.049	1.10.3.2
LAC	TR6546|c1_g1_i3	TPA: laccase family					-3.49	0.004	-3.65	0.001	1.10.3.2

| LAC | TR6554\|c0_g1_i2 | laccase-17-like | | | | | | | 5.37 | 6.960E-11 | 1.10.3.2 |
| LAC | TR7969\|c1_g1_i3 | laccase-12 13-like | | | | | | | 5.24 | 4.208E-06 | 1.10.3.2 |

Binary logarithm of FC

(A)

ANOVA
treatment, p < 0.001
time, p < 0.001
treatment x time, p < 0.001

apigenin derivatives (mg g⁻¹ DW)

(B)

ANOVA
treatment, p < 0.001
time, p < 0.001
treatment x time, p < 0.001

quercitin (mg g⁻¹ DW)

(C)

ANOVA
treatment, p < 0.001
time, p < 0.001
treatment x time, p < 0.001

kaempferol derivatives (mg g⁻¹ DW)

(A)

ANOVA
treatment, p < 0.05
time, p < 0.01
treatment x time, p < 0.01

(B)

ANOVA
treatment, p < 0.05
time, p < 0.001
treatment x time, p < 0.001

(C)

ANOVA
treatment, p < 0.001
time, p < 0.001
treatment x time, p < 0.001

117

2.   CONCLUSIONS AND FUTURE PERSPECTIVES

The first goal of this study was the *de novo* assembly of the transcriptome of *A. donax* L. under stress conditions. The assembly quality was high as indicated by BUSCO (Benchmarking Sets of Universal Single-Copy Orthologues) analysis, with 74.8% complete gene groups compared to the set of Embryophyta genes; moreover, functional annotation allowed to identify that more than 50% of arundo transcripts were orthologues of other Poaceae (paper I). Differential gene expression highlighted that stresses combination (+NaP) has the major impact, stating clearly that arundo is able to respond to changes in the environment, modifying rapidly its transcriptional machinery. Growth and biomass production were affected, as indicated by physiological measures. Plants, nevertheless, retain the ability to fully recover after one month of wash out from stress treatment. Single stresses seemed to have a lower impact on the plant: +P affects carbon metabolism and isoprene emission but does not hamper photosynthesis; +Na affects principally leaf cells ultrastucture. The enhanced biosynthesis of antioxidant carotenoids, sucrose and isoprene in +Na could have a protective role against salt stress, explaining arundo ability to growth in saline soils.

The functional annotation of transcripts allowed to reconstruct the lignin biosynthetic pathway and determine the differential expression of genes belonging to this pathway in response to different stresses. Analysis of class III peroxidases activity and total lignin content (paper III) showed that lignin content is not altered in any treatment. However, +NaP treatment, a 2-fold increment of peroxidases activity with guaiacol substrate (G) in respect to control and up-regulation of a peroxidase 17 orthologue plus a down-regulation of peroxidases involved in syringal monomers deposition suggest a remodulation on lignin composition, that could influence the final S/G ratio. As already described, S/G ratio is an important measure to assess sugars accessibility: a higher lignin S/G ratio lead to a different lignin structural composition, that could increase the susceptibility to carbohydrate solubilization, lowering the recalcitrance. The data obtained seem to suggest that growing arundo in marginal lands could result in a biomass more suitable for bioethanol production. More specific analysis on lignin composition would be required. If this hypothesis prove to be true, it would be a great boost in arundo usage in both bioenergy production and land restoration usage.

Identification of miRNAs, through smallRNA-seq, and their targets, through deg-seq, was another important step: it was the first time that a catalogue of conserved miRNAs and candidate novel miRNAs for arundo was built (paper II). Until now, only miRNAs inferred from *in silico* analysis of RNA-seq data were available. Among the miRNA identified in arundo by this work, 134 miRNAs were conserved among dicotiledons and monocotiledons and 27 were targeted as candidate novel miRNAs. Stress-responsive miRNAs and their probable targets were identified. Few interesting examples follows:

- miR169a targets a mRNA cleavage and polyadenylation factor (CLP1) homolog, involved in in the 3′-end cleavage and polyadenylation of eukaryotic mRNAs, a critical step of gene expression, that has been recently related also to the regulation of stress responses;
- miR169c-5p a Vascular Plant One-Zinc-Finger (VOZ) 1-like transcription factor, involved in the defense against pathogens, and response to multiple types of abiotic stress. VOZ transcription factors positively affect salt stress tolerance through the regulation of many stress-responsive genes. It may be a promising target for salt-tolerant crops production;
- miR528-5p targets an L-ascorbate oxidase (AAO), an enzyme involved in salt and oxidative stress responses. The slightly higher expression of miR528 in arundo treated with excess of salt, both +Na and +NaP treatments, suggests a conserved mechanism among plants. It also could be an interesting target for salt-tolerant crops generation;
- miRC35861-11 targets a geranylgeranyl pyrophosphate synthase coding transcript, that is involved in the biosynthesis of carotenoids and is likely associated with tolerance to osmotic stress. In arundo under salt stress, carotenoids synthesis seemed to be enhanced. Therefore, this novel miRNA could be involved in osmotic stress response through regulation of carotenoids and, in turn, in salt stress response;
- miRC37052-11 targets a PAD4 lipase-like coding transcript, involved in salicylic acid-mediated response. Salicylic acid is a phytohormone and its role in stress-tolerance is already known. Hence, the novel miRC37052-11 could be involved in salicylic acid-mediated stress responses in arundo.

Those miRNA-target pairs could be a promising list for further investigations with the final aim of biotechnological crop improvement, for both stress tolerance and biomass

yield. In general, deepening the knowledge on arundo ability to cope with salt stress and nutrients imbalance could help in using this plant for requalification of marginal and abandoned lands, helping to lighten the pressure on soil usage and mitigating climate change effects.

Funding information

Acknowledgment